NCAT Report 10-05

EVALUATION OF MIXTURE PERFORMANCE AND STRUCTURAL CAPACITY OF PAVEMENTS USING SHELL THIOPAVE®

Comprehensive Laboratory Performance Evaluation

By
Nam Tran
Adam Taylor
David Timm
Mary Robbins
Buzz Powell
Raj Dongre

September 2010

National Center for Asphalt Technology
NCAT
at AUBURN UNIVERSITY

277 Technology Parkway ■ Auburn, AL 36830

EVALUATION OF MIXTURE PERFORMANCE AND STRUCTURAL CAPACITY OF PAVEMENTS UTILIZING SHELL THIOPAVE®

Comprehensive Laboratory Performance Evaluation

By

Nam Tran
Adam Taylor
David Timm
Mary Robbins
Buzz Powell
Raj Dongre

National Center for Asphalt Technology
Auburn University, Alabama

Sponsored by

Shell Oil Products, USA

September 2010

ACKNOWLEDGEMENTS

This project was sponsored by Shell Oil Products, USA. The project team appreciates and thanks Shell Oil Products, USA for their sponsorship of this project.

DISCLAIMER

The contents of this report reflect the views of the authors who are responsible for the facts and accuracy of the data presented herein. The contents do not necessarily reflect the official views or policies of Shell Oil Products, USA or the National Center for Asphalt Technology, or Auburn University. This report does not constitute a standard, specification, or regulation. Comments contained in this paper related to specific testing equipment and materials should not be considered an endorsement of any commercial product or service; no such endorsement is intended or implied.

TABLE OF CONTENTS

1. INTRODUCTION

1.1 Background

The use of sulfur in hot mix asphalt (HMA) (known as SEA or sulfur-extended asphalt) was originally tried in the 1970s and continued into the 1980s (*1*). The hot liquid sulfur was used in HMA as a binder extender (replacing a portion of the asphalt binder) and a mixture modifier.

In a field evaluation of 26 SEA projects built between 1977 and 1982 in 18 states, Beatty et al. (*2*) reported that the overall performance and level of distress in the SEA pavements were not significantly different from that of the control pavement sections. The mixtures used in the SEA pavements contained between 20 and 40 percent (by weight) of sulfur as a replacement for the asphalt binder. The material performance benefit was an increase in stiffness of the mixtures with a reduction in rutting susceptibility. The increase in stiffness of these mixtures also resulted in performance drawbacks. Bayomy and Khedr (*3*) reported that the sulfur-modified mixtures were more prone to moisture damage than conventional asphalt mixtures.

In the late 1980s, a sharp rise in the price of sulfur in addition to the fact that the use of hot liquid sulfur during production generated a significant amount of fumes and odors brought its use in road paving to an end (*1*). However, the recent rise in asphalt prices coupled with the production of low sulfur fuels has once again made sulfur a marketable product in the asphalt industry. To overcome the problems with hot liquid sulfur used in asphalt concrete (AC), a solid sulfur pellet technology, known as Shell Thiopave[1], was developed. The technology consists of small modified sulfur pellets that are added together with a compaction agent to the asphalt mixture during the mixing process. The technology is designed to lower the mixing temperature of the sulfur-modified mixture so that it can be produced as warm-mix asphalt (WMA) which reduces odors and fumes during production and placement. The modified sulfur pellets melt rapidly on contact with the heated mix and are dispersed throughout the asphalt mixture by aggregate shear during mixing (*4*). FIGURE 1 shows the modified sulfur pellets and compaction agent used in the sulfur-modified WMA evaluated in this study.

Technological improvements to the solid-modified sulfur pellet technology have led to the resurgence in the exploration of the use of sulfur in asphalt concrete. Part of this exploration is an extensive study being conducted at the National Center for Asphalt Technology (NCAT) at Auburn University.

1.2 Objective

This study was divided into two phases. Phase I included laboratory testing as well as theoretical structural pavement analysis and design. Phase II is a field study at the NCAT Pavement Test Track. A set of objectives was defined below for each phase.

The objectives of Phase I were to:

- Perform Thiopave mix designs using the Superpave mix design method;

[1] Shell Thiopave is a trade mark of the Shell Group of Companies

- Measure mechanistic and performance properties of the Thiopave asphalt mixture in the laboratory for use in structural pavement analysis and design as well as laboratory performance evaluation;
- Perform theoretical structural pavement analysis using mechanistic analysis and design to determine appropriate structural pavements for the field study in Phase II.

The objectives of Phase II are to:

- Evaluate the mixture performance and structural capacity of the pavement structure designed in Phase I through a field study at the NCAT Pavement Test Track;
- Incorporate any needed modifications and/or additional information to the findings of Phase I.

FIGURE 1 Modified Sulfur Pellets (left) and Compaction Agent (right) Used in Sulfur-Modified WMA.

Parts of Phase I, including mix design, laboratory performance testing, and theoretical structural pavement analysis, to support the field study in Phase II have been completed and presented in NCAT Report 09-05 (*5*). Phase II field evaluation is underway through 2012 at the NCAT Pavement Test Track.

More laboratory testing has been conducted under Phase I after NCAT Report 09-05 (*5*) was completed. The objective of this comprehensive laboratory testing was to thoroughly quantify the laboratory performance (moisture susceptibility, rutting, fatigue cracking, low temperature cracking, and reflective cracking) of multiple Shell Thiopave warm mixes relative to the performance of control HMA mixtures using binders at various PG grades.

1.3 Scope of Work Presented in This Report

The work presented in this report is part of a two phase study currently being conducted at NCAT regarding the sulfur pellet WMA technology. This report focuses on the comprehensive laboratory investigation of lab-produced sulfur-modified WMA mixtures and control HMA mixtures with multiple binders completed in Phase I of this study.

2. LABORATORY EXPERIMENTAL PLAN

A wide array of testing was utilized for this project to quantify the laboratory performance of asphalt mixtures with varying amounts of Thiopave versus that of control asphalt mixtures using asphalt binders at different performance grades. As shown in TABLE 1, a total of ten asphalt mixtures were tested during Phase I of the study. Each of these mixtures had the same target aggregate gradation. The differences in these mixtures were in the base binder, the percentage of Thiopave utilized as a replacement of the base binder, and the design air voids.

TABLE 1 Asphalt Mixtures Evaluated in Phase I

Mix ID	Base Binder	Percent Thiopave	Design Air Voids	Aggregate	NMAS
Control_67	PG 67-22	0%	4%	Lms, Grn, Sand**	19 mm
Control_76	PG 76-22	0%	4%	Lms, Grn, Sand	19 mm
Thio_67_30_2	PG 67-22	30%	2%	Lms, Grn, Sand	19 mm
Thio_67_30_3.5	PG 67-22	30%	3.5%	Lms, Grn, Sand	19 mm
Thio_67_40_2	PG 67-22	40%	2%	Lms, Grn, Sand	19 mm
Thio_67_40_3.5	PG 67-22	40%	3.5%	Lms, Grn, Sand	19 mm
Thio_58_30_2	PG 58-28*	30%	2%	Lms, Grn, Sand	19 mm
Thio_58_30_3.5	PG 58-28	30%	3.5%	Lms, Grn, Sand	19 mm
Thio_58_40_2	PG 58-28	40%	2%	Lms, Grn, Sand	19 mm
Thio_58_40_3.5	PG 58-28	40%	3.5%	Lms, Grn, Sand	19 mm

* Approximately equivalent to AC-10; ** Limestone, granite and natural sand

Two control mixtures (containing no Thiopave) utilized PG 67-22 and PG 76-22 and were designed to have 4 percent air voids. The PG 67-22 control mixture (Control_67) was based on a mix design used in the bottom binder and base asphalt courses (layers 3 and 4) of Section S11 in the 2006 research cycle at the NCAT Pavement Test Track.

Eight Thiopave mixes were designed based on two base binders (PG 67-22 and PG 58-28). For each base binder, four Thiopave mix designs were prepared. Two mix designs contained 30 percent Thiopave as a replacement of the base binder. One of these mixes was designed as a binder layer mixture with a design air void content of 3.5 percent, and the other was designed as a fatigue-resistant rich bottom layer with a design air void content of 2 percent. The other two mixes contained 40 percent Thiopave and had design air void levels of 3.5 and 2 percent, respectively. In this report, the mixtures with a design air void level of 2 percent are referred to as ‘rich bottom’ mixtures. The mixtures with 4 or 3.5 percent design air voids are referred to as ‘base’ layer mixtures. The change in base layer air void content from 4 percent for the control mix to 3.5 percent for the Thiopave mixes was done to offset the increased brittleness of the stiffer Thiopave mixtures as well as to provide additional moisture and fatigue resistance in these mixtures.

A testing plan for this study was designed so that there would be multiple tests, if possible, used to assess the performance characteristics of the sulfur-modified asphalt mixtures. The relevant performance characteristics, along with the relevant testing procedures, are listed in TABLE 2.

These tests were conducted on each of the ten mixtures, with one exception--moisture susceptibility testing via the determination of a tensile strength ratio (TSR) was not performed on the rich bottom mixes. Reasons are given later with a discussion of the test results.

TABLE 2 Performance Testing of Each Asphalt Mixture

Property Evaluated	Test Name	Test Specification	Number of Specimens Per Mix and Testing Condition
Moisture susceptibility	Moisture Resistance of HMA	ALDOT 361, AASHTO T 283-07	6 specimens (14 days cured) at 7±0.5% air voids (3 conditioned and 3 unconditioned)
Moisture and rutting susceptibility	Hamburg Wheel-Track	AASHTO T 324-04	3 twin specimens (14 days cured) at 7±1% air voids subjected to 20,000 passes at 50°C (wet test)
Rutting susceptibility	Asphalt Pavement Analyzer	AASHTO TP 63-07	6 specimens (14 days cured) at 7±0.5% air voids subjected to 8,000 cycles at 64°C
Rutting susceptibility	Flow Number	AASHTO TP 79-09	3 specimens (14 days cured) at 7±0.5% air voids tested at 58°C using a deviator stress of 70 psi and no confinement
Stiffness for master curve	Dynamic Modulus	AASHTO TP 79-09	2 specimens (14 days cured) at 7±0.5% air voids tested at 3 temperatures (4, 21, 46°C) and at 6 frequencies (0.01, 0.1, 0.5, 1, 5, 10 Hz) to construct master curve
Stiffness development	Dynamic Modulus	AASHTO TP 79-09	4 specimens at 7±0.5% air voids: 2 tested at 1 day and 2 tested at 14 days (at 21°C and 0.01 Hz to 10 Hz)
Fatigue Cracking	Bending Beam Fatigue	ASTM D7460-08	6 beams (14 days cured) at 7 ± 1% voids tested at 3 strain levels (200, 400 and 600 μstrain) and at 20°C
Low temperature cracking	Thermal Stress-Restrained Specimen Tensile Strength	AASHTO TP 10-00	3 beam specimens (14 days cured) at 7±1% air voids
Low temperature cracking	Semi-Circular Bending	Proposed Procedure	6 replicates tested at -18 and -30°C
Low temperature cracking	Bending Beam Rheometer for Mixture	Proposed Procedure	6 replicates tested at -12 and 16°C
Reflective Cracking	Overlay Test	Tex-248-F	6 replicates tested using two maximum displacements (0.01 and 0.025 in.)

2.1 Mix Design

For this project, a mix design was conducted for each of the control and sulfur-modified asphalt mixtures with 30 and 40 percent of Thiopave. These mix designs were conducted in accordance

with AASHTO M 323-07, *Standard Specification for Superpave Volumetric Mix Design,* and AASHTO R 35-04, *Standard Practice for Superpave Volumetric Design for Hot-Mix Asphalt.*

For the control mix, the optimum binder content was determined corresponding to 4 percent air voids. For each Thiopave mix, the optimum content of combined Thiopave and asphalt binder was determined according to Equation 1, to account for the presence of Thiopave materials in the mixture. For each Thiopave percentage level, two optimum contents of combined Thiopave and asphalt binder were determined for mixtures that would be used in the base and rich bottom layers. The optimum Thiopave and asphalt content for the base layer mix was determined at 3.5 percent air voids, and the optimum Thiopave and asphalt content for the rich bottom mix was determined at 2 percent air voids. The mix designs were carried out using a spreadsheet provided by Shell, being modified for use in this project.

$$Thiopave + Binder\% = A * \frac{100R}{[100R - P_s(R - G_{binder})]} \quad (1)$$

where:

A = weight percentage of binder in conventional mix design
R = Thiopave to binder substitution ratio
R = $G_{Thiopave}/G_{Binder}$ (R = 1.90 for this study)
P_s = weight percentage of Thiopave in Thiopave-blended binder
G = specific gravity of the unmodified binder

As mentioned earlier, the mix design with Thiopave was based on the mix design used for the two bottom lifts of Section S11 (S11-3 and S11-4). This was a 19.0 mm mix consisting of four aggregate stockpiles. The coarse aggregate used in the mix designs was a limestone obtained from stockpiles at Martin-Marietta Quarry in Auburn, Alabama. Two different stockpiles (#57 and #78) of this limestone were used. The fine granite (M10) was obtained from Vulcan Materials Barin Quarry in Columbus, Georgia. Finally, the natural sand was from Martin Marietta Sand and Gravel in Shorter, Alabama.

The percentages of each stockpile were generated from the original laboratory mix design used at the Test Track. The gradations of individual stockpiles, the gradation of the total blend, and the percentages of each stockpile used in the final blend are shown in TABLE 3. FIGURE 2 shows a plot of the design gradation curve that was within the Superpave aggregate gradation control points. The aggregate specific gravities, absorptions, and consensus properties (crushed face count, uncompacted voids in fine aggregate, sand equivalency, and flat and elongated particle percentages) for each of the four stockpiles are shown in TABLE 4. The weighted average of each of the four consensus properties fell within the specification for an acceptable mix design set forth in AASHTO M 323.

All the asphalt binders used in this study were modified with 0.5 percent (by weight of the binder) of a liquid anti-strip agent (Ad-here 1500). For the Thiopave mixes, a compaction additive, as shown in FIGURE 1, was also added at 1.52 percent (by the binder weight). This compaction additive (CA), consisting of fine wax crystals, aids in the compaction of Thiopave mixes to the target air voids at the lower compaction temperatures that are necessary to control sulfur emissions.

TABLE 3 Aggregate Gradations

Sieve Size (mm)	Sieve Size (Inches)	Percent Passing				
		EAP Limestone #78	EAP Limestone #57	Columbus Granite M10	Shorter Natural Sand	Total Blend
50.0	2.0"	100.0	100.0	100.0	100.0	100.0
37.5	1.5"	100.0	100.0	100.0	100.0	100.0
25.0	1.0"	100.0	98.0	100.0	100.0	99.6
19.0	3/4"	100.0	63.0	100.0	100.0	92.6
12.5	1/2"	92.0	23.0	100.0	100.0	82.1
9.5	3/8"	61.0	15.0	100.0	100.0	70.9
4.75	# 4	10.0	3.0	99.0	99.2	52.2
2.36	# 8	4.0	2.0	86.0	91.6	44.8
1.18	# 16	3.0	1.0	65.0	75.2	34.9
0.600	# 30	2.0	1.0	47.0	46.1	23.7
0.300	# 50	1.0	1.0	31.0	11.6	12.0
0.150	#100	1.0	1.0	19.0	3.6	6.9
0.075	#200	0.4	1.0	10.6	2.2	3.9
Cold Feed		**31%**	**20%**	**30%**	**19%**	

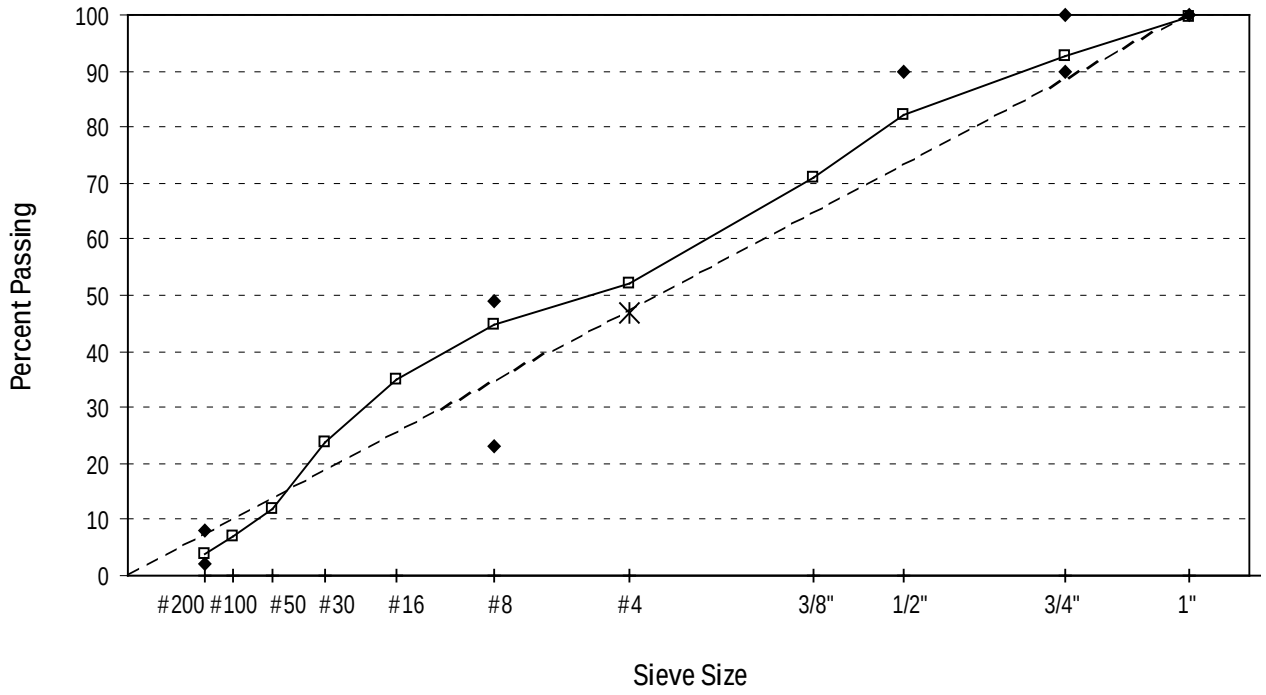

FIGURE 2 Design Aggregate Gradation Curve.

To mix the Thiopave samples in the laboratory, the Thiopave additive was added to the hot aggregate and asphalt binder immediately after the start of the mixing process. The mixing

process using the Thiopave materials was conducted in a well-ventilated mixing room. All the samples were short-term aged in the oven at a temperature of 140°C for two hours before compaction. The design pills were compacted to an N_{des} level of 60 gyrations and a target height of 115 ±5 mm. The control mixtures for this project were short-term aged for two hours at 157°C to achieve a compaction temperature between 149°C and 152°C.

The loose mixes and compacted specimens were cooled down in the laboratory. After cooling, the bulk specific gravity of the compacted specimens was determined according to AASHTO T 166, and the maximum theoretical specific gravity of the loose mixtures was determined in accordance with AASHTO T 209. The specific gravity information was used to determine the volumetric properties of the mixes that are presented later in this report.

TABLE 4 Aggregate Properties

Consensus Property	EAP Limestone #78	EAP Limestone #57	Columbus Granite M10	Shorter Natural Sand	Total Blend (Weighted Average)
Bulk Specific Gravity	2.819	2.833	2.707	2.614	2.746
%Absorption	0.5	0.4	0.3	0.2	0.3
%Crushed Face*	100/100*	100/100*	N/A	N/A	100/100
Uncompacted Void	N/A	N/A	50.2	45.8	48.4
Sand Equivalency	N/A	N/A	72	81	75.2
%Flat and Elongated Particle**	<1	<1	N/A	N/A	<1

* - Blasted and Crushed Limestone Material
** - Weighted Average Based on Gradation (5:1)

2.2 Mechanistic and Performance Testing

2.2.1 Moisture Susceptibility

Moisture susceptibility testing was performed according to two different methods (ALDOT 361 and AASHTO T 283) on specimens that had been allowed to cure at room temperature for 14 days. For each of the following mixtures, three sets of three specimens were used to determine the tensile strength ratio (TSR):

- Control mix using PG 67-22 at 4 percent design air voids
- Control mix using PG 76-22 at 4 percent design air voids
- Thiopave mix using PG 67-22 and 30 percent Thiopave at 3.5 percent design air voids
- Thiopave mix using PG 67-22 and 40 percent Thiopave at 3.5 percent design air voids
- Thiopave mix using PG 58-28 and 30 percent Thiopave at 3.5 percent design air voids
- Thiopave mix using PG 58-28 and 40 percent Thiopave at 3.5 percent design air voids

The first set of three specimens was tested with no moisture conditioning while the other two sets were conditioned in accordance with the ALDOT and AASHTO procedures. All the specimens were compacted to a height of 95 mm and an air void level of 7 ± 0.5 percent. For the ALDOT

method, the conditioned specimens were vacuum saturated to the point at which 55 to 80 percent of the internal voids were filled with water. These specimens were then conditioned in 60 ± 1°C water bath for 24 ±1 hours. All samples, conditioned and unconditioned, were brought to room temperature in a 25 ± 0.5°C water bath to equilibrate the sample temperature just prior to testing. The indirect tensile strength was then calculated using Equation 2 based on the failure loading and measured specimen dimensions. The tensile strength ratio was then calculated for each set by dividing the average tensile strength of the conditioned specimens by the average tensile strength of the unconditioned specimens. ALDOT 361 recommends a TSR value of 0.8 and above for moisture resistant mixes. The Pine Instruments Marshall Stability Press used for determining indirect tensile strength is shown in FIGURE 3.

$$S_t = \frac{2 * P}{3.14 * D * t} \tag{2}$$

where:

S_t = tensile strength (psi)
P = average load (lb)
D = specimen diameter (in.)
t = specimen thickness (in.)

FIGURE 3 Pine Instruments Marshall Stability Press.

For the AASHTO method, the conditioned specimens were vacuum saturated so that 70 to 80 percent of the internal voids were filled with water. These specimens were then wrapped in plastic wrap and placed in a leak-proof plastic bag with 10 mL of water prior to being placed in the freezer at -18 ± 3°C for a minimum of 16 hours. After the freezing process, the conditioned samples were placed in a 60 ± 1°C water bath for 24 ±1 hours to thaw. All samples, conditioned

and unconditioned, were brought to room temperature in a 25 ± 0.5°C water bath to equilibrate the sample temperature for two hours just prior to testing. Calculation of the failure load, splitting tensile strength, and TSR value is done using the same procedure as the ALDOT method.

2.2.2 Dynamic Modulus

Dynamic modulus (E*) testing was conducted generally in accordance with AASHTO TP 79-09. This testing was performed using an IPC Global Asphalt Mixture Performance Tester (AMPT), shown in FIGURE 4. Dynamic modulus testing was performed for each of the ten mix designs listed in TABLE 1. A Pine Instruments gyratory compactor was used to compact specimens to 150 mm in diameter and 170 mm in height. These specimens were then cored using a 100 mm core drill and trimmed to 150 mm in height. The air voids for these cut specimens were 7 ± 0.5 percent.

FIGURE 4 IPC Global Asphalt Mixture Performance Tester.

For each mix design, two sets of specimens were tested at two different room-temperature curing times to assess the effect of aging on the mixtures. The first set of specimens was tested with 1 day between compaction and testing time to quantify the strength parameters of the mix post-compaction. The second set of specimens was tested after 14 days of curing had passed to assess the effects of curing time on the modulus of the different mixtures. For the evaluation of the effects of aging, the specimens were tested at a chamber temperature of 21.1°C and the following frequencies: 25, 10, 5, 1, 0.5, 0.1, and 0.01 Hz.

To provide the necessary information for mechanistic-empirical (M-E) pavement analyses, the ten sets of dynamic modulus test specimens used for "14-day" testing (referring to the curing time) were re-tested using three temperatures (4.4, 21.1, and 46.1°C) and six frequencies (10, 5, 1, 0.5, 0.1, and 0.01 Hz). This testing produced a data set for generating master curves for the control and Thiopave mixtures using the procedure outlined in NCHRP Report 614 (*6*).

To ensure quality of the measured data, the coefficient of variation (COV) between measured moduli when tested at the same temperatures and frequencies was required to be less than 15 percent. If a high level of variation was determined between specimens, the specimens were re-tested. Equations 3 and 4 were used to generate the master curve for each mix design. Equation 3 is the master curve equation, while Equation 4 shows how the reduced frequency is determined. The regression coefficients and shift factors, which are used to shift the modulus data at various test temperatures to the reference temperature of 21.1°C, are determined simultaneously during the optimization process using the Solver function in an Excel® spreadsheet.

$$\log|E^*| = \delta + \frac{\alpha}{1 + e^{\beta + \gamma \log f_r}} \tag{3}$$

$$\log f_r = \log f + \log a(T) \tag{4}$$

where:

$\|E^*\|$	= dynamic modulus, psi
f	= loading frequency at the test temperature, Hz
f_r	= reduced frequency at the reference temperature, Hz
$\alpha, \delta, \beta, \gamma$	= regression coefficients
$a(T)$	= temperature shift factor

2.2.3 Flow Number

Flow number (F_n) testing was performed using the specimens that were tested for E* for each of the ten mix designs listed in TABLE 1. The testing was performed using the AMPT (FIGURE 4). F_n tests were conducted at a temperature of 58°C. The specimens were tested at a deviator stress of 70 psi and were unconfined. The tests were terminated when the samples reached 10 percent axial strain. For the determination of tertiary flow, two model forms were utilized. The first model form is the classical power model in Equation 5. The second model form was the Francken model in Equation 6 (*7*). The non-linear regression analysis used to fit both models to the test data was performed within the testing software (Universal Testing Systems (UTS) SPT Flow Software – Version 1.37).

$$\varepsilon_p(N) = aN^b \tag{5}$$

$$\varepsilon_p(N) = aN^b + c(e^{dN} - 1) \tag{6}$$

where:

$\varepsilon_p(N)$	= permanent strain at 'N' cycles
N	= number of cycles
a,b,c,d	= regression coefficients

2.2.4 Asphalt Pavement Analyzer

The rutting susceptibility of all ten mix designs (listed in TABLE 1) was evaluated using the Asphalt Pavement Analyzer (APA) as shown in FIGURE 5. Testing was performed in accordance with AASHTO TP 63. The specimens used for this testing were prepared to a height of 75 mm and an air void level of 7 ± 0.5 percent. Six replicates were tested for each mix. All specimens were cured at room temperature 14 days prior to testing to allow for development of the time-dependent stiffness properties of the Thiopave-asphalt mixtures. The samples were tested at a temperature of 64^{o}C (the 98 percent reliability temperature for the high PG grade of the binder in Opelika, Alabama). The samples were loaded by a steel wheel (loaded to 100 lbs) resting on a pneumatic hose pressurized to 100 psi for 8,000 cycles. Manual depth readings were taken at two locations on each specimen before and after the loading was applied to determine the specimen rut depth.

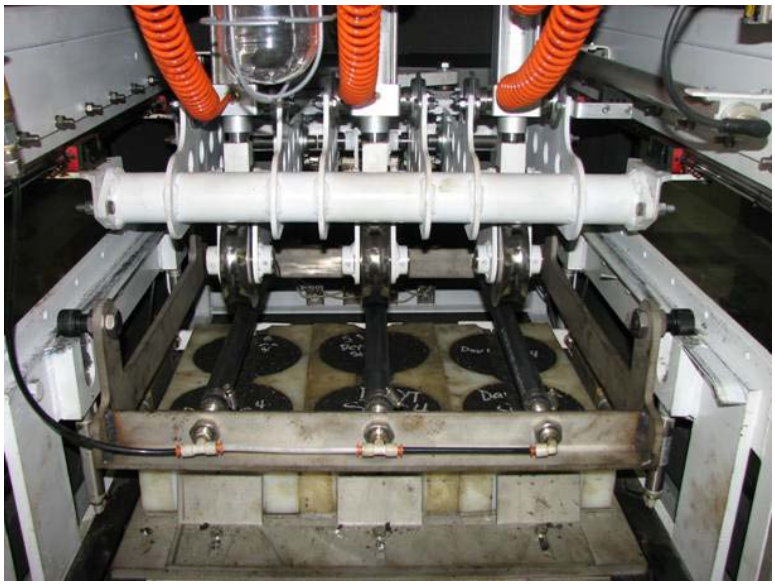

FIGURE 5 Asphalt Pavement Analyzer.

2.2.5 Hamburg Wheel Tracking Device

Hamburg wheel-track (Hamburg) testing, shown in FIGURE 6, was performed to determine both the rutting and stripping susceptibility of the ten mixtures listed in TABLE 1. Testing was performed in accordance with AASHTO T 324. For each mix, a minimum of two replicates were tested. The specimens were originally compacted to a diameter of 150 mm and a height of 115 mm. These specimens were then trimmed so that two specimens, with a height between 38 mm and 50 mm, were cut from the top and bottom of each gyratory-compacted specimen. The air voids on these cut specimens were 7 ± 2 percent, as specified in AASHTO T 324. All specimens were cured at room temperature for 14 days prior to testing.

The specimens were tested under a 158 ± 1 lbs wheel load for 10,000 cycles (20,000 passes) while submerged in a water bath which was maintained at a temperature of 50^{o}C. While being

tested, rut depths were measured by an LVDT which recorded the relative vertical position of the load wheel after each load cycle. After testing, these data were used to determine the point at which stripping occurred in the mixture under loading and the relative rutting susceptibility of those mixtures. FIGURE 7 illustrates typical data output from the Hamburg device. These data show the progression of rut depth with number of cycles. From this curve two tangents are evident, the steady-state rutting portion of the curve and the portion of the curve after stripping. The intersection of these two curve tangents defines the stripping inflection point of the mixture. The slope of the steady-state portion of the curve is also quantified and multiplied by the number of cycles per hour (2520) to determine the rutting rate per hour. Comparing the stripping inflection points and rutting rates of the ten different mixtures gives a measure of the relative moisture and deformation susceptibility of these mixtures.

FIGURE 6 Hamburg Wheel-Tracking Device.

2.2.6 Bending Beam Fatigue

Bending beam fatigue testing was performed in accordance with ASTM D7460 to determine the fatigue limits of the ten asphalt mixtures listed in TABLE 1. Six beam specimens were tested for each mix. Within each set of six, two beams each were tested at 200, 400, and 600 microstrain. The specimens were originally compacted in a kneading beam compactor, shown in FIGURE 8, then were trimmed to the dimensions of 380 ± 6 mm in length, 63 ± 2 mm in width, and 50 ± 2 mm in height. Additionally, the orientation in which the beams were compacted (top and bottom) was marked and maintained for the fatigue testing as well.

The beam fatigue apparatus, shown in FIGURE 9, applies haversine loading at a frequency of 10 Hz. During each cycle, a constant level of strain is applied to the bottom of the specimen. The loading device consists of 4-point loading and reaction positions which allow for the application of the target strain to the bottom of the test specimen. Testing was performed at 20 ± 0.5°C. The data acquisition software was used to record load cycles, applied loads, beam deflections. The

software also computed and recorded the maximum tensile stress, maximum tensile strain, phase angle, beam stiffness, dissipated energy, and cumulative dissipated energy at user specified load cycle intervals.

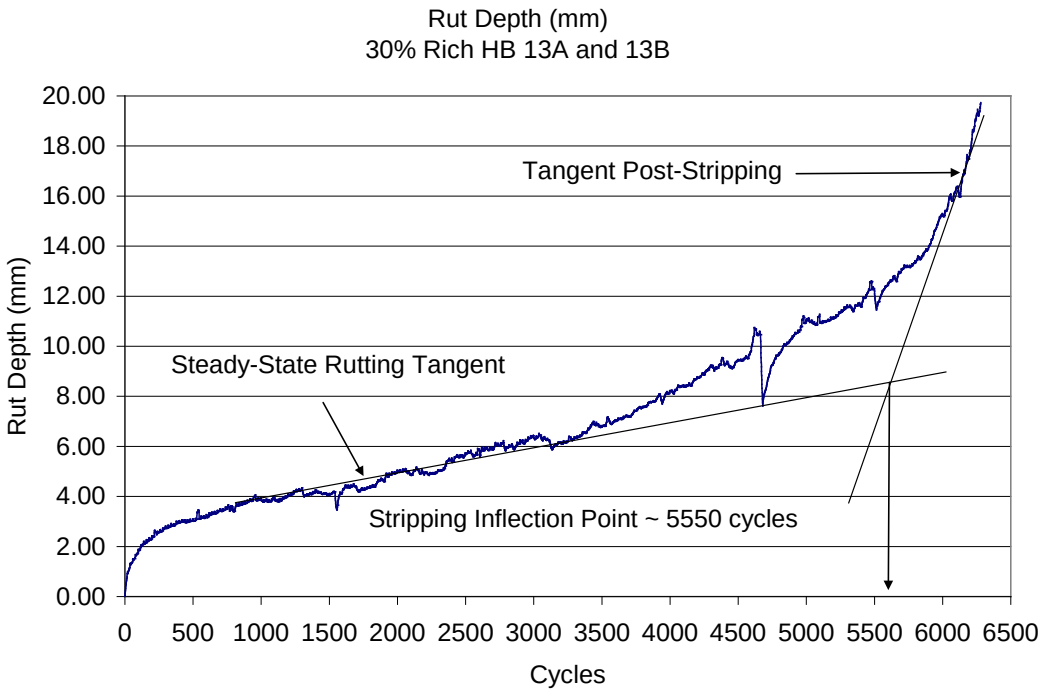

FIGURE 7 Example of Hamburg Raw Data Output.

FIGURE 8 Kneading Beam Compactor.

FIGURE 9 IPC Global Beam Fatigue Testing Apparatus.

At the beginning of each test, the initial beam stiffness was calculated by the data acquisition software after 50 conditioning cycles. ASTM D7460 recommends the test be terminated when the beam stiffness is reduced to 40 percent of the initial stiffness. As a factor of safety and to ensure a complete data set, the beams for this project were allowed to run until the beam stiffness was reduced to 30 percent of the initial stiffness. Based on the collected data, the value of Normalized Modulus × Cycles was calculated using Equation 7 to help interpret the point of failure. According to ASTM D7460, the failure point of the beam occurs at the maximum point on a plot of Normalized Modulus × Cycles versus number of testing cycles. An example of this type of plot is shown in FIGURE 10. This also corresponds to a sudden reduction in stiffness of the specimen. Given the cycles to failure for three different strain levels, the fatigue limit was then calculated for each mix design.

$$NM = \frac{S_i x N_i}{S_o x N_o} \tag{7}$$

where:

NM = Normalized Modulus × Cycles
S_i = flexural beam stiffness at cycle i
N_i = cycle i
S_o = initial flexural beam stiffness (estimated at 50 cycles)
N_o = actual cycle number where initial flexural beam stiffness is estimated

Using a proposed procedure developed under NCHRP 9-38 (*8*), the endurance limit for each of the ten mixes was estimated using Equation 8 based on a 95 percent lower prediction limit of a linear relationship between the log-log transformation of the strain levels (200, 400, and 600

microstrain) and cycles to failure. All the calculations were conducted using a spreadsheet developed under NCHRP Project 9-38.

$$\text{Endurance Limit} = \hat{y}_0 - t_\alpha s\sqrt{1+\frac{1}{n}+\frac{(x_0-\bar{x})^2}{S_{xx}}} \quad (8)$$

where:

$\hat{y}_0$ = log of the predicted strain level (microstrain)
t_α = value of *t* distribution for n-2 degrees of freedom = 2.131847 for n = 6 with $\alpha = 0.05$
s = standard error from the regression analysis
n = number of samples = 6
S_{xx} = $\sum_{i=1}^{n}(x_i-\bar{x})^2$ (Note: log of fatigue lives)
x_o = log (50,000,000) = 7.69897
$\bar{x}$ = log of average of the fatigue life results

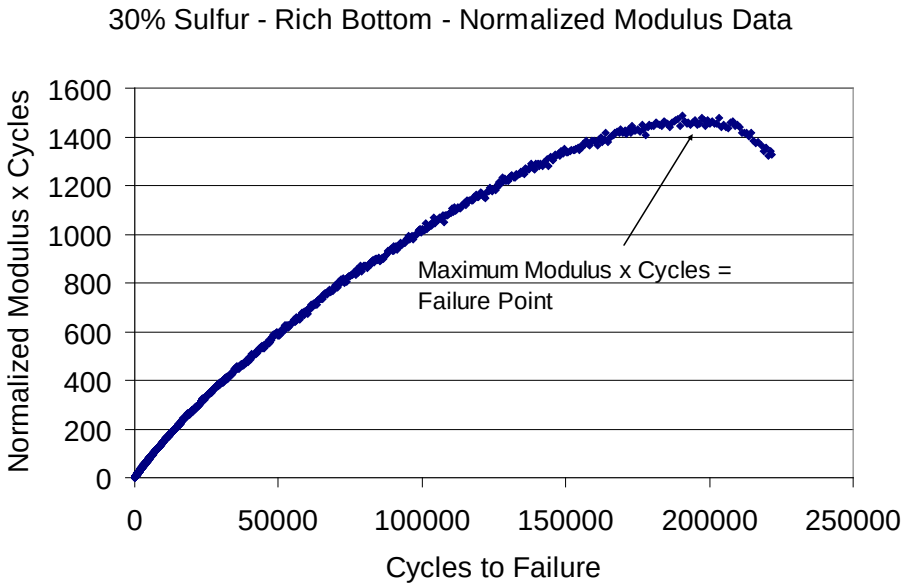

FIGURE 10 Sample Plot of Normalized Modulus × Cycles versus Number of Cycles.

2.2.7 Thermal Stress Restrained Specimen Test

The thermal stress restrained specimen testing (TSRST) shown in FIGURE 11 was conducted at the Western Regional Superpave Center at the University of Nevada at Reno. The tests were conducted in accordance with AASHTO TP 10. The test specimens were prepared in the NCAT laboratory. For this testing, five beams for each of the ten mix designs listed in TABLE 1 were compacted. The specimens were compacted to 7 ± 1 percent air voids and were trimmed to be 10 inches in length and 2 inches square in cross-section. The specimens were compacted using

the same kneading beam compactor used for the compaction of the bending beam fatigue test specimens. Only three beams from each mix design were tested at UNR, the extra beams were compacted in the event some of the specimens were damaged during shipping.

FIGURE 11 Thermal Stress Restrained Specimen Test.

2.2.8 Semi-Circular Bending Test

Semi-Circular Bending (SCB) testing was conducted to determine the fracture toughness and fracture energy of the ten mix designs tested in this study. A schematic of the instrumentation is shown in FIGURE 12. For each test, a load controlled by a constant rate of crack mouth opening displacement (CMOD) was applied vertically on the top of the semi-circular specimen. The CMOD was measured and controlled by a clip-gage placed over a notch which had been cut at the bottom-center of the semi-circular specimen. This notch was the location at which cracking was initiated. The load-line displacement (LLD) was measured using a vertically-mounted extensometer. The fracture toughness was calculated from the peak load, and the fracture energy was determined from the area under load-LLD curve. An example of three load-LLD curves measured at high, intermediate and low temperatures is given in FIGURE 13. For this study, the SCB tests were performed at -18 and -30^{o}C.

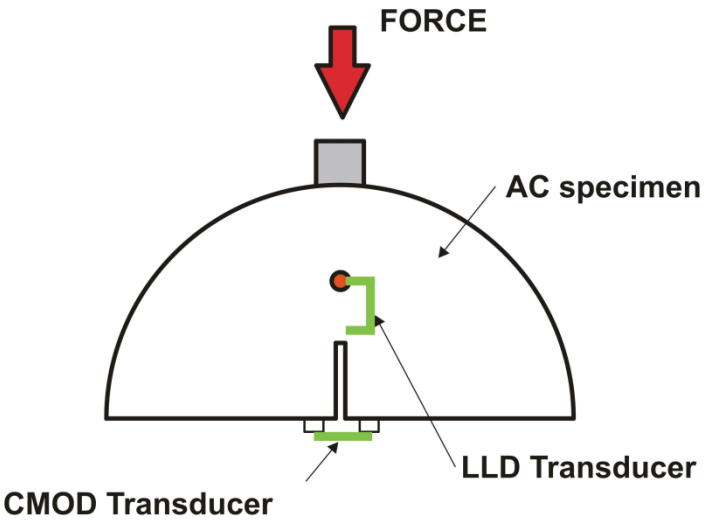

FIGURE 12 Semi-Circular Bending Test Setup.

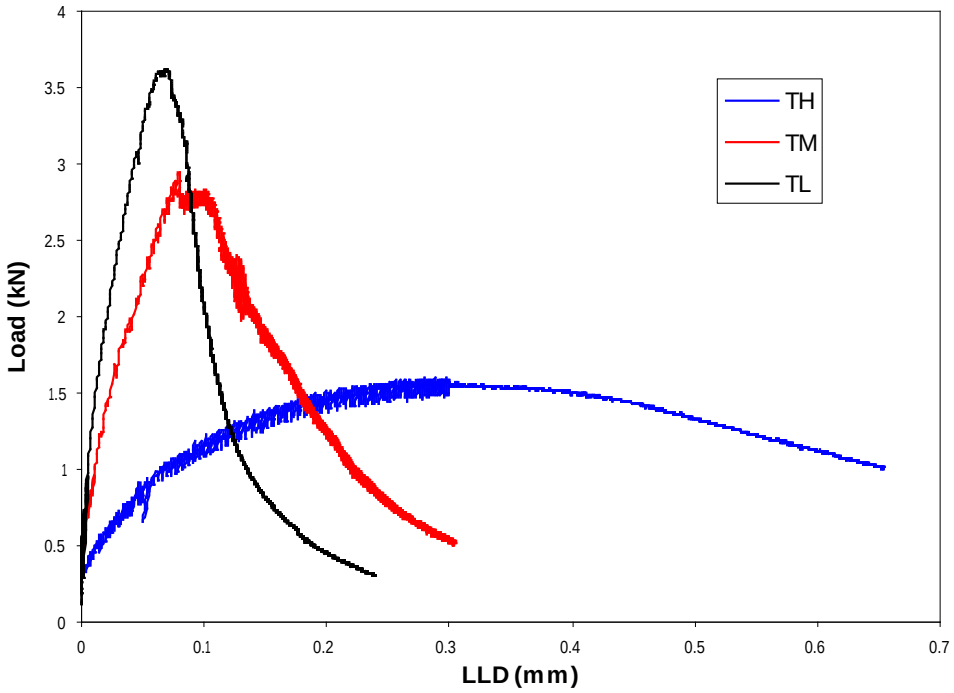

FIGURE 13 Example of LLD Curves Measured at Three Temperatures.

2.2.9 Bending Beam Rheometer Testing for Asphalt Mixture

In this study, the Bending Beam Rheometer (BBR) was utilized to perform creep tests on asphalt mixture beams. Beam specimens (6.35 ± 0.05 mm thick by 12.70 ±0.05 mm wide by 127 ± 2.0 mm long) were cut from Superpave gyratory compacted specimens. FIGURE 14 shows an asphalt mixture beam in the BBR. The BBR testing procedure for asphalt mixture beams is similar to that used for asphalt binder beams (AASHTO T 313-05), except that loading up to

1000 g was applied to maintain a large enough deflection during the creep test. The BBR creep tests for asphalt mixture beams were conducted for 240 seconds, the same as that used for testing asphalt binder beams. For this study, the BBR tests were conducted at 16 and -12°C. Based on the load and deflection results measured during the test, the creep stiffness and m-value for each beam were determined at 60 seconds using the calculation procedure presented in the Annex of AASHTO T 313-05.

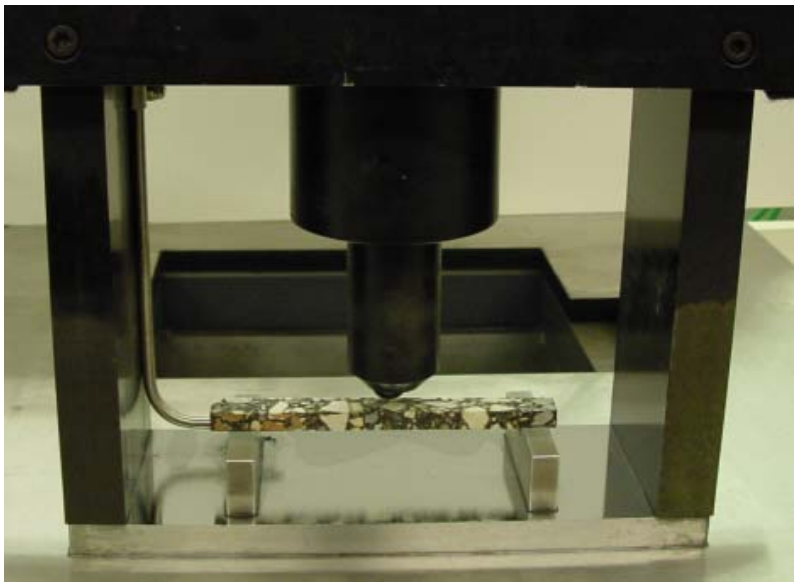

FIGURE 14 Bending Beam Rheometer with Asphalt Mixture Beam.

2.2.10 Overlay Test

The Overlay Test (OT) was performed in accordance with TxDOT test procedure Tex-248-F. The test device simulates the expansion and contraction movements that occur in the joint/crack vicinity of PCC pavements. Although this test procedure is essentially a fatigue-type test, it currently represents the best method to truly simulate horizontal joint movements of PCC pavements in the laboratory. FIGURE 15 shows a picture of the Overlay Tester used in this study.

As specified in TxDOT test procedure Tex-248-F, the OT tests were conducted at 25°C (77°F) with two maximum displacements of (displacement controlled) of 0.025 and 0.01 inches. Each test cycle lasted 10 seconds (5 seconds loading and 5 seconds unloading). Specimen failure was defined as 93 percent reduction in initial load.

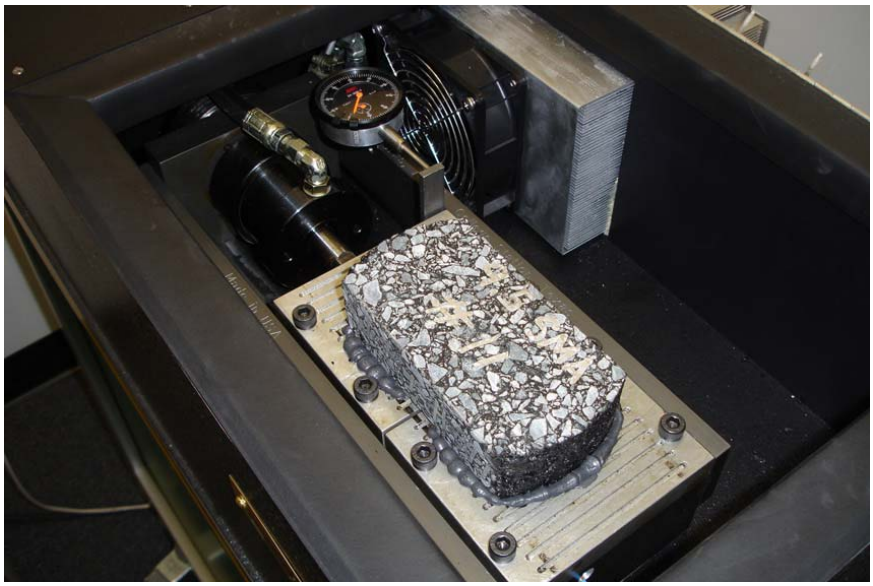

FIGURE 15 Overlay Tester.

3. LABORATORY TEST RESULTS AND ANALYSIS

This section details the results of the laboratory testing conducted for this project. First, the volumetric properties of each mix design are presented, followed by the results of the mechanistic and performance testing on both the control and Thiopave modified mixes. These test results show how the Thiopave mixes performed relative to the control mixes in terms of moisture susceptibility, fatigue resistance, rutting and deformation resistance, resistance to low temperature cracking, and overall mixture stiffness.

3.1 Volumetric Properties

Mix designs were conducted without Thiopave and two percentages—30 and 40 percent—of Thiopave for replacing a part of the asphalt binder. Details regarding the methodology and materials used for this mix design process were presented in Section 2.1.

A summary of the volumetric properties for the ten mixes listed in TABLE 1 is shown in TABLE 5. The volumetric properties for the Thiopave modified mixes were calculated using the modified mix design spreadsheet provided by Shell to account for the higher specific gravity of sulfur. According to AASHTO M 323, the minimum VMA (Voids in Mineral Aggregate) requirement for a 19 mm NMAS mix is 13 percent. However, the specification states that mixes with VMA higher than 2 percent above the minimum value may be prone to flushing and rutting. It can be seen from TABLE 5 that the only mixture with a higher-than-recommended VMA is the control mixture using PG 67-22. The VFA (Voids Filled with Asphalt) requirement in AASHTO M 323 for a 19 mm NMAS mix with a design traffic level of higher than 10 million ESAL is between 65 and 75 percent. The only mixes that strictly adhere to this requirement are the control mixes (without Thiopave) and the 30 percent Thiopave base layer mix (design air voids = 3.5 percent) using PG 67-22. The other Thiopave base layer mixes have a VFA that is less than 1 percent above the specified upper limit. The high VFA of the rich bottom mixes (design air voids = 2 percent) was expected due to the low design air void levels. All the ten mix designs fell within the AASHTO M 323 required range for dust proportion (0.6-1.2).

TABLE 5 Summary of Volumetric Properties

Mix ID	Base Binder	%Thio. by Binder Weight	Design Air (%)	%(Thio. + Bitumen)	Equiv. Binder (%)	%VMA (>13%)	%VFA (65-75%)	Dust Proportion (0.6-1.2)
Control_67	PG 67-22	0	4.0	N/A	5.3	15.3	74.2	0.82
Control_76	PG 76-22	0	4.0	N/A	4.7	13.9	71.5	0.90
Thio_67_30_2	PG 67-22	30	2.0	6.3	5.5	13.9	86.0	0.69
Thio_67_30_3.5	PG 67-22	30	3.5	5.5	4.8	14.0	74.5	0.80
Thio_67_40_2	PG 67-22	40	2.0	6.9	5.7	14.5	86.5	0.62
Thio_67_40_3.5	PG 67-22	40	3.5	6.2	5.1	14.5	75.9	0.71
Thio_58_30_2	PG 58-28	30	2.0	6.2	5.4	14.2	85.9	0.67
Thio_58_30_3.5	PG 58-28	30	3.5	5.6	4.9	14.4	75.6	0.75
Thio_58_40_2	PG 58-28	40	2.0	6.6	5.4	14.3	86.0	0.64
Thio_58_40_3.5	PG 58-28	40	3.5	5.9	4.9	14.3	75.5	0.72

3.2 Mechanistic and Performance Testing Results

3.2.1 Moisture Susceptibility

Moisture susceptibility testing was performed on six mix designs, including two control mixes, two 30 percent Thiopave mixes with 3.5 percent design air voids, and two 40 percent Thiopave mixes with 3.5 percent design air voids. Testing was conducted in accordance with both ALDOT 361-88 and AASHTO T 283-07 (both are described in detail in Section 2.2.1) after the specimens were allowed to cure for 14 days at room temperature. A detailed summary of the TSR test results for the ALDOT method with 14 days of curing is presented in TABLE A.1 of Appendix A. A detailed summary of the TSR test results for the AASHTO method with 14 days of curing is presented in TABLE A.2 of Appendix A. Both the saturation and air void requirements specified in ALDOT 361 and AASHTO T 283 were met for each specimen tested.

TABLE 6 shows a summary of the TSR results for the six mixes using the ALDOT method after the specimens were allowed to cure for 14 days. TABLE 7 lists a summary of the TSR testing results for these mixes using the AASHTO method. FIGURE 16 compares the TSR results determined using both the AASHTO and ALDOT TSR methods. As shown in FIGURE 16, the Thiopave modified mixes had lower TSR values than the control mixtures tested by both the ALDOT and AASHTO methods. In this study, the TSR values for the Thiopave mixtures were lower than the commonly accepted failure threshold of 0.8.

TABLE 6 Summary of TSR Testing for Base Layer Mixes (ALDOT Method – More than 14 Days of Curing)

Mix ID	Treatment	Sample Air Voids (%)	Saturation (%)	Splitting Tensile Strength (psi)	TSR
Control_67	Conditioned	6.7	64.6	132.0	0.99
	Unconditioned	6.9	N/A	133.0	
Control_76	Conditioned	6.6	63.4	127.0	0.90
	Unconditioned	6.7	N/A	141.7	
Thio_67_30_3.5	Conditioned	7.1	56.5	73.0	0.60
	Unconditioned	7.1	N/A	122.1	
Thio_67_40_3.5	Conditioned	7.6	59.7	74.8	0.67
	Unconditioned	7.0	N/A	111.6	
Thio_58_30_3.5	Conditioned	7.2	73.1	51.0	0.68
	Unconditioned	7.3	N/A	75.5	
Thio_58_40_3.5	Conditioned	7.0	74.6	52.4	0.57
	Unconditioned	7.2	N/A	91.3	

TABLE 7 Summary of TSR Testing for Base Layer Mixes (AASHTO Method – More than 14 Days of Curing)

Mix ID	Treatment	Sample Air Voids (%)	Saturation (%)	Splitting Tensile Strength (psi)	TSR
Control_67	Conditioned	6.6	73.1	115.0	0.87
	Unconditioned	6.8	N/A	133.0	
Control_76	Conditioned	6.9	73.0	147.2	1.04
	Unconditioned	6.7	N/A	141.7	
Thio_67_30_3.5	Conditioned	7.0	71.4	86.5	0.71
	Unconditioned	7.1	N/A	122.1	
Thio_67_40_3.5	Conditioned	7.1	74.5	81.6	0.73
	Unconditioned	7.0	N/A	111.6	
Thio_58_30_3.5	Conditioned	7.1	71.5	52.6	0.70
	Unconditioned	7.3	N/A	75.5	
Thio_58_40_3.5	Conditioned	7.2	75.3	57.2	0.63
	Unconditioned	7.2	N/A	91.3	

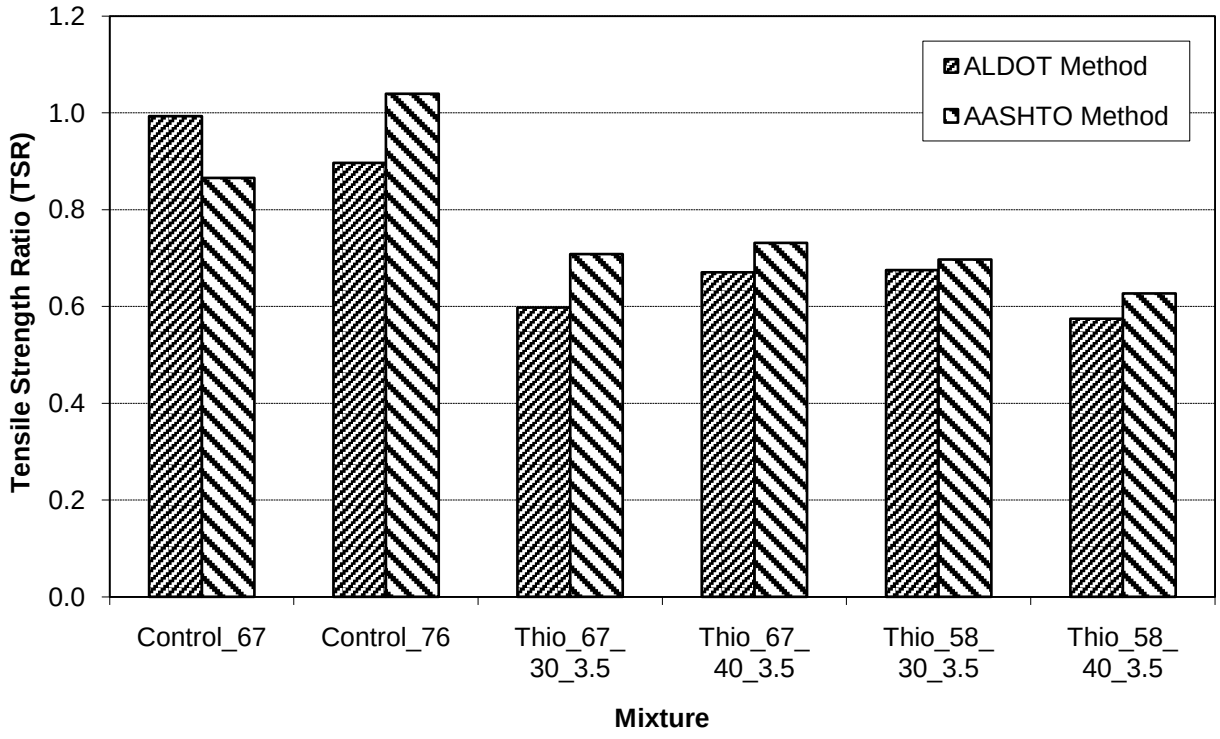

FIGURE 16 Summary of TSR Results (after 14 Days of Curing).

3.2.2 Dynamic Modulus Testing Results

The first phase of the dynamic modulus investigation involved testing specimens after both 1 day and 14 days of curing. This was done to assess the time-dependent stiffness properties of the Thiopave mixtures. A description of the test procedure was outlined in Section 2.2.2. A detailed summary of the E* results is included in Appendix B.

FIGURE 17 and FIGURE 18 show the average dynamic moduli for each of the ten mix designs tested at 10 Hz and 0.1 Hz, respectively, and at 21°C after both 1 day and 14 days of curing. These figures also show the percent increase in stiffness of each mix due to curing after 1 and 14 days.

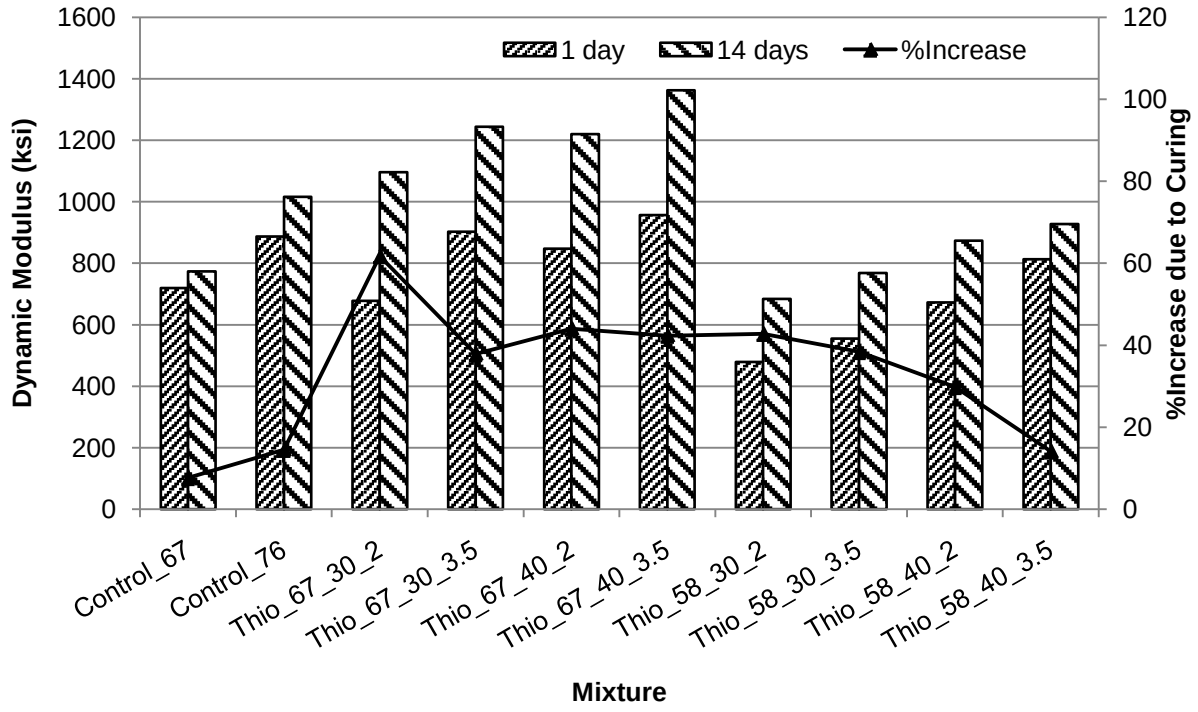

FIGURE 17 Average E* Results at 10 Hz & 21°C for All Mixtures After 1 and 14 Days.

When a PG 67-22 was used as the base binder in four Thiopave mixes, the average 1-day E* results of these Thiopave mixes were comparable or greater than the respective average 1-day E* values for the PG 67-22 control mix. In addition, except for the 30 percent Thiopave mix with 2 percent design air voids, the other Thiopave mixes yielded average 1-day E* results comparable to those of the PG 76-22 control mix. The average 14-day E* results of the Thiopave mixes were comparable or greater than the respective average 14-day E* values for both the control mixes.

As shown in FIGURE 17 and FIGURE 18, when a PG 58-28 was used as the base binder for four Thiopave mixes, the two 30 percent Thiopave mixes appeared to yield slightly lower average 1-day E* results than the PG 67-22 control mix. The 40 percent Thiopave mixes at 2 and 3.5 percent design air voids had average 1-day E* results comparable to those of the PG 67-22 and PG 76-22 control mixes, respectively. After 14 days of curing at the room temperature, the two

30 percent Thiopave mixes and the 40 percent Thiopave mix with 2 percent design air voids showed comparable or greater average E* results than the PG 67-22 control mix. In addition, the 40 percent Thiopave mix with 3.5 percent design air voids showed average E* results comparable to those of the PG 76-22 control mix.

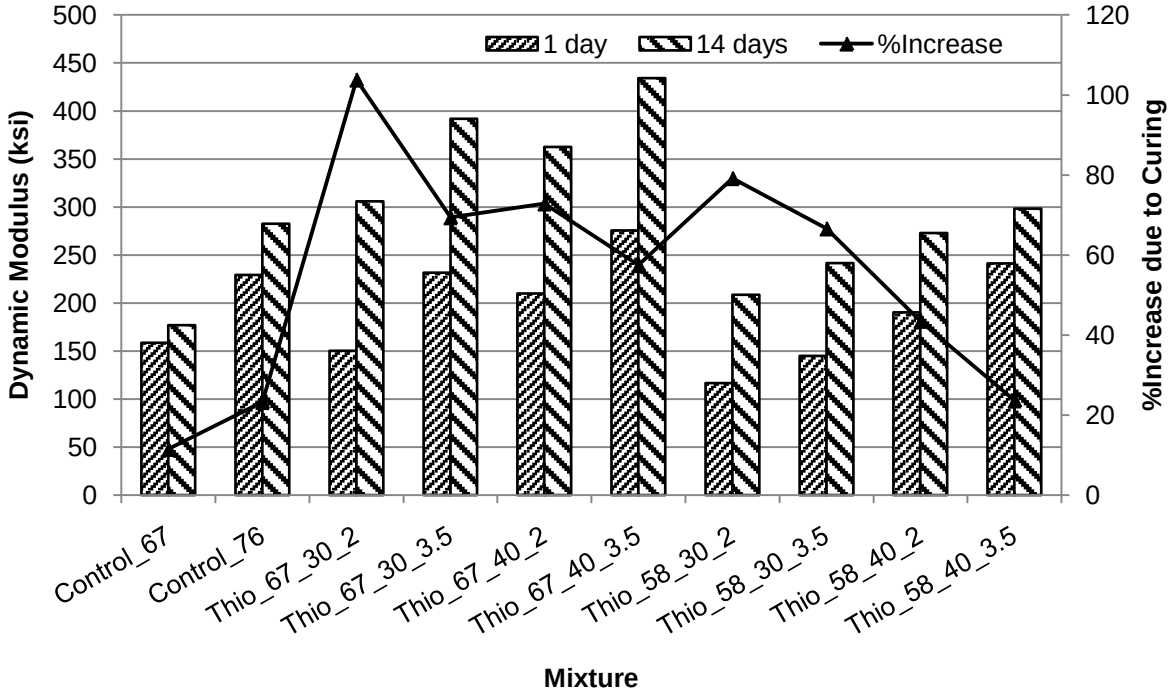

FIGURE 18 Average E* Results at 0.1 Hz & 21°C for All Mixtures After 1 and 14 Days.

The percent increase in stiffness due to curing was the most significant for the two 30 percent Thiopave mixes with 2 percent design air voids. The percent increase in stiffness was lower for the Thiopave mixes with higher design air voids and/or higher sulfur contents, as shown in FIGURE 17 and FIGURE 18. The two control mixes exhibited the least increase in stiffness due to curing at the room temperature.

The second phase of the dynamic modulus investigation involved laboratory E* testing at three temperatures and six frequencies to develop a master curve for each of the ten mix designs. Detailed E* test results are presented in Appendix B. The procedure for developing the master curves was explained in detail in Section 2.2.2.

FIGURE 19 and FIGURE 20 compare the master curves of the Thiopave mixes using PG 67-22 and PG 58-28, respectively, with those of the two control mixes. As shown in FIGURE 19, there was a distinct separation between the curve of the PG 67-22 control mix and those of the Thiopave mixtures across the range of testing temperatures and frequencies. In addition, the Thiopave mixes appeared stiffer than the PG 76-22 control mix at the lower reduced frequencies (which are corresponding to the high temperature and low frequency testing condition in the laboratory) but yielded comparable stiffness at the higher reduced frequencies (lower testing temperatures).

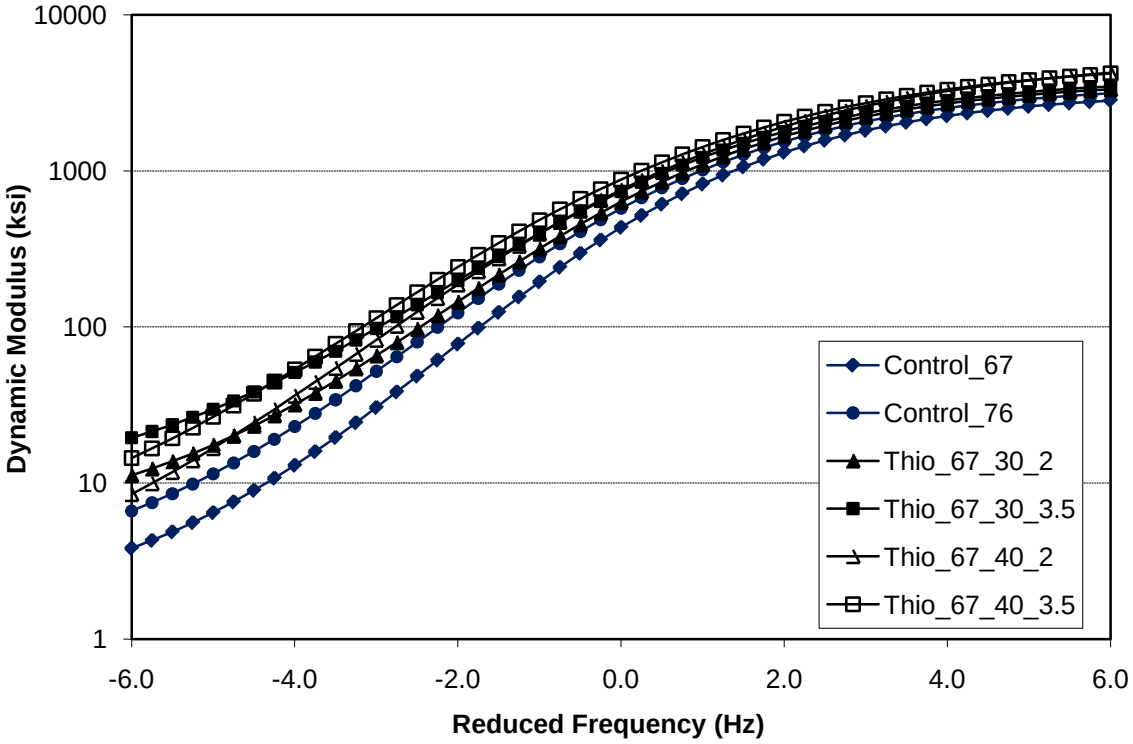

FIGURE 19 E* Master Curves for PG 67-22 Thiopave Mixes and Two Control Mixtures.

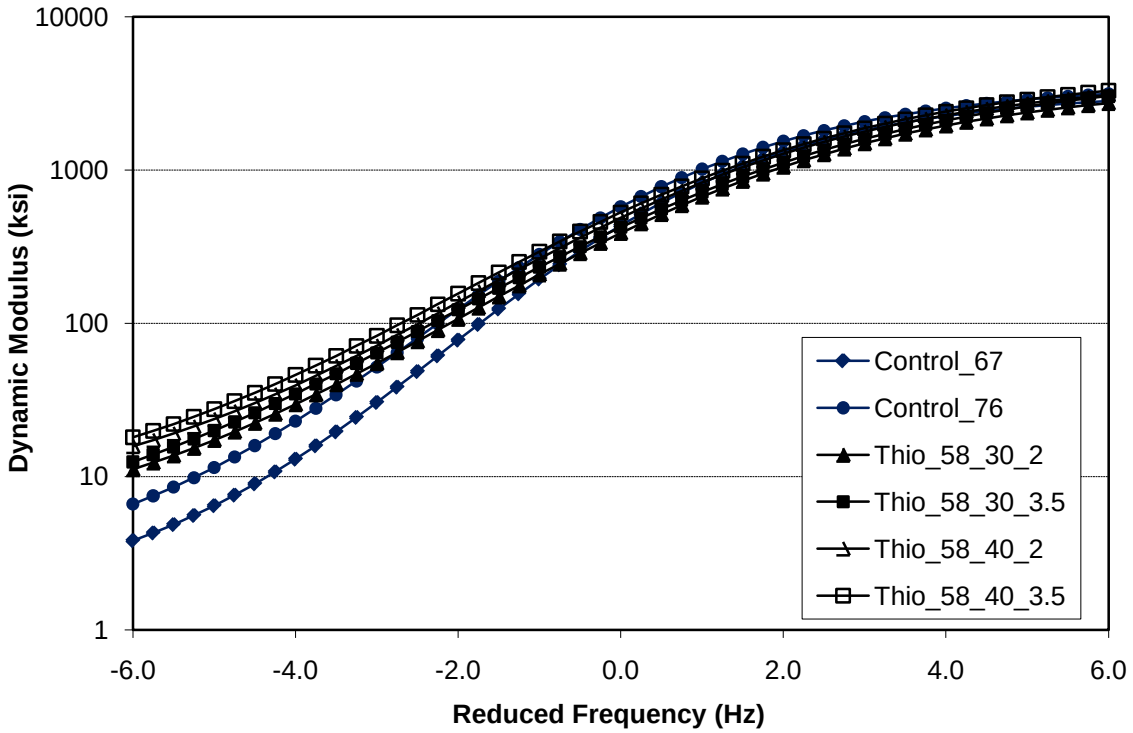

FIGURE 20 E* Master Curves for PG 58-28 Thiopave Mixes and Two Control Mixtures.

Even with the softer PG 58-28 binder, the Thiopave mixes still appeared stiffer than the two control mixes at the higher temperatures (lower frequencies), but they were comparable at the lower temperatures, as shown in FIGURE 20.

As shown in FIGURE 19 and FIGURE 20, within each group of the Thiopave mixes using the same base binder, the 40 percent Thiopave mix with 3.5 percent design air voids appeared to be stiffer than the 40 percent Thiopave mix with 2 percent design air voids and the 30 percent Thiopave mix with 3.5 percent design air voids, followed by the 30 percent Thiopave mix with 2 percent design air voids. This behavior was anticipated because the rich bottom mixes (with 2 percent design air voids) were designed with more asphalt for improving fatigue cracking resistance.

3.2.3 Flow Number Testing Results

Flow number testing was performed on the specimens that had been used for 14-day dynamic modulus testing discussed in Section 3.2.2. Flow number testing was performed in accordance with the procedure outlined in Section 2.2.3, and the flow number for each of these specimens were determined using two different model forms—the Power and Francken models. FIGURE 21 compares the flow number test results for the ten mixes evaluated in this study. Detailed results of the flow number testing, including the permanent strain values at the flow point, are presented in Appendix C.

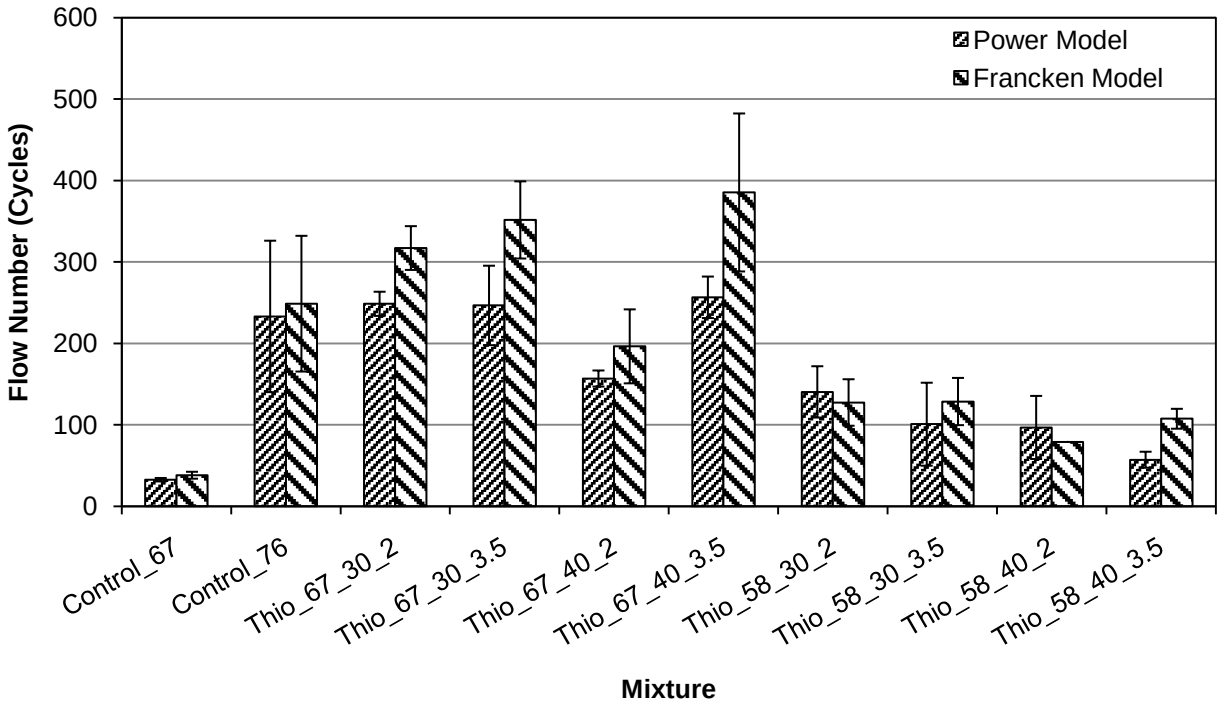

FIGURE 21 Average Flow Numbers and Standard Deviations Determined using Power and Francken Models.

From these results, it appeared that all the Thiopave mixes had higher resistance to rutting than the PG 67-22 control mix, given these specimens took greater numbers of cycles to fail. The PG 76-22 control mix showed better rutting resistance than the Thiopave mixtures using the PG 58-28 binder but did not exhibit statistically different rutting resistance to the Thiopave mixtures using the PG 67-22 binder in an ANOVA with a 5 percent significance level ($\alpha = 0.05$). This finding showed that use of 30 to 40 percent Thiopave in an asphalt mixture may increase the high critical temperature (resistance to rutting) of its binder by approximately 9^{o}C (1.5 PG grade).

Among the Thiopave mixtures using the PG 67-22 binder, the 40 percent Thiopave mix with 3.5 percent design air voids had the highest resistance to rutting, then the 30 percent Thiopave mixes, and followed by the 40 percent Thiopave mix with 2 percent design air voids. For the Thiopave mixtures using the PG 58-28 binder, the 40 percent Thiopave mix with 2 percent design air voids had the lowest resistance to rutting, and the other three mixes showed comparable flow number results determined using the Francken model. There was seemingly no relationship between the relative deformation susceptibility of the mixes and the Thiopave percentage or the combined Thiopave and asphalt content.

3.2.4 Asphalt Pavement Analyzer Testing Results

Asphalt Pavement Analyzer (APA) testing was performed on each of the ten mix designs used for this project in accordance with AASHTO TP 63. More details regarding the test procedure can be found in Section 2.2.4. For each mix, a total of six specimens were tested. It should be noted that for the control mix, the automated rut depth measurement system and one of the hoses failed during the testing, resulting in only four manually-measured data points being available. A summary of test results is included in Appendix D.

FIGURE 22 summarizes the average values and variability (plus and minus one standard deviation) of the manually- and automatically-measured rut depths for the ten mixtures. It can be seen that the PG 67-22 control mix had higher manually-measured APA rut depths than the Thiopave mixes. In addition, the PG 76-22 control mix exhibited lower manually-measured APA rut depths than the four Thiopave mixtures using the PG 67-22 binder and the two 30 percent Thiopave mixtures using the PG 58-28 binder. However, the PG 76-22 control mix did not show statistically different APA rut depths from those of the two 40 percent Thiopave mixtures using the PG 58-28 binder in an ANOVA with $\alpha = 0.05$.

While the APA appeared to separate the rutting performance of the PG 67-22 control mix, Thiopave mixtures, and PG 76-22 control mix, it did not seem to differentiate the rutting susceptibility of the Thiopave mixtures using different base binders (PG 67-22 and PG 58-28) as the flow number test shown in the previous section.

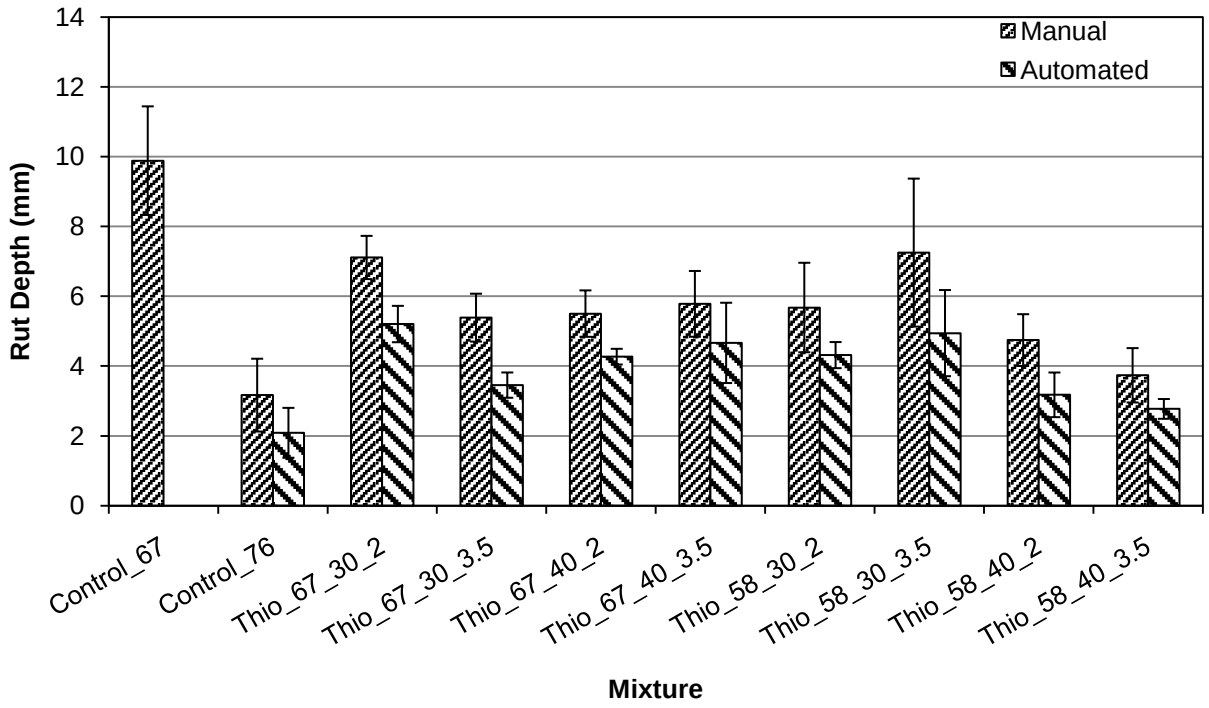

FIGURE 22 APA Manually and Automatically Measured Rut Depths.

3.2.5 Hamburg Wheel Tracking Results

Rutting and moisture susceptibility testing was also performed using the Hamburg Wheel Tracking device. This testing was performed in accordance with AASHTO T 324 and more detail regarding the testing procedure and analysis of results is discussed in Section 2.2.5.

FIGURE 23 summarizes the results of the Hamburg Wheel Tracking testing. This plot summarizes the average values and variability (plus and minus one standard deviation) of the steady-state rutting rate and stripping inflection points for the ten mix designs tested. Definitions of these quantities are given in Section 2.2.5. A complete database of all Hamburg data analysis results can be found in Appendix E.

FIGURE 23 shows that the PG 67-22 control mix and the 30 percent Thiopave mixes using the PG 58-28 binder had much higher average rutting rates than the other mixtures evaluated in this testing. Based on an ANOVA with $\alpha = 0.05$, there was no statistical difference between the rutting rates for the PG 67-22 control mix and the 30 percent Thiopave mixes using the PG 58-28 binder. In addition, the rutting rates for all the Thiopave mixes, except the 30 percent Thiopave mixes using the PG 58-28 binder, were comparable or lower than that of the PG 76-22 control mix.

It appeared that the Thiopave mixes with 3.5 percent design air voids had similar or lower average rutting rates than those of the respective Thiopave mixes with 2 percent design air voids, which had higher design binder contents. These rutting data seemed to compare well with the

flow number testing results from the AMPT, given the dramatic difference in deformation resistance between the Thiopave mixtures and the control mixtures.

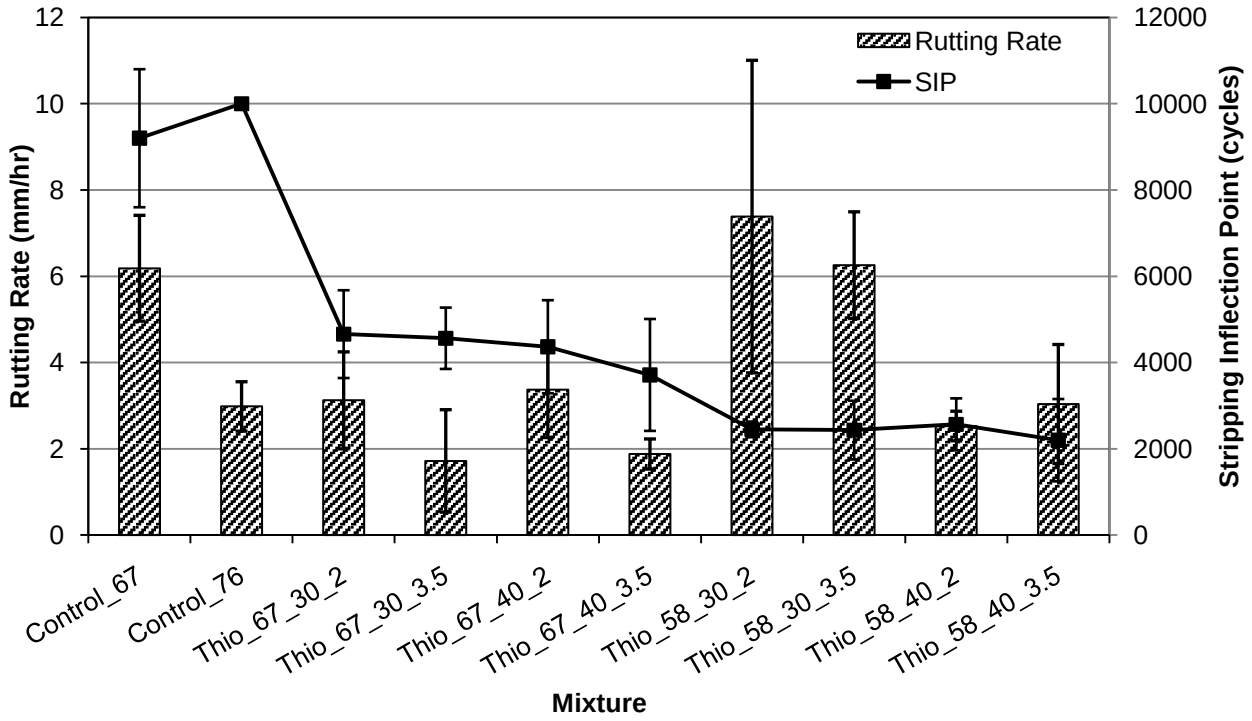

FIGURE 23 Hamburg Wheel-Tracking Data Analysis Summary

The data from the Hamburg testing is also useful in that it gives a measure of the moisture sensitivity of the different mixtures. For the purposes of reporting a numerical average, a specimen that did not show any evidence of stripping during testing was assigned a stripping inflection point of 10,000 cycles (the maximum number of cycles allowed by the test). The average and variability of the stripping inflection points for the ten mix designs are also shown in FIGURE 23. Based on an ANOVA with $\alpha = 0.05$, there was a significant difference between the average stripping inflection points of the control mixtures versus those of the Thiopave mixtures. The average stripping inflection points of the Thiopave mixtures using the PG 67-22 binder was higher than those of the Thiopave mixes using the PG 58-28 binder. However, based on the ANOVA, there was no significant difference in the stripping behavior of the four Thiopave mixtures using the same base binder (PG 67-22 or PG 58-28).

FIGURE 24 shows photographs of five sets of tested Hamburg specimens made from the PG 67-22 control mix (1A and 1B) and the Thiopave mixes using the PG 67-22 binder. Based on visual inspection, the mixture appeared more brittle as the amount of Thiopave in the mixture was increased. This can be seen in the additional fracturing of the specimen surrounding the rutting path in the Thiopave mixes while little additional fracturing can be seen in the control mixture. Given the results of the TSR testing (higher TSR values for the control mixtures), the results of this testing served to validate the fact that the Thiopave mixtures were more susceptible to

moisture induced damage than the control mixtures for the liquid anti-strip used in this evaluation.

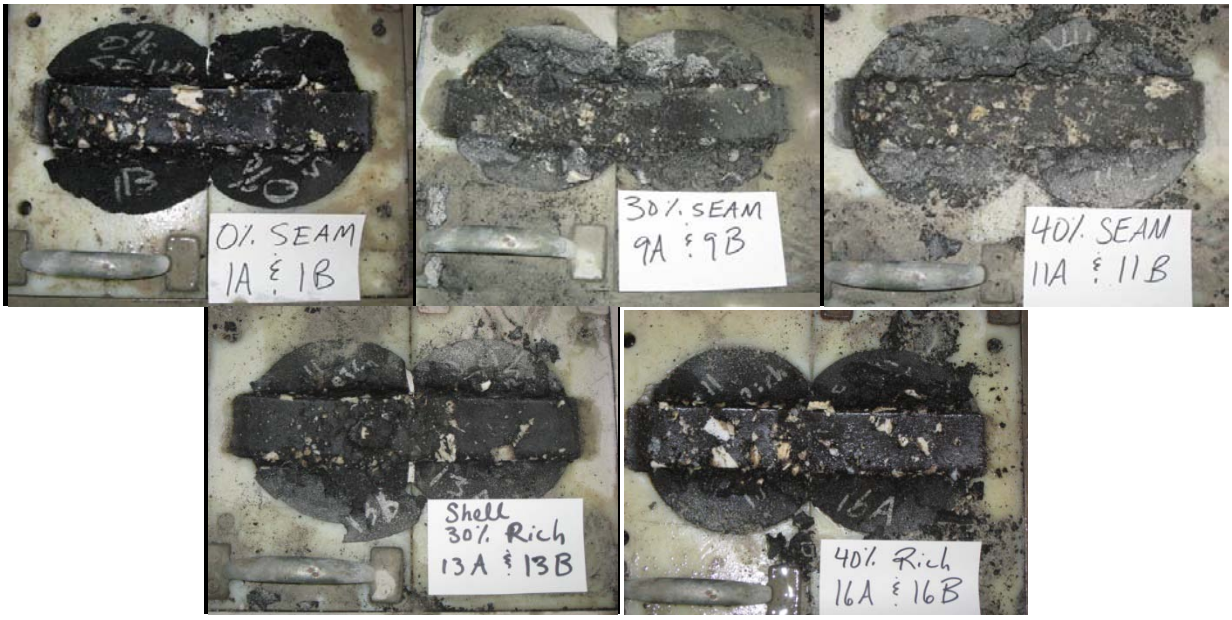

FIGURE 24 Tested Hamburg Wheel Tracking Specimens.

3.2.6 Bending Beam Fatigue Testing Results

The fatigue life of each of the ten mixes was quantified using the bending beam fatigue testing apparatus. The mixes were tested in accordance with ASTM D7460 at three different strain levels with two replicates per strain level. Full details regarding the bending beam testing methodology can be found in Section 2.2.6.

A detailed summary of the bending beam fatigue test results is presented in Appendix F. Despite adherence to the specification and tight control of specimen air voids, dimensions, and beam orientation, significant variability could still be seen in the duplicate results (the numbers of cycles to failure) for a given mixture at a given strain level. This variability was especially evident for testing performed at the lowest strain level (200 microstrain).

According to ASTM D7460, failure of the beam specimen is defined as the maximum point on a plot of Normalized Modulus × Cycles versus number of cycles (see Section 2.2.6). As discussed in Section 2.2.6, the test was terminated when the beam stiffness was reduced to 30 percent of the initial stiffness. This allowed the determination of the number of cycles to failure according to ASTM D 7460 and at 50 percent of the initial stiffness according to AASHTO T 321, and both sets of the results are presented in Appendix F. It should be noted that the beams for the PG 76-22 control mix and the 30 percent Thiopave mix with PG 58-28 and 3.5 percent design air voids were not failed after 12,000,000 cycles tested at 200 microstrain. The numbers of cycles to failure for these beams at 50 percent of the initial stiffness according to AASHTO T 321 were extrapolated using the three-stage Weibull procedure proposed under NCHRP Project 9-38 (*8*).

However, there is no procedure for extrapolating the numbers of cycles to failure for the beams determined based on the ASTM D7460 failure criterion.

FIGURE 25 and FIGURE 26 compare the fatigue cracking resistance of four Thiopave mixtures using the PG 67-22 binder to that of the two control mixes determined in accordance with ASTM D7460 and AASHTO T 321, respectively. A power model was used to fit the results for each of the six mixtures. The two figures show similar relative fatigue resistance relationships between the mixtures. There appeared to be three groups of fatigue curves:

- The first group included the fatigue curve for the PG 76-22 control mix that had the highest fatigue resistance.
- The second group included the fatigue curves for the PG 67-22 control mix and the 30 percent Thiopave mix with the PG 67-22 binder and 2 percent design air voids. The control mix had higher fatigue resistance than the Thiopave mix at higher strain levels (800 and 400 microstrain), but the two mixtures had similar fatigue resistance at the low strain level (200 microstrain).
- The last group included the fatigue curves for the other three Thiopave mixtures using the PG 67-22 binder. These mixtures exhibited similar fatigue resistance at the three strain levels tested in this study.

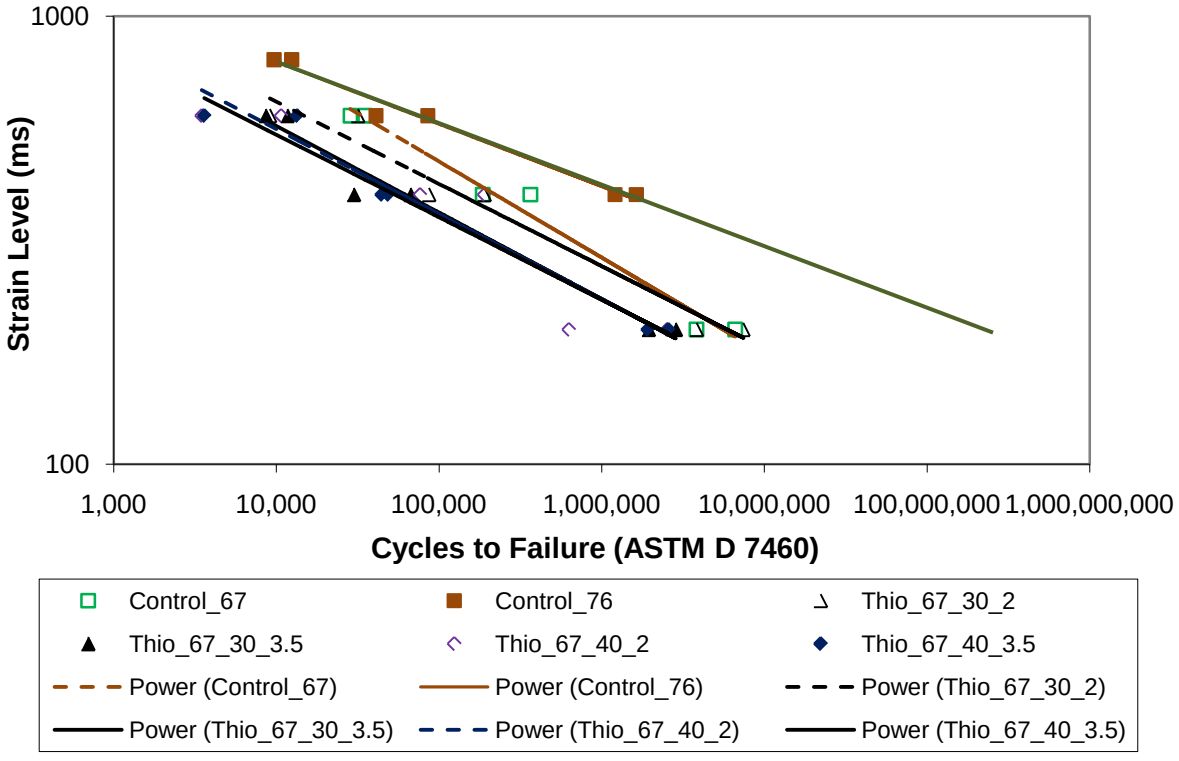

FIGURE 25 Fatigue Resistance (ASTM D7460) of Thiopave Mixtures Using PG 67-22.

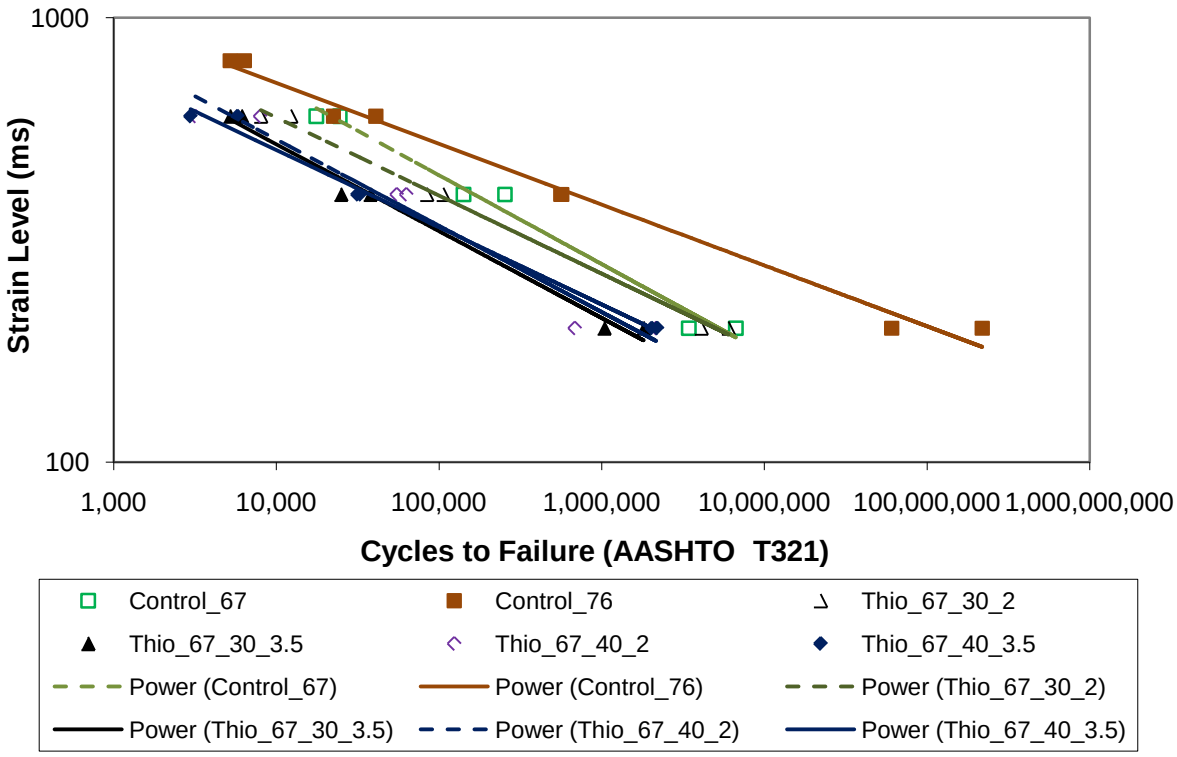

FIGURE 26 Fatigue Resistance (AASHTO T 321) of Thiopave Mixtures Using PG 67-22.

The fatigue cracking resistance determined according to ASTM D7460 and ASTM T 321 for four Thiopave mixtures using PG 58-28 was compared to that of the two control mixes in FIGURE 27 and FIGURE 28, respectively. The relative fatigue resistance relationships were similar between the mixtures in the two figures, except for the 30 percent Thiopave mix with the PG 58-28 binder and 3.5 percent design air voids. In FIGURE 28, the fatigue curve for this mix was plotted based on four sets of test results, including three sets determined at 800, 600 and 400 microstrain; and one set extrapolated based on testing results at 200 microstrain. However, the fatigue curve for this mixture shown in FIGURE 27 was plotted based on only three sets of test results determined at 800, 600 and 400 microstrain because there is no procedure for extrapolating the numbers of cycles to failure determined based on the ASTM D7460 failure criterion, as previously mentioned.

By examining FIGURE 28, there appeared to be four groups of fatigue curves:

- The first group included the fatigue curve for the PG 76-22 control mix. The beams made from this mix did not fail after 12,000,000 cycles tested at 200 microstrain. The PG 76-22 control mix had the highest fatigue resistance.
- The second group included the 30 percent Thiopave mix with the PG 58-28 binder and 3.5 percent design air voids. The beams made from this mix did not fail after 12,000,000 cycles tested at 200 microstrain. The test results determined at 800, 600 and 400 microstrain for the 30 percent Thiopave mix with PG 58-28 and 3.5 percent design air voids suggested the fatigue of this mix would be in the third group as shown in FIGURE

27, but this mix had much higher fatigue resistance at 200 microstrain, which changed the overall trend of the fatigue curve.

- The third group included the fatigue curves for the PG 67-22 control mix and the 30 percent Thiopave mix with the PG 58-28 binder and 2 percent design air voids. The two mixtures showed similar fatigue resistance at the three strain levels tested in this study.
- The last group included the fatigue curves for the two 40 percent Thiopave mixtures using the PG 58-28 binder. These mixtures exhibited similar fatigue resistance at the three strain levels tested in this study.

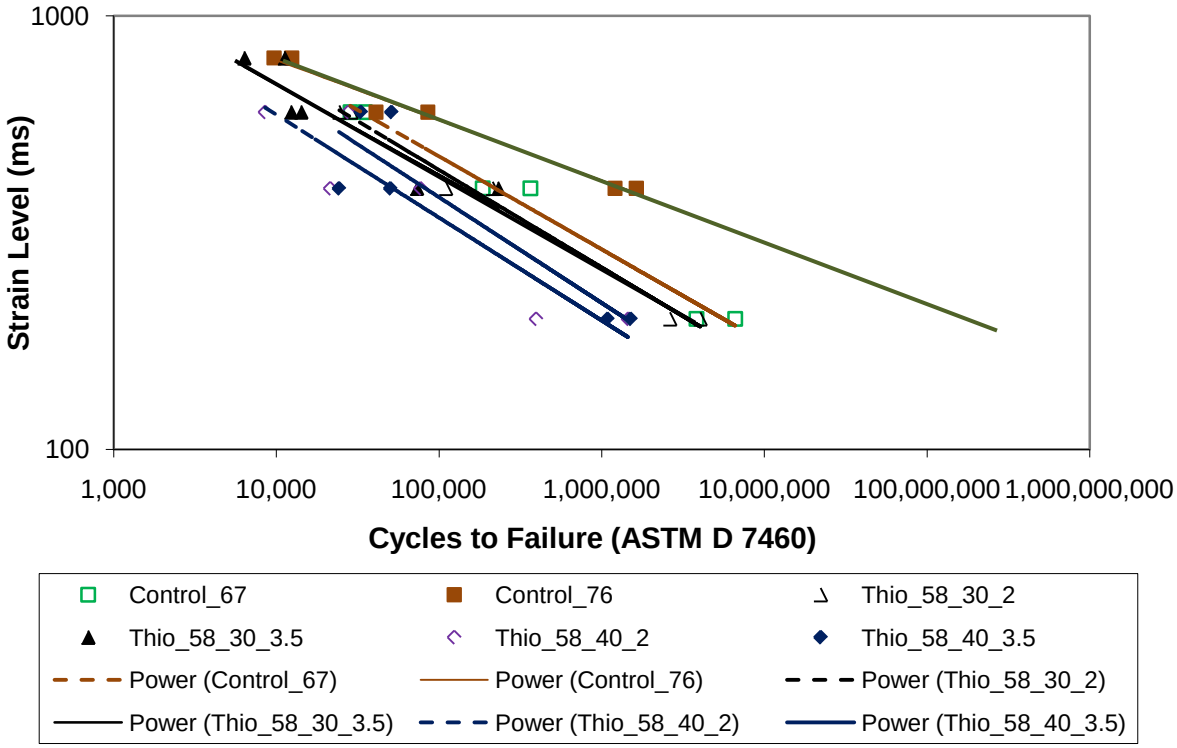

FIGURE 27 Fatigue Resistance (ASTM D7460) of Thiopave Mixtures Using PG 58-28.

TABLE 8 shows the 95 percent one-sided lower prediction of endurance limit for each of the ten mixes tested in this study based on the number of cycles to failure determined in accordance with ASTM D 7460 and AASHTO T 321. The procedure for estimating the endurance limit was developed under NCHRP 9-38 (see Section 2.2.6). Based on the results shown in TABLE 8, the PG 76-22 control mix had the highest predicted endurance limit among the mixtures tested in this study (according to the AASHTO failure criteria). The 30 percent Thiopave mix using the PG 67-22 binder and 2 percent design air voids and the 30 percent Thiopave mix using the PG 58-28 binder and 3.5 percent design air voids had the highest endurance limits among the Thiopave mixtures tested in this study according to the AASHTO failure criteria. Both the mixtures had the estimated endurance limits higher than that of the PG 67-22 control mix. The other Thiopave mixtures had similar or lower estimated endurance limits than the PG 67-22 control mix.

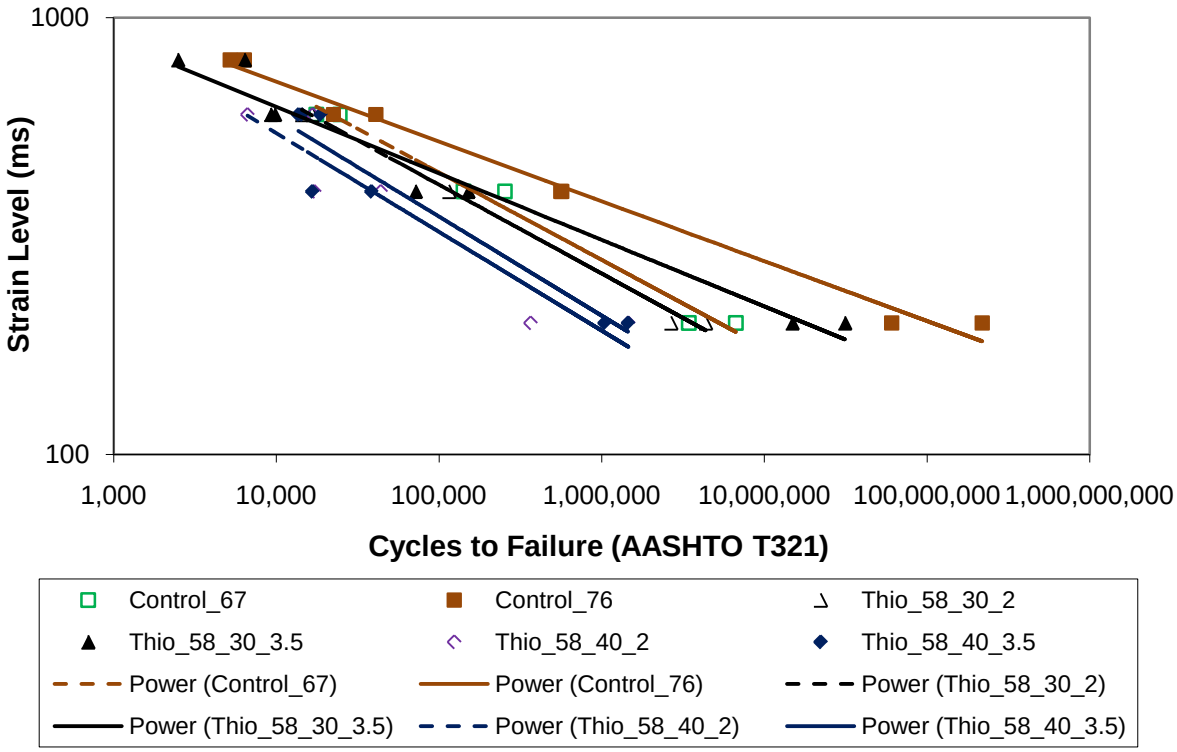

FIGURE 28 Fatigue Resistance (AASHTO T 321) of Thiopave Mixtures Using PG 58-28.

TABLE 8 Predicted Endurance Limits

Base Binder	Thiopave (%)	Design Air Voids (%)	Endurance Limit* (Microstrain)	
			ASTM D7460	AASHTO T 321
67 -22	0	4	99	102
76 -22	0	4	204	176
67 -22	30	2	98	119
67 -22	30	3.5	83	79
67 -22	40	2	60	69
67 -22	40	3.5	84	98
58 -28	30	2	88	102
58 -28	30	3.5	N/A	132
58 -28	40	2	35	39
58 -28	40	3.5	33	50

Note: * 95% one-sided lower prediction limit

3.2.7 Thermal Stress-Restrained Specimen Testing Results

The low temperature cracking resistance of each of the ten mix designs was quantified using thermal stress-restrained specimen testing (TSRST). The mixes were tested in accordance with

AASHTO TP 10 with three replicates per mix to determine the stress level and temperature at which low temperature cracking occurred. More details regarding the TSRST testing methodology can be found in Section 2.2.7. A detailed summary of TSRST testing results, including sample air voids, sample dimensions, fracture stress, and fracture temperature (temperature at which low temperature cracking occurred), is presented in Appendix G. In TSRST testing, a mixture that exhibits a lower fracture stress and lower fracture temperature is considered to have better resistance to low temperature cracking.

FIGURE 29 shows the average and standard deviation of the fracture stress for the ten mixtures that underwent TSRST testing. TABLE 9 shows ANOVA results of TSRST fracture stress data. At a 5 percent significance level ($\alpha = 0.05$), there was no statistical difference in the means of the fracture stress data (p-value = 0.157) determined for the ten mixtures tested in this study.

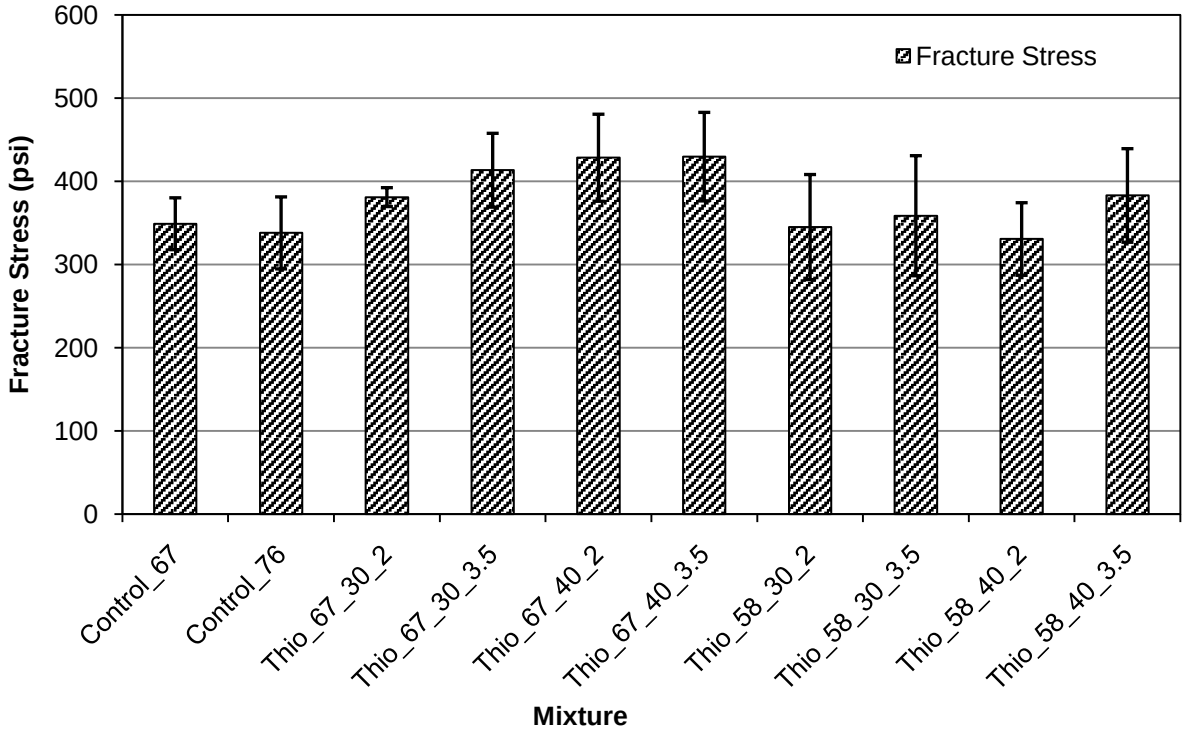

FIGURE 29 Fracture Stress Measured using TSRST.

TABLE 9 ANOVA Results for TSRST Fracture Stress

Source	df	Seq. SS	Adj. SS	Adj. MS	F	P-value
Mixture	9	37725	37725	4192	1.69	0.157
Error	20	49543	49543	2477		
Total	29	87269				

FIGURE 30 shows the average and standard deviation of the fracture temperature for the ten mixtures that underwent TSRST testing. As expected, the facture temperatures determined for the mixtures using the PG XX-22 and PG 58-28 binders were different. The average values of

fracture temperature for the six mix designs using the PG 67-22 and PG 76-22 binders fell between -19.3°C and -23.3°C. An ANOVA test (TABLE 10) indicated that there was no statistical difference in the means of the fracture temperature data for the mixtures using the PG 67-22 and PG 76-22 binders (p-value = 0.134). As shown in TABLE 11, there was also no statistical difference in the means of the fracture temperature data for the mixtures using the PG 58-28 binder (p-value = 0.737) at a 5 percent significance level. Therefore, it could be said that the addition of the Thiopave material had no tangible impact on the low temperature cracking susceptibility of the mixture.

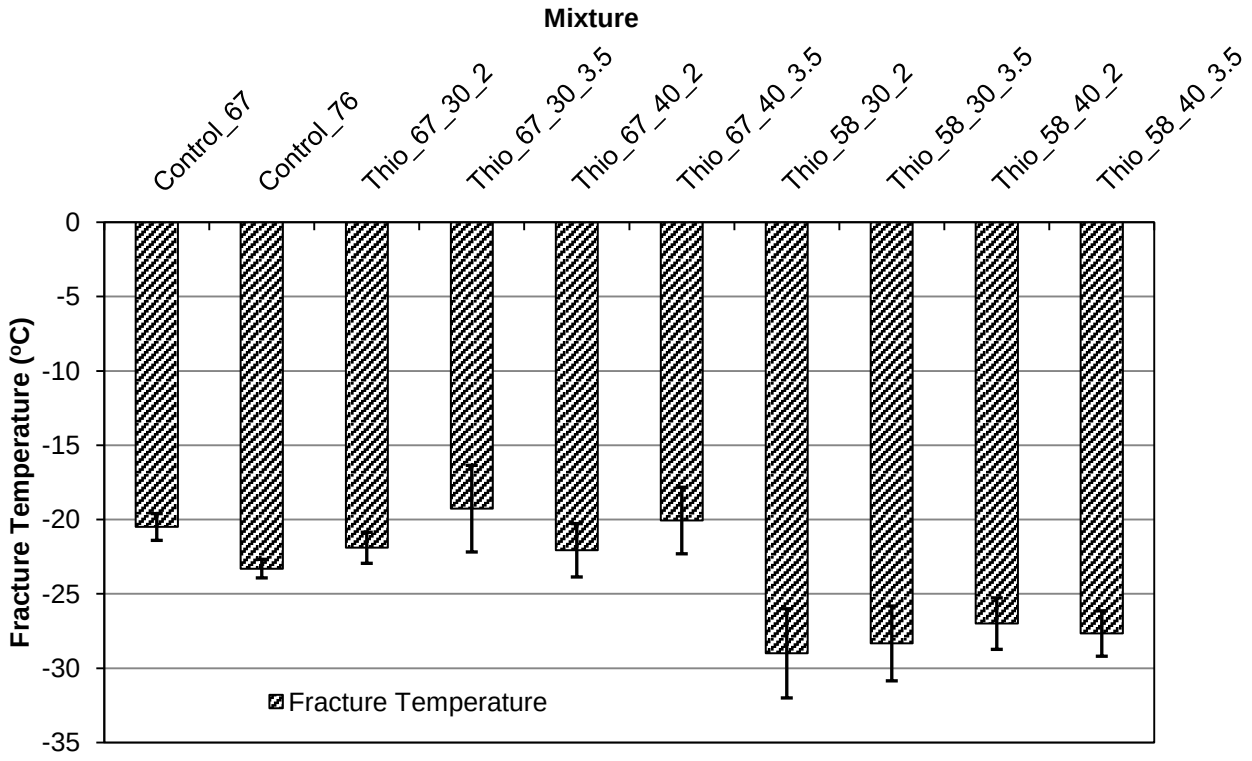

FIGURE 30 Fracture Temperature Measured using TSRST.

TABLE 10 ANOVA Results for Fracture Temperature of Six Mixtures Using PG XX-22

Source	df	Seq. SS	Adj. SS	Adj. MS	F	P-value
Mixture	5	33.485	33.485	6.697	2.11	0.134
Error	12	38.020	38.020	3.168		
Total	17	71.505				

TABLE 11 ANOVA Results for Fracture Temperature of Four Mixtures Using PG 58-28

Source	df	Seq. SS	Adj. SS	Adj. MS	F	P-value
Mixture	3	6.667	6.667	2.222	0.43	0.737
Error	8	41.333	41.333	5.167		
Total	11	48.000				

3.2.8 Semi-Circular Bending Test Results

Semi-circular bending testing was conducted for nine mix designs, including the PG 67-22 control mix and the eight Thiopave mixtures. The SCB tests were performed at -18 and -30°C with three replicates per mix design to determine the mixture fracture energy and fracture toughness at the maximum load recorded during testing. Both the parameters can be used to describe the fracture resistance of asphalt mixtures at low temperatures. The fracture energy describes the energy required to create a unit surface area of a crack while the fracture toughness measured at the maximum load is a stress intensity factor corresponding to the initiation of the crack. More details regarding the SCB testing methodology can be found in Section 2.2.8. A detailed summary of SCB test results, including test temperature, fracture toughness, and fracture energy, is presented in Appendix H.

FIGURE 31 and FIGURE 32 show the average and standard deviation of the fracture toughness and fracture energy, respectively, for the nine mixtures that underwent SCB testing. Based on the average values, it appeared that the 30 percent Thiopave mixtures using the PG 58-28 binder would have higher fracture energy.

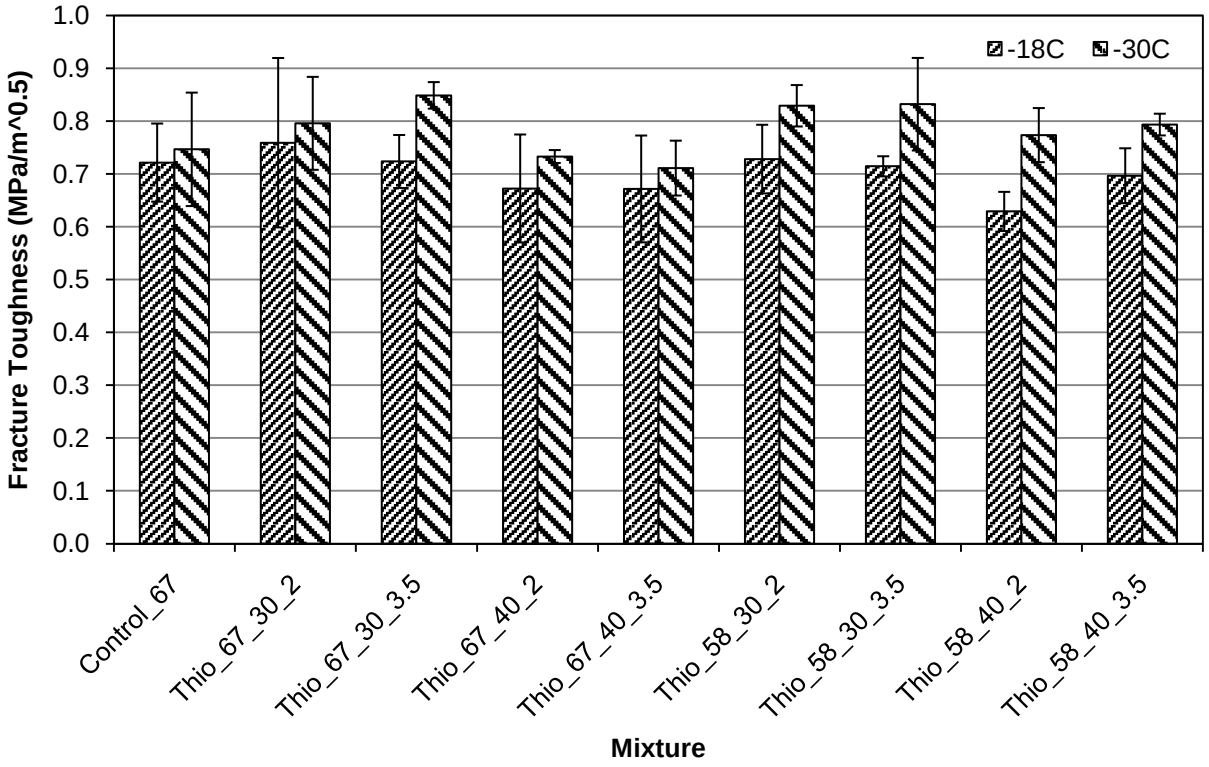

FIGURE 31 Fracture Toughness Measured using SCB.

However, based on the ANOVA results shown in TABLE 12 and TABLE 13, which took into account the variability of the SCB test, there was no statistical difference in the means of the fracture toughness data (p-value = 0.729 and 0.154) at a 5 percent significance level. There was also no statistical difference in the means of the fracture energy data measured at -18°C (TABLE

14). However, the difference in the means of the fracture energy data measured at -30°C (TABLE 15) was statistically significant. Further analysis using Tukey's test showed that only the means of the fracture energy data measured at -30°C for two mixtures, including the 40 percent Thiopave mix using the PG 67-22 binder at 2 percent design air voids and the 30 percent Thiopave mix using the PG 58-28 binder at 3.5 percent design air voids, were statistically different. Therefore, it could be said that with the one exception (30 percent Thiopave mix at 3.5 percent design air voids), the effect of using a softer base binder (PG 58-28) in the Thiopave mixtures was not statistically significant based on the fracture parameters determined in SCB testing.

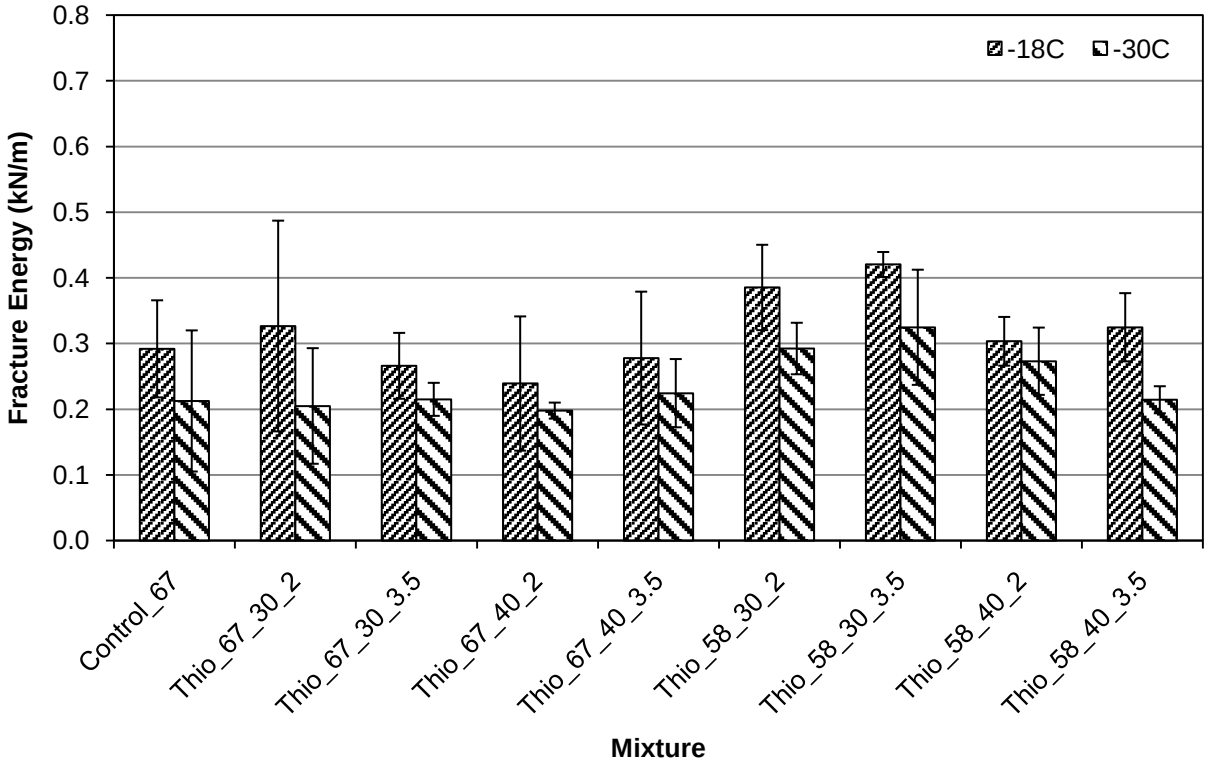

FIGURE 32 Fracture Energy Measured using SCB.

TABLE 12 ANOVA Results for Fracture Toughness Measured at -18°C

Source	df	Seq. SS	Adj. SS	Adj. MS	F	P-value
Mixture	8	0.036315	0.036315	0.004539	0.65	0.729
Error	18	0.126111	0.126111	0.007006		
Total	26	0.162426				

TABLE 13 ANOVA Results for Fracture Toughness Measured at -30°C

Source	df	Seq. SS	Adj. SS	Adj. MS	F	P-value
Mixture	8	0.054565	0.054565	0.006821	1.75	0.154
Error	18	0.070075	0.070075	0.003893		
Total	26	0.124640				

TABLE 14 ANOVA Results for Fracture Energy Measured at -18°C

Source	df	Seq. SS	Adj. SS	Adj. MS	F	P-value
Mixture	8	0.079420	0.079420	0.009927	2.09	0.092
Error	18	0.085377	0.085377	0.004743		
Total	26	0.164797				

TABLE 15 ANOVA Results for Fracture Energy Measured at -30°C

Source	df	Seq. SS	Adj. SS	Adj. MS	F	P-value
Mixture	8	0.048896	0.048896	0.006112	3.12	0.021
Error	18	0.035279	0.035279	0.001960		
Total	26	0.084176				

3.2.9 Bending Beam Rheometer Test Results

As previously described, BBR was used to determine the mixture resistance to low temperature cracking in this study. The BBR tests were conducted at -12 and 16°C to determine the creep stiffness (S) and creep rate (m-value) at 60 seconds for the nine mixtures that included the PG 67-22 control mix and the eight Thiopave mixtures.

FIGURE 33 and FIGURE 34 show the average creep stiffness of each mixture tested at 16 and -12°C, respectively. The variation of the average creep stiffness between the mixtures was similar at 16 and -12°C. As the creep stiffness increases, the thermal stresses developed in asphalt mixtures due to thermal shrinking also increase, and low temperature cracking becomes more likely. Therefore, it appeared that based on the stiffness measured at -12°C, the following five mixtures would have better resistance to low temperature cracking than the remaining four Thiopave mixtures: the PG 67-22 control mix, the 40 percent Thiopave mixture with the PG 67-22 binder and 2 percent design air voids, the two 30 percent Thiopave mixes using the PG 58-28 binder, and the 40 percent Thiopave mixture with the PG 58-28 binder and 2 percent design air voids.

FIGURE 35 shows the creep rate for each mixture measured at -12 and 16°C. As the m-value decreases, the slope of the asphalt binder stiffness curve flattens, and the ability of the mixture to relax thermal stress decreases. Thus, the PG 67-22 control mix and the Thiopave mixture with 2 percent design air voids appeared to have comparable or better low temperature cracking resistance than the Thiopave mixtures with 3.5 percent air voids, except for the 40 percent Thiopave mixture with the PG 58-28 binder.

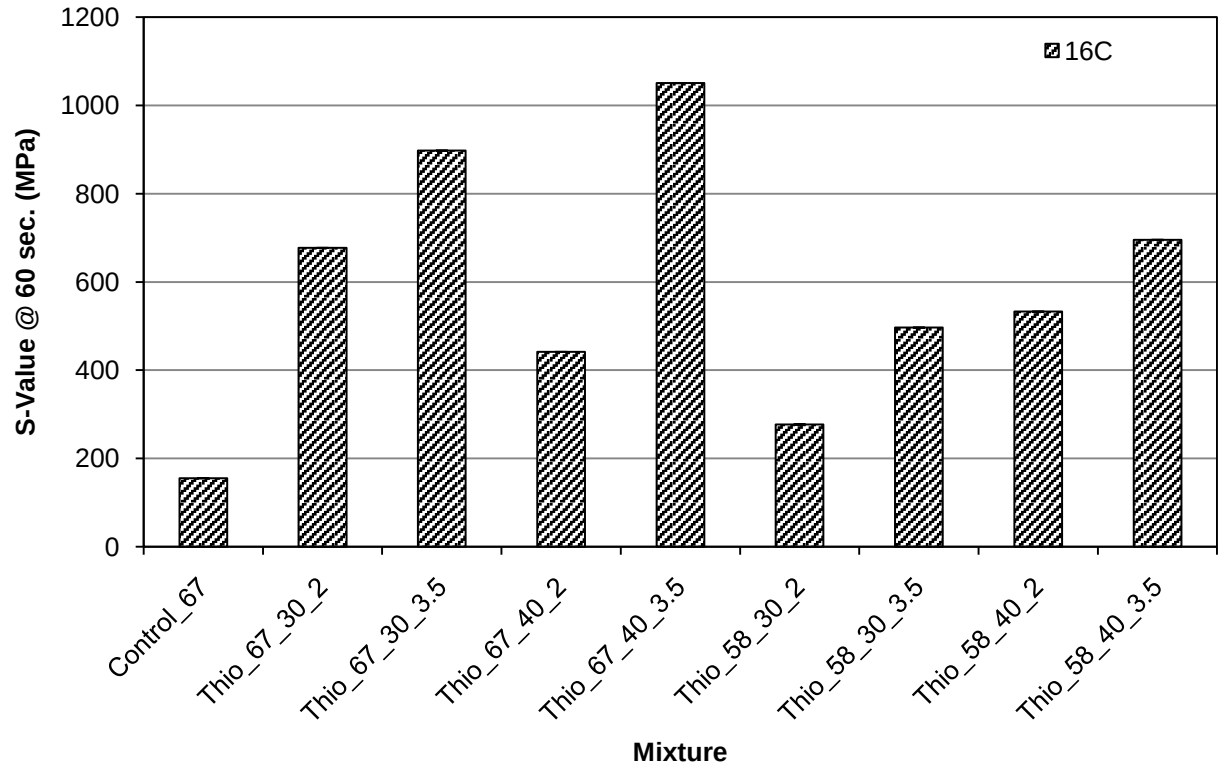

FIGURE 33 Creep Stiffness @ 60 Seconds Measured at 16°C using BBR.

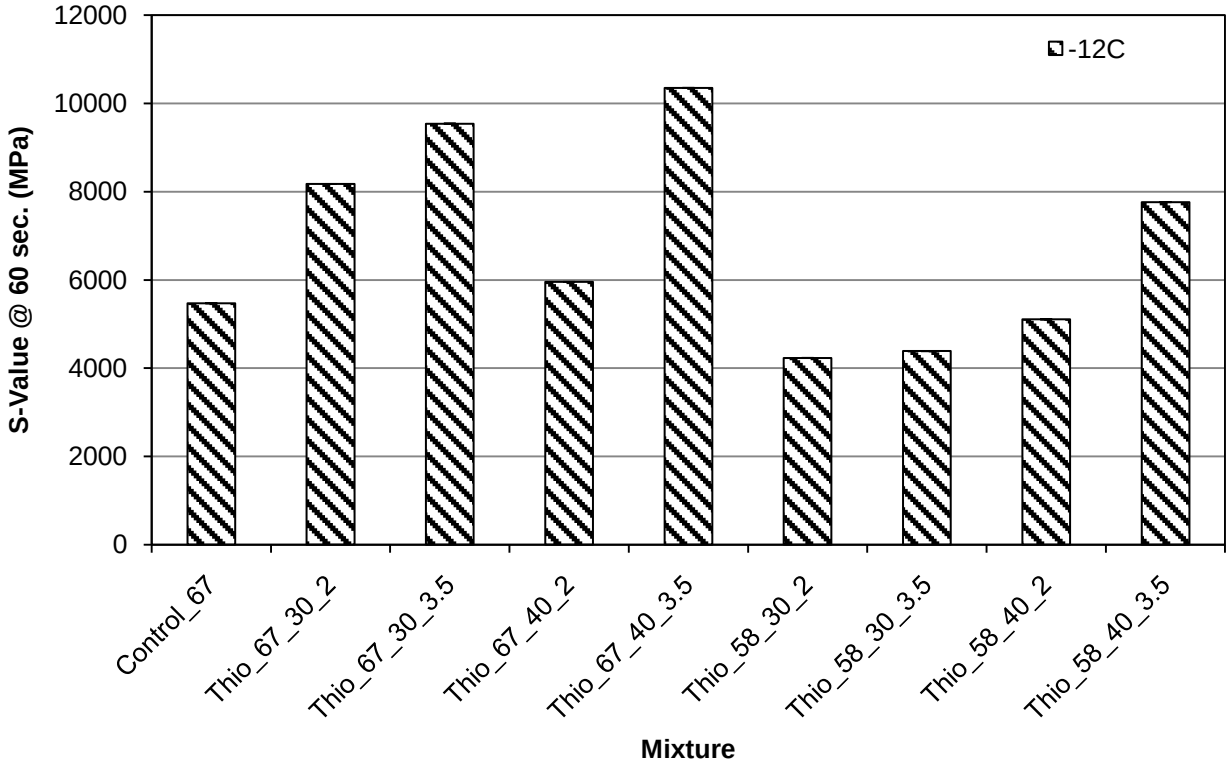

FIGURE 34 Creep Stiffness @ 60 Seconds Measured at -12°C using BBR.

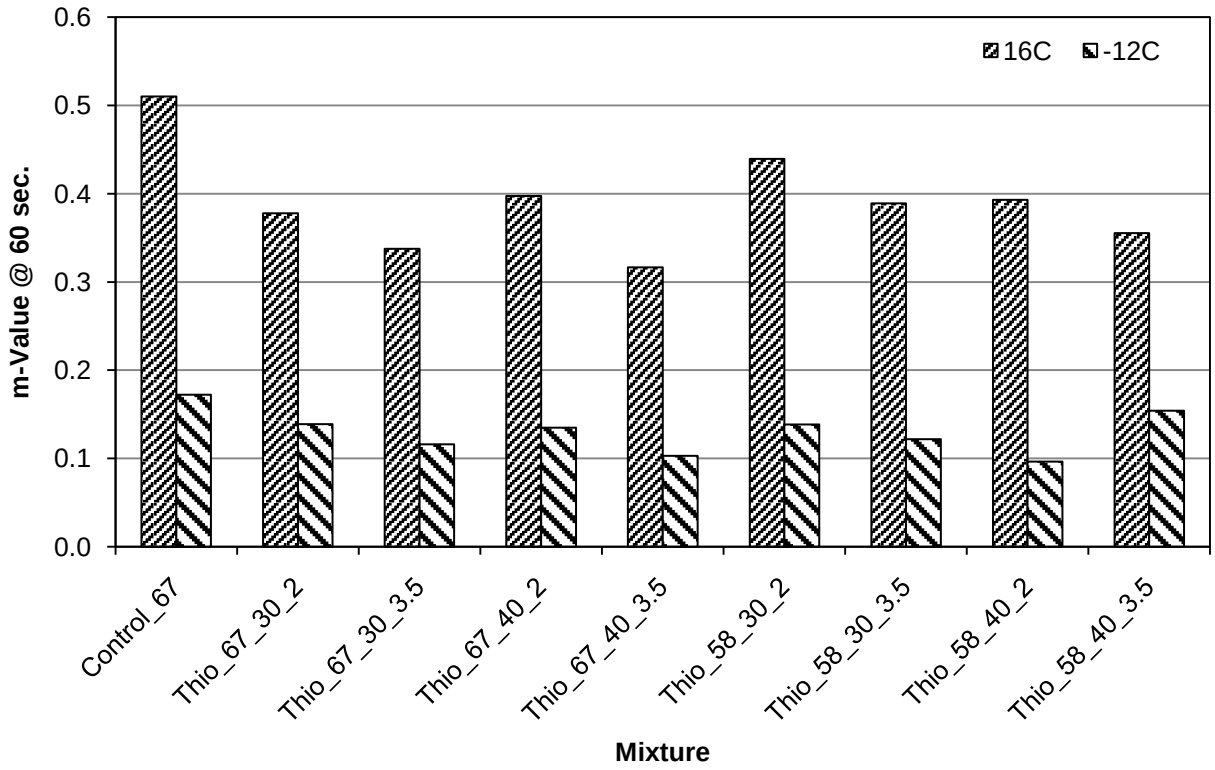

FIGURE 35 Creep Rate @ 60 Seconds Measured at -12 and 16°C using BBR.

3.2.10 Overlay Test Results

Overlay testing was conducted for nine mix designs, including the PG 67-22 control mix and the eight Thiopave mixtures. The overlay tests were performed at 25°C (77°F) with three replicates per mix design to determine the number of cycles to failure. Overlay testing was conducted using two maximum displacements of 0.01 and 0.025 inches. The latter displacement value was used to test asphalt mixtures used for overlays over old concrete pavements to simulate the joint opening due to the contraction and expansion reactions of the concrete slabs. More details regarding the Overlay testing methodology can be found in Section 2.2.10. Detailed Overlay test results are presented in Appendix J.

FIGURE 36 shows the average and standard deviation of the number of cycles to failure for the nine mixtures. It appears that when tested at the higher displacement, some of the mixtures failed within a few cycles, including the PG 67-22 control mix. This made it difficult to evaluate the cracking resistance of the mixtures. Therefore, this analysis was focused on the numbers of cycles to failure measured using the maximum displacement of 0.01 inches. As shown in FIGURE 36, the 30 percent Thiopave mixtures using the PG 58-28 binder had much higher numbers of cycles to failure, especially the mixture with 2 percent design air voids. A closer look at the results of the control and Thiopave mixtures using the PG 67-22 binder (FIGURE 37) showed that the 30 percent Thiopave mixture with 3.5 percent design air voids had the highest number of cycles to failure among the mixtures using the PG 67-22 binder.

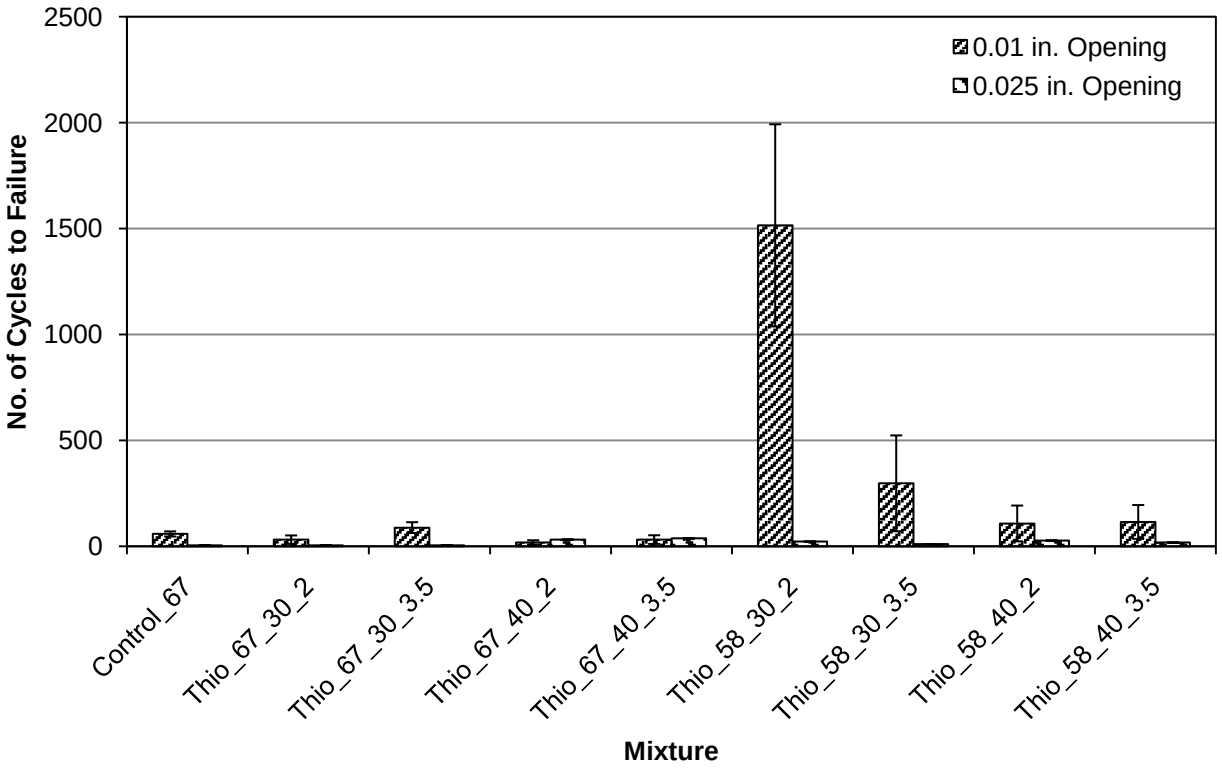

FIGURE 36 Overlay Test Results.

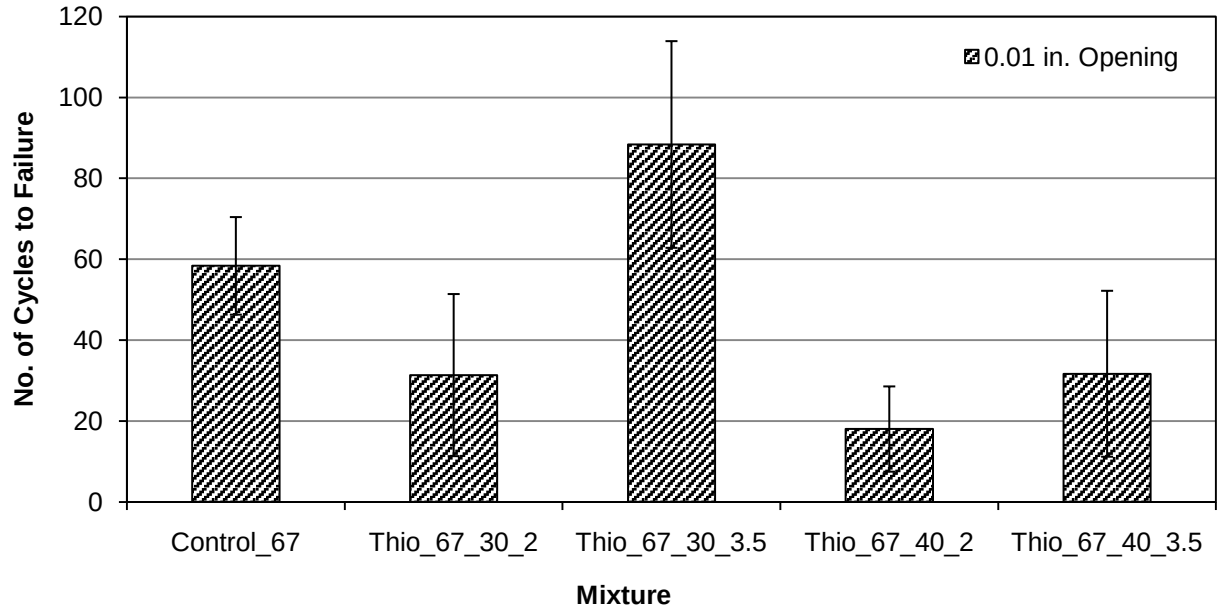

FIGURE 37 Overlay Test Results for Mixtures Using PG 67-22.

4. CONCLUSIONS AND RECOMMENDATIONS

This study conducted the mix designs and evaluated the mechanistic and performance properties of ten mixtures—two control and eight Thiopave-modified mixes—in the laboratory. The testing plan for this study was designed so that there would be multiple tests, if possible, used to assess the performance characteristics (moisture susceptibility, mixture stiffness, rutting, fatigue cracking, low temperature cracking, and reflective cracking) of the sulfur-modified asphalt mixtures relative to those of the control HMA mixtures. The following conclusions and recommendations are offered based on the results of the laboratory study.

To evaluate the moisture susceptibility of the mixtures, three tests, including ALDOT 361, AASHTO T 283 and AASHTO T 324, were conducted in this study. Both ALDOT 361 and AASHTO T 283 measured the splitting tensile strength and tensile strength ratio of each mix but using different methods for conditioning. For AASHTO T 324, the stripping inflection point was determined to evaluate the moisture susceptibility of each mix. For the liquid anti-strip used in this evaluation, the Thiopave mixtures were more susceptible to moisture induced damage than the control mixtures.

Dynamic modulus testing (AASHTO TP 79) was used to determine mixture stiffness. The average modulus of the Thiopave mixtures increased significantly (up to 100 percent) after 14 days of curing at the room temperature. After 14 days of curing, the Thiopave mixtures exhibited comparable or higher average E* results than the control mixes for all combinations of test temperatures and frequencies, especially at the high temperature and low frequency region, which meant the Thiopave mixes would have higher rutting resistance.

To evaluate the mixture resistance to permanent deformation, three tests, including flow number (AASHTP TP 79), APA (AASHTO TP 63) and Hamburg (AASHTO T 324), were conducted. Except for the APA results, the results from the other tests showed that in general, the Thiopave mixtures using the PG 67-22 binder and the PG 76-22 control mixture were stiffer and had higher rutting resistance than the Thiopave mixes using the PG 58-28 binder and then the PG 67-22 control mixture.

Bending beam fatigue testing in accordance with ASTM D7460 and AASHTO T 321 was used to evaluate the mixture resistance to fatigue cracking. Based on the AASHTO T 321 results, there appeared to be four groups of fatigue curves. The first group included the PG 76-22 control mix, which had the longest fatigue life at all the levels tested. The second group consisted of the 30 percent Thiopave mix with the PG 58-28 binder and 3.5 percent design air voids, which did not fail after 12,000,000 cycles tested at 200 microstrain. The third group included three mixtures—the PG 67-22 control mix and two 30 percent Thiopave mixes with the PG 67-22 and PG 58-28 binders, respectively, and 2 percent design air voids. The last group consisted of the remaining three Thiopave mixtures using the PG 67-22 binder and two Thiopave mixes using the PG 58-22 binder.

Based on the estimated endurance limit, the PG 76-22 control mix was ranked first, then two Thiopave mixtures, including the 30 percent Thiopave mix using the PG 67-22 binder and 2 percent design air voids and the 30 percent Thiopave mix using the PG 58-28 binder and 3.5

percent design air voids. The PG 67-22 control mix and two other Thiopave mixtures were ranked third, and then the other four Thiopave mixtures.

Based on the TSRST results, the addition of the Thiopave material had no tangible impact on the low temperature performance grades of the base asphalt binder used in the asphalt mixtures. While the two 30 percent Thiopave mixtures using the PG 58-28 binder had higher mean SCB fracture energy values, they were not significantly different from the SCB results of the other mixtures.

Regarding mixture resistance to reflective cracking, the two 30 percent Thiopave mixtures had higher numbers of cycles to failure tested at an opening displacement of 0.01 in. in the Overlay Tester.

Since the standard binder for Alabama is a PG 67-22 and the 30 percent Thiopave mixture with PG 67-22 and 2 percent design air voids had the best fatigue resistance among the Thiopave mixtures using the PG 67-22 binder, this mix was used in the bottom layers of two Thiopave test sections at the NCAT Pavement Test Track. The 40 percent Thiopave mixture with PG 67-22 and 3.5 percent design air voids was used in the intermediate layers of the test track sections because this mix was stiffer, providing better load stress distribution.

REFERENCES

1. Strickland, D., J. Colange, M. Martin, and I. Deme. Performance Properties of Sulphur Extended Asphalt Mixtures with Modified Sulphur Pellets, *Proceedings of the International Society for Asphalt Pavements*, 2008.
2. Beatty T., K. Dunn, E.T. Harrigan, K. Stuart, and H. Weber. Field Evaluation of Sulfur-Extended Asphalt Pavements, *Journal of the Transportation Research Board: Transportation Research Record No. 1115*, 1987, pp. 161-170.
3. Bayomy, F., and S.A. Khedr. Sulfur as a Partial Replacement for Asphalt in Pavement, *Journal of the Transportation Research Board: Transportation Research Record No. 1115*, 1987, pp. 150-160.
4. Deme, I., and B. Kennedy. Use of Sulfur in Asphalt Pavements. Presented at *the 5th International Symposium on Pavement Surface Characteristics*, Roads and Airfields, Toronto, 2004.
5. Timm, D., N. Tran, A.J. Taylor, M.M. Robbins and R.B. Powell. *Evaluation of Mixture Performance and Structural Capacity of Pavements Using Shell Thiopave.* NCAT Report 09-05, National Center for Asphalt Technology, Auburn University, 2009.
6. Bonaquist, R. *Refining the Simple Performance Tester for Use in Routine Practice*. NCHRP Report 614, TRB, Washington, D.C., 2008.
7. Biligiri, K.P., Kaloush, K.E., Mamlouk, M.S., and Witczak, M.W. Rational Modeling of Tertiary Flow for Asphalt Mixtures. *Journal of the Transportation Research Board: Transportation Research Record No. 2001*, 2007, pp. 63-72.
8. Prowell, B., et al. Endurance Limit of Hot Mix Asphalt Mixtures to Prevent Fatigue Cracking in Flexible Pavements. Draft Final Report for NCHRP 9-38, NCAT, Alabama, 2009.
9. Shell. *Shell THIOPAVE – Miscellaneous Lab Properties.* Powerpoint Presentation.
10. Eres Consultants Division, Guide For Mechanistic-Empirical Pavement Design of New and Rehabilitated Pavement Structures. Final Report, NCHRP 1-37A, 2004.
11. American Association of State Highway and Transportation Officials, AASHTO Guide for Design of Pavement Structures, Washington, D.C., 1993.
12. Taylor, A.J., "Mechanistic Characterization of Resilient Moduli for Unbound Pavement Layer Materials," M.S. Thesis, Auburn University, 2008.
13. Timm, D.H. and A.L. Priest, "Material Properties of the 2003 NCAT Test Track Structural Study," Report No. 06-01, National Center for Asphalt Technology, Auburn University, 2006.
14. Timm, D.H. and D.E. Newcomb, "Perpetual Pavement Design for Flexible Pavements in the U.S.," International Journal of Pavement Engineering, Vol. 7, No. 2, June 2006, pp. 111-119.
15. Timm, D.H. and A.L. Priest, "Flexible Pavement Fatigue Cracking and Measured Strain Response at the NCAT Test Track," Proceedings of the 87th Annual Transportation Research Board, Washington, D.C., 2008.
16. Priest, A.L. and D.H. Timm, "Methodology and Calibration of Fatigue Transfer Functions for Mechanistic-Empirical Flexible Pavement Design," Report No. 06-03, National Center for Asphalt Technology, Auburn University, 2006.
17. Monismith, C.L. and F. Long (1999). Overlay Design for Cracked and Seated Portland Cement Concrete (PCC) Pavement – Interstate Route 710. Technical Memorandum TM

UCB PRC 99-3, Pavement Research Center, Institute for Transportation Studies, University of California, Berkeley.

18. Willis, J.R., “Field-Based Strain Thresholds for Flexible Perpetual Pavement Design,” PhD. Dissertation, Auburn University, 2008.

APPENDIX A TSR Testing Results

TABLE A.1 Test Results for TSR Testing (ALDOT Method – With 14 days of Curing)

Binder	Thiopave (%)	Design Air (%)	Treatment	Curing Time (days)	Sample Air Voids (%)	Saturation (%)	Splitting Tensile Strength (psi)	TSR
PG 67-22	0	4	Conditioned	1	6.9	66.6	132.49	0.99
	0	4	Conditioned	1	6.9	64.8	125.29	
	0	4	Conditioned	1	6.3	62.2	138.25	
	0	4	Unconditioned	1	6.4	N/A	149.77	
	0	4	Unconditioned	1	7.2	N/A	128.17	
	0	4	Unconditioned	1	7.0	N/A	120.97	
PG 76-22	0	4	Conditioned	1	6.4	67.5	127.40	0.90
	0	4	Conditioned	1	6.6	66.8	133.19	
	0	4	Conditioned	1	6.7	55.9	120.31	
	0	4	Unconditioned	1	6.5	N/A	143.63	
	0	4	Unconditioned	1	6.8	N/A	131.97	
	0	4	Unconditioned	1	6.7	N/A	149.36	
PG 67-22	30	3.5	Conditioned	14	7.3	56.2	68.65	0.60
	30	3.5	Conditioned	14	7.1	54.7	74.29	
	30	3.5	Conditioned	14	7.0	58.6	76.04	
	30	3.5	Unconditioned	14	7.1	N/A	120.28	
	30	3.5	Unconditioned	14	7.1	N/A	127.26	
	30	3.5	Unconditioned	14	7.0	N/A	118.72	
PG 67-22	40	3.5	Conditioned	14	7.5	60.6	74.49	0.67
	40	3.5	Conditioned	14	7.6	60.9	78.66	
	40	3.5	Conditioned	14	7.7	57.7	71.26	
	40	3.5	Unconditioned	14	7.4	N/A	99.69	
	40	3.5	Unconditioned	14	6.9	N/A	115.23	
	40	3.5	Unconditioned	14	6.8	N/A	119.94	
PG 58-28	30	3.5	Conditioned	14	7.3	73.2	49.40	0.68
	30	3.5	Conditioned	14	7.1	73.3	52.90	
	30	3.5	Conditioned	14	7.3	72.7	50.70	
	30	3.5	Unconditioned	14	7.6	N/A	84.00	
	30	3.5	Unconditioned	14	7.3	N/A	72.40	
	30	3.5	Unconditioned	14	7.1	N/A	70.20	
PG 58-28	40	3.5	Conditioned	14	6.1	71.8	52.90	0.57
	40	3.5	Conditioned	14	7.3	75.4	54.40	
	40	3.5	Conditioned	14	7.5	76.7	50.00	
	40	3.5	Unconditioned	14	7.1	N/A	99.30	
	40	3.5	Unconditioned	14	7.4	N/A	86.90	
	40	3.5	Unconditioned	14	7.1	N/A	87.70	

TABLE A.2 Test Results for TSR Testing (AASHTO Method – With 14 days of Curing)

Binder	Thiopave (%)	Design Air (%)	Treatment	Curing Time (days)	Sample Air Voids (%)	Saturation (%)	Splitting Tensile Strength (psi)	TSR
PG 67-22	0	4	Conditioned	1	6.5	73.8	120.2	0.865
	0	4	Conditioned	1	7.1	71.6	111.7	
	0	4	Conditioned	1	6.4	73.9	113.2	
	0	4	Unconditioned	1	6.4	N/A	149.8	
	0	4	Unconditioned	1	7.2	N/A	128.2	
	0	4	Unconditioned	1	7.0	N/A	121.0	
PG 76-22	0	4	Conditioned	1	6.6	71.9	156.6	1.039
	0	4	Conditioned	1	6.7	70.9	148.2	
	0	4	Conditioned	1	7.4	76.3	136.7	
	0	4	Unconditioned	1	6.5	N/A	143.6	
	0	4	Unconditioned	1	6.8	N/A	132.0	
	0	4	Unconditioned	1	6.7	N/A	149.4	
PG 67-22	30	3.5	Conditioned	14	6.7	73.3	95.7	0.708
	30	3.5	Conditioned	14	7.2	70.6	78.1	
	30	3.5	Conditioned	14	7.0	70.1	85.6	
	30	3.5	Unconditioned	14	7.1	N/A	120.3	
	30	3.5	Unconditioned	14	7.1	N/A	127.3	
	30	3.5	Unconditioned	14	7.0	N/A	118.7	
PG 67-22	40	3.5	Conditioned	14	7.0	77.3	89.3	0.731
	40	3.5	Conditioned	14	7.1	73.6	79.5	
	40	3.5	Conditioned	14	7.2	72.4	76.0	
	40	3.5	Unconditioned	14	7.4	N/A	99.7	
	40	3.5	Unconditioned	14	6.9	N/A	115.2	
	40	3.5	Unconditioned	14	6.8	N/A	119.9	
PG 58-28	30	3.5	Conditioned	14	7.0	72.8	48.8	0.696
	30	3.5	Conditioned	14	6.9	70.3	48.0	
	30	3.5	Conditioned	14	7.4	71.4	61.0	
	30	3.5	Unconditioned	14	7.6	N/A	84.0	
	30	3.5	Unconditioned	14	7.3	N/A	72.4	
	30	3.5	Unconditioned	14	7.1	N/A	70.2	
PG 58-28	40	3.5	Conditioned	14	7.3	75.8	57.2	0.627
	40	3.5	Conditioned	14	6.9	73.9	60.8	
	40	3.5	Conditioned	14	7.5	76.2	53.6	
	40	3.5	Unconditioned	14	7.1	N/A	99.3	
	40	3.5	Unconditioned	14	7.4	N/A	86.9	
	40	3.5	Unconditioned	14	7.1	N/A	87.7	

APPENDIX B Dynamic Modulus Test Results

TABLE B.1 Test Results of Dynamic Modulus Testing

Base Binder	Thiopave (%)	Design Air Voids (%)	Curing Time (days)	Test Temp (Deg_C)	Frequency (Hz)	E* (ksi)	Phase Angle (Deg)
67-22	0	4	1	21.1	25	907.9	23.9
67-22	0	4	1	21.1	10	724.0	26.7
67-22	0	4	1	21.1	5	603.6	28.4
67-22	0	4	1	21.1	1	368.8	32.2
67-22	0	4	1	21.1	0.5	294.7	33.1
67-22	0	4	1	21.1	0.1	163.5	35.1
67-22	0	4	1	21.1	0.01	67.7	34.9
67-22	0	4	1	21.1	25	918.7	25.6
67-22	0	4	1	21.1	10	713.4	27.8
67-22	0	4	1	21.1	5	589.9	29.2
67-22	0	4	1	21.1	1	354.6	33.0
67-22	0	4	1	21.1	0.5	279.9	33.5
67-22	0	4	1	21.1	0.1	154.0	34.7
67-22	0	4	1	21.1	0.01	67.1	34.1
67-22	30	3.5	1	21.1	25	1386.1	25.3
67-22	30	3.5	1	21.1	10	1026.4	25.1
67-22	30	3.5	1	21.1	5	856.0	26.5
67-22	30	3.5	1	21.1	1	554.5	29.9
67-22	30	3.5	1	21.1	0.5	453.4	30.5
67-22	30	3.5	1	21.1	0.1	276.6	31.7
67-22	30	3.5	1	21.1	0.01	139.4	30.7
67-22	30	3.5	1	21.1	25	987.1	24.2
67-22	30	3.5	1	21.1	10	777.4	26.9
67-22	30	3.5	1	21.1	5	645.4	28.5
67-22	30	3.5	1	21.1	1	400.9	31.7
67-22	30	3.5	1	21.1	0.5	320.1	32.1
67-22	30	3.5	1	21.1	0.1	186.2	32.4
67-22	30	3.5	1	21.1	0.01	92.8	31.1
67-22	30	2	1	21.1	25	826.4	24.9
67-22	30	2	1	21.1	10	639.3	27.6
67-22	30	2	1	21.1	5	523.4	29.2
67-22	30	2	1	21.1	1	315.7	32.5
67-22	30	2	1	21.1	0.5	249.5	33.0
67-22	30	2	1	21.1	0.1	141.3	33.6
67-22	30	2	1	21.1	0.01	142.8	46.8
67-22	30	2	1	21.1	25	925.2	25.1
67-22	30	2	1	21.1	10	715.9	27.9

Base Binder	Thiopave (%)	Design Air Voids (%)	Curing Time (days)	Test Temp (Deg_C)	Frequency (Hz)	E* (ksi)	Phase Angle (Deg)
67-22	30	2	1	21.1	5	588.9	29.3
67-22	30	2	1	21.1	1	354.9	32.4
67-22	30	2	1	21.1	0.5	279.6	32.6
67-22	30	2	1	21.1	0.1	159.1	32.7
67-22	30	2	1	21.1	0.01	75.0	30.7
67-22	40	3.5	1	21.1	25	1120.3	21.2
67-22	40	3.5	1	21.1	10	904.0	24.2
67-22	40	3.5	1	21.1	5	760.9	26.0
67-22	40	3.5	1	21.1	1	492.0	29.6
67-22	40	3.5	1	21.1	0.5	402.5	30.4
67-22	40	3.5	1	21.1	0.1	246.7	31.2
67-22	40	3.5	1	21.1	0.01	130.9	29.6
67-22	40	3.5	1	21.1	25	1241.5	19.5
67-22	40	3.5	1	21.1	10	1009.9	22.3
67-22	40	3.5	1	21.1	5	859.1	24.0
67-22	40	3.5	1	21.1	1	577.1	27.4
67-22	40	3.5	1	21.1	0.5	475.4	28.3
67-22	40	3.5	1	21.1	0.1	304.6	29.6
67-22	40	3.5	1	21.1	0.01	168.8	28.7
67-22	40	2	1	21.1	25	1187.1	23.4
67-22	40	2	1	21.1	10	924.0	25.9
67-22	40	2	1	21.1	5	769.7	27.5
67-22	40	2	1	21.1	1	487.6	30.9
67-22	40	2	1	21.1	0.5	392.0	31.4
67-22	40	2	1	21.1	0.1	235.4	31.7
67-22	40	2	1	21.1	0.01	118.0	30.0
67-22	40	2	1	21.1	25	1061.4	28.8
67-22	40	2	1	21.1	10	769.4	27.1
67-22	40	2	1	21.1	5	635.4	28.7
67-22	40	2	1	21.1	1	392.5	32.0
67-22	40	2	1	21.1	0.5	314.4	32.5
67-22	40	2	1	21.1	0.1	184.2	32.7
67-22	40	2	1	21.1	0.01	91.3	30.4
67-22	0	4	14	21.1	25	1049.1	22.9
67-22	0	4	14	21.1	10	818.7	25.4
67-22	0	4	14	21.1	5	678.5	26.9
67-22	0	4	14	21.1	1	421.3	30.9
67-22	0	4	14	21.1	0.5	335.9	31.9
67-22	0	4	14	21.1	0.1	190.3	34.0

Base Binder	Thiopave (%)	Design Air Voids (%)	Curing Time (days)	Test Temp (Deg_C)	Frequency (Hz)	E* (ksi)	Phase Angle (Deg)
67-22	0	4	14	21.1	0.01	79.8	34.1
67-22	0	4	14.1	4.4	10	2139.5	12.5
67-22	0	4	14.1	4.4	5	1952.6	13.6
67-22	0	4	14.1	4.4	1	1525.5	16.5
67-22	0	4	14.1	4.4	0.5	1342.8	17.8
67-22	0	4	14.1	4.4	0.1	971.6	21.7
67-22	0	4	14.1	4.4	0.01	599.7	26.2
67-22	0	4	14.1	21.1	10	847.7	25.1
67-22	0	4	14.1	21.1	5	718.4	26.2
67-22	0	4	14.1	21.1	1	463.0	29.9
67-22	0	4	14.1	21.1	0.5	378.7	30.5
67-22	0	4	14.1	21.1	0.1	212.8	32.4
67-22	0	4	14.1	21.1	0.01	86.3	33.1
67-22	0	4	14.1	46.1	10	106.4	43.5
67-22	0	4	14.1	46.1	5	76.9	40.2
67-22	0	4	14.1	46.1	1	34.9	39.1
67-22	0	4	14.1	46.1	0.5	26.6	36.8
67-22	0	4	14.1	46.1	0.1	14.8	33.7
67-22	0	4	14.1	46.1	0.01	8.1	30.5
67-22	0	4	14	21.1	25	913.7	23.7
67-22	0	4	14	21.1	10	728.7	26.1
67-22	0	4	14	21.1	5	602.6	27.8
67-22	0	4	14	21.1	1	369.6	31.5
67-22	0	4	14	21.1	0.5	293.7	32.4
67-22	0	4	14	21.1	0.1	163.7	33.8
67-22	0	4	14	21.1	0.01	65.0	33.3
67-22	0	4	14.1	4.4	10	1963.4	13.9
67-22	0	4	14.1	4.4	5	1787.6	14.4
67-22	0	4	14.1	4.4	1	1380.3	17.4
67-22	0	4	14.1	4.4	0.5	1208.3	18.8
67-22	0	4	14.1	4.4	0.1	868.5	22.5
67-22	0	4	14.1	4.4	0.01	518.1	26.8
67-22	0	4	14.1	21.1	10	759.3	26.6
67-22	0	4	14.1	21.1	5	630.0	27.1
67-22	0	4	14.1	21.1	1	393.8	30.0
67-22	0	4	14.1	21.1	0.5	314.4	30.5
67-22	0	4	14.1	21.1	0.1	178.3	31.6
67-22	0	4	14.1	21.1	0.01	74.5	31.3
67-22	0	4	14.1	46.1	10	93.5	45.0

Base Binder	Thiopave (%)	Design Air Voids (%)	Curing Time (days)	Test Temp (Deg_C)	Frequency (Hz)	E* (ksi)	Phase Angle (Deg)
67-22	0	4	14.1	46.1	5	73.5	39.9
67-22	0	4	14.1	46.1	1	33.2	38.3
67-22	0	4	14.1	46.1	0.5	24.8	36.1
67-22	0	4	14.1	46.1	0.1	14.1	33.1
67-22	0	4	14.1	46.1	0.01	7.4	31.6
67-22	30	3.5	14	21.1	25	2124.5	23.7
67-22	30	3.5	14	21.1	10	1294.0	19.8
67-22	30	3.5	14	21.1	5	1104.3	21.7
67-22	30	3.5	14	21.1	1	759.6	25.3
67-22	30	3.5	14	21.1	0.5	636.3	26.1
67-22	30	3.5	14	21.1	0.1	419.2	27.9
67-22	30	3.5	14	21.1	0.01	229.2	27.7
67-22	30	3.5	14.1	4.4	10	2652.5	9.8
67-22	30	3.5	14.1	4.4	5	2417.2	11.1
67-22	30	3.5	14.1	4.4	1	1970.5	13.3
67-22	30	3.5	14.1	4.4	0.5	1796.6	14.3
67-22	30	3.5	14.1	4.4	0.1	1375.8	17.9
67-22	30	3.5	14.1	4.4	0.01	921.7	22.1
67-22	30	3.5	14.1	21.1	10	1267.9	20.2
67-22	30	3.5	14.1	21.1	5	1094.9	21.7
67-22	30	3.5	14.1	21.1	1	764.1	24.9
67-22	30	3.5	14.1	21.1	0.5	649.3	25.7
67-22	30	3.5	14.1	21.1	0.1	423.2	27.6
67-22	30	3.5	14.1	21.1	0.01	225.7	27.6
67-22	30	3.5	14.1	46.1	10	246.9	35.3
67-22	30	3.5	14.1	46.1	5	194.1	32.8
67-22	30	3.5	14.1	46.1	1	111.8	31.2
67-22	30	3.5	14.1	46.1	0.5	85.8	30.2
67-22	30	3.5	14.1	46.1	0.1	57.2	27.9
67-22	30	3.5	14.1	46.1	0.01	37.0	25.2
67-22	30	3.5	14	21.1	25	1493.7	18.5
67-22	30	3.5	14	21.1	10	1192.8	20.8
67-22	30	3.5	14	21.1	5	998.0	22.9
67-22	30	3.5	14	21.1	1	679.8	27.0
67-22	30	3.5	14	21.1	0.5	567.5	28.3
67-22	30	3.5	14	21.1	0.1	364.8	30.4
67-22	30	3.5	14	21.1	0.01	195.2	30.1
67-22	30	3.5	14.1	4.4	10	2582.0	10.1
67-22	30	3.5	14.1	4.4	5	2403.1	10.8

Base Binder	Thiopave (%)	Design Air Voids (%)	Curing Time (days)	Test Temp (Deg_C)	Frequency (Hz)	E* (ksi)	Phase Angle (Deg)
67-22	30	3.5	14.1	4.4	1	1975.8	12.8
67-22	30	3.5	14.1	4.4	0.5	1784.8	13.7
67-22	30	3.5	14.1	4.4	0.1	1381.2	16.6
67-22	30	3.5	14.1	4.4	0.01	905.8	21.6
67-22	30	3.5	14.1	21.1	10	1147.7	21.5
67-22	30	3.5	14.1	21.1	5	987.7	23.1
67-22	30	3.5	14.1	21.1	1	683.4	26.7
67-22	30	3.5	14.1	21.1	0.5	577.4	27.6
67-22	30	3.5	14.1	21.1	0.1	368.1	29.8
67-22	30	3.5	14.1	21.1	0.01	190.0	29.5
67-22	30	3.5	14.1	46.1	10	206.4	38.6
67-22	30	3.5	14.1	46.1	5	166.6	35.5
67-22	30	3.5	14.1	46.1	1	90.5	33.7
67-22	30	3.5	14.1	46.1	0.5	69.5	32.7
67-22	30	3.5	14.1	46.1	0.1	44.4	30.7
67-22	30	3.5	14.1	46.1	0.01	28.9	26.0
67-22	30	2	14	21.1	25	1377.4	20.8
67-22	30	2	14	21.1	10	1102.9	23.4
67-22	30	2	14	21.1	5	923.0	25.2
67-22	30	2	14	21.1	1	603.4	28.7
67-22	30	2	14	21.1	0.5	490.7	29.4
67-22	30	2	14	21.1	0.1	302.3	30.8
67-22	30	2	14	21.1	0.01	156.9	29.9
67-22	30	2	14.1	4.4	10	2296.1	11.8
67-22	30	2	14.1	4.4	5	2092.6	12.7
67-22	30	2	14.1	4.4	1	1638.5	15.7
67-22	30	2	14.1	4.4	0.5	1453.1	17.1
67-22	30	2	14.1	4.4	0.1	1074.3	21.0
67-22	30	2	14.1	4.4	0.01	717.6	24.1
67-22	30	2	14.1	21.1	10	1080.0	23.4
67-22	30	2	14.1	21.1	5	919.8	24.7
67-22	30	2	14.1	21.1	1	607.4	28.0
67-22	30	2	14.1	21.1	0.5	500.1	28.8
67-22	30	2	14.1	21.1	0.1	302.1	30.3
67-22	30	2	14.1	21.1	0.01	148.4	29.6
67-22	30	2	14.1	46.1	10	189.6	38.5
67-22	30	2	14.1	46.1	5	145.5	37.9
67-22	30	2	14.1	46.1	1	71.5	37.0
67-22	30	2	14.1	46.1	0.5	55.8	35.0

Base Binder	Thiopave (%)	Design Air Voids (%)	Curing Time (days)	Test Temp (Deg_C)	Frequency (Hz)	E* (ksi)	Phase Angle (Deg)
67-22	30	2	14.1	46.1	0.1	32.5	32.2
67-22	30	2	14.1	46.1	0.01	18.8	28.7
67-22	30	2	14	21.1	25	1359.0	19.9
67-22	30	2	14	21.1	10	1089.1	22.7
67-22	30	2	14	21.1	5	911.9	24.6
67-22	30	2	14	21.1	1	602.5	28.2
67-22	30	2	14	21.1	0.5	496.9	29.0
67-22	30	2	14	21.1	0.1	309.8	30.6
67-22	30	2	14	21.1	0.01	160.0	30.5
67-22	30	2	14.1	4.4	10	2586.9	11.6
67-22	30	2	14.1	4.4	5	2391.1	12.7
67-22	30	2	14.1	4.4	1	1912.5	15.2
67-22	30	2	14.1	4.4	0.5	1709.1	16.4
67-22	30	2	14.1	4.4	0.1	1276.0	19.9
67-22	30	2	14.1	4.4	0.01	793.8	24.7
67-22	30	2	14.1	21.1	10	1103.0	22.8
67-22	30	2	14.1	21.1	5	947.5	24.3
67-22	30	2	14.1	21.1	1	637.7	27.9
67-22	30	2	14.1	21.1	0.5	528.5	28.7
67-22	30	2	14.1	21.1	0.1	322.9	30.7
67-22	30	2	14.1	21.1	0.01	157.1	30.0
67-22	30	2	14.1	46.1	10	180.3	43.4
67-22	30	2	14.1	46.1	5	139.3	37.2
67-22	30	2	14.1	46.1	1	73.7	35.3
67-22	30	2	14.1	46.1	0.5	58.2	33.5
67-22	30	2	14.1	46.1	0.1	36.1	31.6
67-22	30	2	14.1	46.1	0.01	22.9	29.1
67-22	40	3.5	14	21.1	25	1762.6	19.9
67-22	40	3.5	14	21.1	10	1412.1	21.0
67-22	40	3.5	14	21.1	5	1189.0	23.0
67-22	40	3.5	14	21.1	1	812.2	27.2
67-22	40	3.5	14	21.1	0.5	681.8	28.0
67-22	40	3.5	14	21.1	0.1	441.1	29.6
67-22	40	3.5	14	21.1	0.01	239.2	29.3
67-22	40	3.5	14	21.1	25	1569.7	17.0
67-22	40	3.5	14	21.1	10	1312.3	19.4
67-22	40	3.5	14	21.1	5	1135.9	21.2
67-22	40	3.5	14	21.1	1	789.3	24.4
67-22	40	3.5	14	21.1	0.5	668.3	25.0

Base Binder	Thiopave (%)	Design Air Voids (%)	Curing Time (days)	Test Temp (Deg_C)	Frequency (Hz)	E* (ksi)	Phase Angle (Deg)
67-22	40	3.5	14	21.1	0.1	427.0	27.8
67-22	40	3.5	14	21.1	0.01	220.2	27.4
67-22	40	2	14	21.1	25	1418.2	19.5
67-22	40	2	14	21.1	10	1121.9	22.4
67-22	40	2	14	21.1	5	942.7	24.5
67-22	40	2	14	21.1	1	622.1	28.3
67-22	40	2	14	21.1	0.5	503.6	29.1
67-22	40	2	14	21.1	0.1	310.5	30.5
67-22	40	2	14	21.1	0.01	157.8	29.9
67-22	40	2	14	21.1	25	1587.1	17.7
67-22	40	2	14	21.1	10	1317.5	19.9
67-22	40	2	14	21.1	5	1128.7	22.0
67-22	40	2	14	21.1	1	772.9	26.0
67-22	40	2	14	21.1	0.5	647.3	26.9
67-22	40	2	14	21.1	0.1	414.7	28.7
67-22	40	2	14	21.1	0.01	217.8	28.4
67-22	40	3.5	14.1	4.4	10	2830.6	10.4
67-22	40	3.5	14.1	4.4	5	2630.4	11.1
67-22	40	3.5	14.1	4.4	1	2162.1	13.1
67-22	40	3.5	14.1	4.4	0.5	1962.2	14.1
67-22	40	3.5	14.1	4.4	0.1	1522.0	17.3
67-22	40	3.5	14.1	4.4	0.01	1031.5	21.9
67-22	40	3.5	14.1	4.4	10	3020.6	10.7
67-22	40	3.5	14.1	4.4	5	2796.3	12.0
67-22	40	3.5	14.1	4.4	1	2290.6	13.4
67-22	40	3.5	14.1	4.4	0.5	2038.5	14.6
67-22	40	3.5	14.1	4.4	0.1	1560.6	17.2
67-22	40	3.5	14.1	4.4	0.01	1039.6	22.0
67-22	40	3.5	14.1	21.1	10	1398.3	19.9
67-22	40	3.5	14.1	21.1	5	1224.6	21.2
67-22	40	3.5	14.1	21.1	1	852.4	25.1
67-22	40	3.5	14.1	21.1	0.5	722.4	26.0
67-22	40	3.5	14.1	21.1	0.1	466.7	28.3
67-22	40	3.5	14.1	21.1	0.01	244.5	28.8
67-22	40	3.5	14.1	21.1	10	1515.9	20.9
67-22	40	3.5	14.1	21.1	5	1263.6	22.3
67-22	40	3.5	14.1	21.1	1	875.3	25.8
67-22	40	3.5	14.1	21.1	0.5	743.3	26.3
67-22	40	3.5	14.1	21.1	0.1	481.4	28.0

Base Binder	Thiopave (%)	Design Air Voids (%)	Curing Time (days)	Test Temp (Deg_C)	Frequency (Hz)	E* (ksi)	Phase Angle (Deg)
67-22	40	3.5	14.1	21.1	0.01	252.9	30.2
67-22	40	3.5	14.1	46.1	10	361.7	37.2
67-22	40	3.5	14.1	46.1	5	307.6	34.8
67-22	40	3.5	14.1	46.1	1	176.4	33.4
67-22	40	3.5	14.1	46.1	0.5	136.3	32.0
67-22	40	3.5	14.1	46.1	0.1	77.8	29.5
67-22	40	3.5	14.1	46.1	0.01	37.7	26.2
67-22	40	3.5	14.1	46.1	10	285.9	35.4
67-22	40	3.5	14.1	46.1	5	237.9	33.1
67-22	40	3.5	14.1	46.1	1	134.2	31.8
67-22	40	3.5	14.1	46.1	0.5	104.1	31.0
67-22	40	3.5	14.1	46.1	0.1	62.7	30.0
67-22	40	3.5	14.1	46.1	0.01	33.5	25.9
67-22	40	2	14.1	4.4	10	2650.0	15.1
67-22	40	2	14.1	4.4	5	2482.0	14.4
67-22	40	2	14.1	4.4	1	1971.8	16.1
67-22	40	2	14.1	4.4	0.5	1759.2	17.1
67-22	40	2	14.1	4.4	0.1	1311.6	20.2
67-22	40	2	14.1	4.4	0.01	824.8	24.6
67-22	40	2	14.1	4.4	10	3442.2	15.5
67-22	40	2	14.1	4.4	5	2586.7	11.3
67-22	40	2	14.1	4.4	1	2130.6	12.9
67-22	40	2	14.1	4.4	0.5	1938.3	14.0
67-22	40	2	14.1	4.4	0.1	1504.5	16.8
67-22	40	2	14.1	4.4	0.01	992.5	21.7
67-22	40	2	14.1	21.1	10	1205.1	24.7
67-22	40	2	14.1	21.1	5	986.1	23.9
67-22	40	2	14.1	21.1	1	672.0	27.1
67-22	40	2	14.1	21.1	0.5	563.2	27.7
67-22	40	2	14.1	21.1	0.1	350.6	29.8
67-22	40	2	14.1	21.1	0.01	171.6	30.0
67-22	40	2	14.1	21.1	10	1338.3	21.6
67-22	40	2	14.1	21.1	5	1140.4	22.1
67-22	40	2	14.1	21.1	1	795.7	25.4
67-22	40	2	14.1	21.1	0.5	677.3	26.1
67-22	40	2	14.1	21.1	0.1	438.2	28.6
67-22	40	2	14.1	21.1	0.01	227.6	29.3
67-22	40	2	14.1	46.1	10	248.3	37.4
67-22	40	2	14.1	46.1	5	169.3	35.6

Base Binder	Thiopave (%)	Design Air Voids (%)	Curing Time (days)	Test Temp (Deg_C)	Frequency (Hz)	E* (ksi)	Phase Angle (Deg)
67-22	40	2	14.1	46.1	1	85.2	35.3
67-22	40	2	14.1	46.1	0.5	63.9	34.1
67-22	40	2	14.1	46.1	0.1	36.3	32.2
67-22	40	2	14.1	46.1	0.01	18.7	28.3
67-22	40	2	14.1	46.1	10	291.4	36.0
67-22	40	2	14.1	46.1	5	222.1	34.1
67-22	40	2	14.1	46.1	1	117.5	33.9
67-22	40	2	14.1	46.1	0.5	88.0	33.1
67-22	40	2	14.1	46.1	0.1	49.9	31.8
67-22	40	2	14.1	46.1	0.01	26.0	28.2
76-22	0	4	1	21.1	10	899.1	23.3
76-22	0	4	1	21.1	5	761.9	24.9
76-22	0	4	1	21.1	1	490.5	28.7
76-22	0	4	1	21.1	0.5	398.9	29.8
76-22	0	4	1	21.1	0.1	226.4	32.3
76-22	0	4	1	21.1	0.01	92.8	33.2
76-22	0	4	1	21.1	10	888.6	23.4
76-22	0	4	1	21.1	5	763.0	24.7
76-22	0	4	1	21.1	1	490.2	29.2
76-22	0	4	1	21.1	0.5	401.8	30.2
76-22	0	4	1	21.1	0.1	233.8	32.2
76-22	0	4	1	21.1	0.01	101.7	32.5
76-22	0	4	1	21.1	10	872.7	23.1
76-22	0	4	1	21.1	5	739.7	24.8
76-22	0	4	1	21.1	1	479.6	28.9
76-22	0	4	1	21.1	0.5	394.5	30.0
76-22	0	4	1	21.1	0.1	227.7	32.4
76-22	0	4	1	21.1	0.01	98.2	33.4
76-22	0	4	14	21.1	10	1162.9	22.5
76-22	0	4	14	21.1	5	984.2	23.9
76-22	0	4	14	21.1	1	660.1	27.3
76-22	0	4	14	21.1	0.5	547.2	28.0
76-22	0	4	14	21.1	0.1	333.2	30.2
76-22	0	4	14	21.1	0.01	153.4	30.9
76-22	0	4	14	21.1	10	968.3	23.1
76-22	0	4	14	21.1	5	823.1	24.4
76-22	0	4	14	21.1	1	545.8	28.2
76-22	0	4	14	21.1	0.5	450.5	29.0
76-22	0	4	14	21.1	0.1	272.4	31.3

Base Binder	Thiopave (%)	Design Air Voids (%)	Curing Time (days)	Test Temp (Deg_C)	Frequency (Hz)	E* (ksi)	Phase Angle (Deg)
76-22	0	4	14	21.1	0.01	123.3	32.0
76-22	0	4	14	21.1	10	915.6	23.8
76-22	0	4	14	21.1	5	773.2	25.2
76-22	0	4	14	21.1	1	502.0	29.1
76-22	0	4	14	21.1	0.5	410.0	29.9
76-22	0	4	14	21.1	0.1	242.2	32.2
76-22	0	4	14	21.1	0.01	107.9	32.4
76-22	0	4	14.1	4.4	10	2526.4	10.6
76-22	0	4	14.1	4.4	5	2344.1	11.2
76-22	0	4	14.1	4.4	1	1913.3	13.6
76-22	0	4	14.1	4.4	0.5	1727.0	14.6
76-22	0	4	14.1	4.4	0.1	1315.8	18.2
76-22	0	4	14.1	4.4	0.01	849.8	23.0
76-22	0	4	14.1	4.4	10	2162.1	9.7
76-22	0	4	14.1	4.4	5	1998.8	10.6
76-22	0	4	14.1	4.4	1	1626.0	13.1
76-22	0	4	14.1	4.4	0.5	1468.4	14.3
76-22	0	4	14.1	4.4	0.1	1110.4	18.1
76-22	0	4	14.1	4.4	0.01	692.7	23.2
76-22	0	4	14.1	4.4	10	2265.8	12.9
76-22	0	4	14.1	4.4	5	2098.7	13.8
76-22	0	4	14.1	4.4	1	1655.0	16.5
76-22	0	4	14.1	4.4	0.5	1470.0	17.0
76-22	0	4	14.1	4.4	0.1	1079.5	20.6
76-22	0	4	14.1	4.4	0.01	654.1	25.2
76-22	0	4	14.1	21.1	10	1118.7	22.2
76-22	0	4	14.1	21.1	5	959.7	23.4
76-22	0	4	14.1	21.1	1	652.4	26.4
76-22	0	4	14.1	21.1	0.5	544.9	27.1
76-22	0	4	14.1	21.1	0.1	334.9	29.2
76-22	0	4	14.1	21.1	0.01	157.1	29.9
76-22	0	4	14.1	21.1	10	945.9	22.4
76-22	0	4	14.1	21.1	5	809.2	23.7
76-22	0	4	14.1	21.1	1	539.1	27.2
76-22	0	4	14.1	21.1	0.5	443.2	28.0
76-22	0	4	14.1	21.1	0.1	267.2	30.2
76-22	0	4	14.1	21.1	0.01	121.0	30.9
76-22	0	4	14.1	21.1	10	913.0	23.7
76-22	0	4	14.1	21.1	5	772.3	24.8

Base Binder	Thiopave (%)	Design Air Voids (%)	Curing Time (days)	Test Temp (Deg_C)	Frequency (Hz)	E* (ksi)	Phase Angle (Deg)
76-22	0	4	14.1	21.1	1	509.8	28.5
76-22	0	4	14.1	21.1	0.5	412.2	29.4
76-22	0	4	14.1	21.1	0.1	242.1	31.6
76-22	0	4	14.1	21.1	0.01	108.2	32.2
76-22	0	4	14.1	46.1	10	189.3	37.0
76-22	0	4	14.1	46.1	5	148.4	35.2
76-22	0	4	14.1	46.1	1	72.6	34.2
76-22	0	4	14.1	46.1	0.5	55.7	32.5
76-22	0	4	14.1	46.1	0.1	29.8	30.3
76-22	0	4	14.1	46.1	0.01	15.6	26.3
76-22	0	4	14.1	46.1	10	159.4	34.4
76-22	0	4	14.1	46.1	5	113.7	35.0
76-22	0	4	14.1	46.1	1	56.8	34.0
76-22	0	4	14.1	46.1	0.5	44.6	32.0
76-22	0	4	14.1	46.1	0.1	25.8	29.1
76-22	0	4	14.1	46.1	0.01	14.5	24.5
76-22	0	4	14.1	46.1	10	144.3	37.9
76-22	0	4	14.1	46.1	5	110.0	37.0
76-22	0	4	14.1	46.1	1	53.4	36.2
76-22	0	4	14.1	46.1	0.5	41.9	34.2
76-22	0	4	14.1	46.1	0.1	23.0	31.3
76-22	0	4	14.1	46.1	0.01	12.5	26.5
58-28	30	3.5	1	21.1	10	503.9	29.4
58-28	30	3.5	1	21.1	5	414.5	30.2
58-28	30	3.5	1	21.1	1	254.7	32.0
58-28	30	3.5	1	21.1	0.5	205.7	31.8
58-28	30	3.5	1	21.1	0.1	126.6	31.1
58-28	30	3.5	1	21.1	0.01	70.4	28.7
58-28	30	3.5	1	21.1	10	530.8	28.2
58-28	30	3.5	1	21.1	5	436.9	28.7
58-28	30	3.5	1	21.1	1	272.8	30.6
58-28	30	3.5	1	21.1	0.5	222.3	30.5
58-28	30	3.5	1	21.1	0.1	139.2	30.1
58-28	30	3.5	1	21.1	0.01	78.8	28.0
58-28	30	3.5	1	21.1	10	630.2	27.8
58-28	30	3.5	1	21.1	5	513.7	28.0
58-28	30	3.5	1	21.1	1	326.6	30.1
58-28	30	3.5	1	21.1	0.5	266.6	30.0
58-28	30	3.5	1	21.1	0.1	169.3	29.5

Base Binder	Thiopave (%)	Design Air Voids (%)	Curing Time (days)	Test Temp (Deg_C)	Frequency (Hz)	E* (ksi)	Phase Angle (Deg)
58-28	30	3.5	1	21.1	0.01	95.1	27.7
58-28	30	3.5	14	21.1	10	808.2	23.8
58-28	30	3.5	14	21.1	5	683.9	24.7
58-28	30	3.5	14	21.1	1	466.3	27.1
58-28	30	3.5	14	21.1	0.5	391.9	27.6
58-28	30	3.5	14	21.1	0.1	261.9	28.2
58-28	30	3.5	14	21.1	0.01	155.2	27.5
58-28	30	3.5	14	21.1	10	729.1	24.4
58-28	30	3.5	14	21.1	5	615.0	25.2
58-28	30	3.5	14	21.1	1	412.8	27.3
58-28	30	3.5	14	21.1	0.5	344.2	27.6
58-28	30	3.5	14	21.1	0.1	229.6	27.5
58-28	30	3.5	14	21.1	0.01	138.6	26.0
58-28	30	3.5	14	21.1	10	766.5	24.7
58-28	30	3.5	14	21.1	5	642.4	25.5
58-28	30	3.5	14	21.1	1	427.4	27.8
58-28	30	3.5	14	21.1	0.5	354.9	28.2
58-28	30	3.5	14	21.1	0.1	233.4	28.4
58-28	30	3.5	14	21.1	0.01	138.4	27.0
58-28	30	3.5	14.1	4.4	10	1911.2	12.7
58-28	30	3.5	14.1	4.4	5	1741.3	13.7
58-28	30	3.5	14.1	4.4	1	1365.7	16.1
58-28	30	3.5	14.1	4.4	0.5	1207.3	17.3
58-28	30	3.5	14.1	4.4	0.1	888.1	20.4
58-28	30	3.5	14.1	4.4	0.01	573.0	23.1
58-28	30	3.5	14.1	4.4	10	1677.1	13.9
58-28	30	3.5	14.1	4.4	5	1500.4	15.4
58-28	30	3.5	14.1	4.4	1	1135.8	17.9
58-28	30	3.5	14.1	4.4	0.5	1005.4	18.9
58-28	30	3.5	14.1	4.4	0.1	733.6	21.8
58-28	30	3.5	14.1	4.4	0.01	478.0	23.9
58-28	30	3.5	14.1	4.4	10	1773.4	13.3
58-28	30	3.5	14.1	4.4	5	1596.1	14.3
58-28	30	3.5	14.1	4.4	1	1224.1	17.5
58-28	30	3.5	14.1	4.4	0.5	1068.5	19.0
58-28	30	3.5	14.1	4.4	0.1	782.5	21.9
58-28	30	3.5	14.1	4.4	0.01	505.9	24.1
58-28	30	3.5	14.1	21.1	10	800.3	24.7
58-28	30	3.5	14.1	21.1	5	685.0	25.2

Base Binder	Thiopave (%)	Design Air Voids (%)	Curing Time (days)	Test Temp (Deg_C)	Frequency (Hz)	E* (ksi)	Phase Angle (Deg)
58-28	30	3.5	14.1	21.1	1	464.3	27.1
58-28	30	3.5	14.1	21.1	0.5	389.9	27.1
58-28	30	3.5	14.1	21.1	0.1	257.4	27.6
58-28	30	3.5	14.1	21.1	0.01	154.2	26.7
58-28	30	3.5	14.1	21.1	10	665.4	24.9
58-28	30	3.5	14.1	21.1	5	560.4	25.9
58-28	30	3.5	14.1	21.1	1	368.8	27.8
58-28	30	3.5	14.1	21.1	0.5	305.7	28.1
58-28	30	3.5	14.1	21.1	0.1	198.0	27.9
58-28	30	3.5	14.1	21.1	0.01	117.2	26.1
58-28	30	3.5	14.1	21.1	10	727.9	25.8
58-28	30	3.5	14.1	21.1	5	615.5	26.3
58-28	30	3.5	14.1	21.1	1	406.7	28.3
58-28	30	3.5	14.1	21.1	0.5	336.1	28.6
58-28	30	3.5	14.1	21.1	0.1	216.5	29.4
58-28	30	3.5	14.1	21.1	0.01	124.3	28.9
58-28	30	3.5	14.1	46.1	10	209.1	32.3
58-28	30	3.5	14.1	46.1	5	168.7	31.1
58-28	30	3.5	14.1	46.1	1	98.0	30.2
58-28	30	3.5	14.1	46.1	0.5	80.8	28.8
58-28	30	3.5	14.1	46.1	0.1	52.0	27.2
58-28	30	3.5	14.1	46.1	0.01	29.5	24.5
58-28	30	3.5	14.1	46.1	10	158.2	32.2
58-28	30	3.5	14.1	46.1	5	121.7	31.7
58-28	30	3.5	14.1	46.1	1	68.3	30.7
58-28	30	3.5	14.1	46.1	0.5	55.8	29.2
58-28	30	3.5	14.1	46.1	0.1	37.7	27.1
58-28	30	3.5	14.1	46.1	0.01	23.3	24.6
58-28	30	3.5	14.1	46.1	10	184.1	32.4
58-28	30	3.5	14.1	46.1	5	143.9	31.6
58-28	30	3.5	14.1	46.1	1	82.3	30.2
58-28	30	3.5	14.1	46.1	0.5	68.6	28.4
58-28	30	3.5	14.1	46.1	0.1	45.9	27.3
58-28	30	3.5	14.1	46.1	0.01	27.9	25.5
58-28	30	2	1	21.1	10	502.7	30.4
58-28	30	2	1	21.1	5	412.6	30.5
58-28	30	2	1	21.1	1	253.1	31.7
58-28	30	2	1	21.1	0.5	204.1	31.3
58-28	30	2	1	21.1	0.1	125.3	30.3

Base Binder	Thiopave (%)	Design Air Voids (%)	Curing Time (days)	Test Temp (Deg_C)	Frequency (Hz)	E* (ksi)	Phase Angle (Deg)
58-28	30	2	1	21.1	0.01	70.2	28.2
58-28	30	2	1	21.1	10	439.8	30.8
58-28	30	2	1	21.1	5	358.0	31.3
58-28	30	2	1	21.1	1	215.4	32.8
58-28	30	2	1	21.1	0.5	173.2	32.3
58-28	30	2	1	21.1	0.1	105.6	31.1
58-28	30	2	1	21.1	0.01	58.8	28.4
58-28	30	2	1	21.1	10	493.0	31.5
58-28	30	2	1	21.1	5	401.3	31.8
58-28	30	2	1	21.1	1	242.8	33.1
58-28	30	2	1	21.1	0.5	194.4	32.5
58-28	30	2	1	21.1	0.1	118.6	31.3
58-28	30	2	1	21.1	0.01	64.8	28.8
58-28	30	2	14	21.1	10	685.0	24.8
58-28	30	2	14	21.1	5	573.3	25.8
58-28	30	2	14	21.1	1	378.0	27.9
58-28	30	2	14	21.1	0.5	312.6	28.2
58-28	30	2	14	21.1	0.1	205.7	28.1
58-28	30	2	14	21.1	0.01	124.0	26.5
58-28	30	2	14	21.1	10	700.7	25.0
58-28	30	2	14	21.1	5	588.3	25.6
58-28	30	2	14	21.1	1	391.7	27.6
58-28	30	2	14	21.1	0.5	326.0	27.8
58-28	30	2	14	21.1	0.1	216.1	27.6
58-28	30	2	14	21.1	0.01	130.1	25.8
58-28	30	2	14	21.1	10	664.1	24.6
58-28	30	2	14	21.1	5	555.3	25.4
58-28	30	2	14	21.1	1	369.3	27.4
58-28	30	2	14	21.1	0.5	306.6	27.7
58-28	30	2	14	21.1	0.1	204.4	27.7
58-28	30	2	14	21.1	0.01	125.5	26.4
58-28	30	2	14.1	4.4	10	1722.9	13.8
58-28	30	2	14.1	4.4	5	1556.7	14.9
58-28	30	2	14.1	4.4	1	1193.7	17.8
58-28	30	2	14.1	4.4	0.5	1045.7	19.2
58-28	30	2	14.1	4.4	0.1	766.7	21.8
58-28	30	2	14.1	4.4	0.01	504.2	23.7
58-28	30	2	14.1	4.4	10	1778.0	13.6
58-28	30	2	14.1	4.4	5	1605.9	14.8

Base Binder	Thiopave (%)	Design Air Voids (%)	Curing Time (days)	Test Temp (Deg_C)	Frequency (Hz)	E* (ksi)	Phase Angle (Deg)
58-28	30	2	14.1	4.4	1	1229.2	17.7
58-28	30	2	14.1	4.4	0.5	1075.6	18.9
58-28	30	2	14.1	4.4	0.1	784.5	21.6
58-28	30	2	14.1	4.4	0.01	491.7	24.3
58-28	30	2	14.1	4.4	10	1565.4	14.2
58-28	30	2	14.1	4.4	5	1406.6	15.4
58-28	30	2	14.1	4.4	1	1073.9	18.1
58-28	30	2	14.1	4.4	0.5	947.0	19.1
58-28	30	2	14.1	4.4	0.1	693.7	21.5
58-28	30	2	14.1	4.4	0.01	461.4	23.4
58-28	30	2	14.1	21.1	10	695.9	24.5
58-28	30	2	14.1	21.1	5	588.6	25.2
58-28	30	2	14.1	21.1	1	390.6	27.3
58-28	30	2	14.1	21.1	0.5	325.2	27.6
58-28	30	2	14.1	21.1	0.1	210.6	28.0
58-28	30	2	14.1	21.1	0.01	120.5	26.7
58-28	30	2	14.1	21.1	10	690.4	25.3
58-28	30	2	14.1	21.1	5	582.2	26.0
58-28	30	2	14.1	21.1	1	381.4	28.0
58-28	30	2	14.1	21.1	0.5	314.7	28.2
58-28	30	2	14.1	21.1	0.1	200.0	28.3
58-28	30	2	14.1	21.1	0.01	111.9	27.1
58-28	30	2	14.1	21.1	10	651.8	25.8
58-28	30	2	14.1	21.1	5	550.0	26.5
58-28	30	2	14.1	21.1	1	364.0	28.1
58-28	30	2	14.1	21.1	0.5	302.5	28.2
58-28	30	2	14.1	21.1	0.1	195.4	28.6
58-28	30	2	14.1	21.1	0.01	111.0	27.3
58-28	30	2	14.1	46.1	10	142.9	33.0
58-28	30	2	14.1	46.1	5	109.1	32.7
58-28	30	2	14.1	46.1	1	61.1	32.1
58-28	30	2	14.1	46.1	0.5	51.4	30.5
58-28	30	2	14.1	46.1	0.1	35.2	28.4
58-28	30	2	14.1	46.1	0.01	23.0	25.6
58-28	30	2	14.1	46.1	10	143.8	32.7
58-28	30	2	14.1	46.1	5	110.2	32.6
58-28	30	2	14.1	46.1	1	61.1	31.4
58-28	30	2	14.1	46.1	0.5	51.1	29.3
58-28	30	2	14.1	46.1	0.1	33.8	27.6

Base Binder	Thiopave (%)	Design Air Voids (%)	Curing Time (days)	Test Temp (Deg_C)	Frequency (Hz)	E* (ksi)	Phase Angle (Deg)
58-28	30	2	14.1	46.1	0.01	21.9	24.3
58-28	30	2	14.1	46.1	10	161.6	33.9
58-28	30	2	14.1	46.1	5	126.3	33.4
58-28	30	2	14.1	46.1	1	68.8	33.1
58-28	30	2	14.1	46.1	0.5	56.9	31.4
58-28	30	2	14.1	46.1	0.1	36.0	29.6
58-28	30	2	14.1	46.1	0.01	20.1	26.3
58-28	40	3.5	1	21.1	10	835.0	23.2
58-28	40	3.5	1	21.1	5	715.2	24.3
58-28	40	3.5	1	21.1	1	476.3	27.1
58-28	40	3.5	1	21.1	0.5	392.3	27.8
58-28	40	3.5	1	21.1	0.1	241.5	28.5
58-28	40	3.5	1	21.1	0.01	112.5	27.6
58-28	40	3.5	1	21.1	10	796.5	25.1
58-28	40	3.5	1	21.1	5	672.1	25.6
58-28	40	3.5	1	21.1	1	447.2	27.5
58-28	40	3.5	1	21.1	0.5	375.4	27.9
58-28	40	3.5	1	21.1	0.1	243.7	28.0
58-28	40	3.5	1	21.1	0.01	137.4	26.6
58-28	40	3.5	1	21.1	10	807.6	25.6
58-28	40	3.5	1	21.1	5	678.1	26.0
58-28	40	3.5	1	21.1	1	446.6	28.0
58-28	40	3.5	1	21.1	0.5	369.3	28.0
58-28	40	3.5	1	21.1	0.1	238.2	27.8
58-28	40	3.5	1	21.1	0.01	136.1	26.3
58-28	40	3.5	14	21.1	10	918.2	23.2
58-28	40	3.5	14	21.1	5	772.9	24.4
58-28	40	3.5	14	21.1	1	525.6	26.9
58-28	40	3.5	14	21.1	0.5	442.8	27.4
58-28	40	3.5	14	21.1	0.1	296.0	27.9
58-28	40	3.5	14	21.1	0.01	177.7	26.7
58-28	40	3.5	14	21.1	10	935.5	22.3
58-28	40	3.5	14	21.1	5	786.0	23.8
58-28	40	3.5	14	21.1	1	539.3	26.4
58-28	40	3.5	14	21.1	0.5	456.0	26.9
58-28	40	3.5	14	21.1	0.1	307.9	27.7
58-28	40	3.5	14	21.1	0.01	185.9	26.7
58-28	40	3.5	14	21.1	10	929.7	22.4
58-28	40	3.5	14	21.1	5	773.9	24.4

Base Binder	Thiopave (%)	Design Air Voids (%)	Curing Time (days)	Test Temp (Deg_C)	Frequency (Hz)	E* (ksi)	Phase Angle (Deg)
58-28	40	3.5	14	21.1	1	521.8	27.0
58-28	40	3.5	14	21.1	0.5	437.6	27.5
58-28	40	3.5	14	21.1	0.1	290.4	27.8
58-28	40	3.5	14	21.1	0.01	174.2	26.7
58-28	40	3.5	14.1	4.4	10	2124.2	11.6
58-28	40	3.5	14.1	4.4	5	1938.3	12.5
58-28	40	3.5	14.1	4.4	1	1528.7	15.0
58-28	40	3.5	14.1	4.4	0.5	1358.9	16.3
58-28	40	3.5	14.1	4.4	0.1	1013.4	19.9
58-28	40	3.5	14.1	4.4	0.01	657.6	23.2
58-28	40	3.5	14.1	4.4	10	2064.3	11.8
58-28	40	3.5	14.1	4.4	5	1892.6	12.7
58-28	40	3.5	14.1	4.4	1	1497.8	15.2
58-28	40	3.5	14.1	4.4	0.5	1334.9	16.3
58-28	40	3.5	14.1	4.4	0.1	998.9	19.7
58-28	40	3.5	14.1	4.4	0.01	657.2	22.2
58-28	40	3.5	14.1	4.4	10	2096.8	12.0
58-28	40	3.5	14.1	4.4	5	1918.1	12.9
58-28	40	3.5	14.1	4.4	1	1514.2	15.4
58-28	40	3.5	14.1	4.4	0.5	1342.0	16.8
58-28	40	3.5	14.1	4.4	0.1	988.1	20.4
58-28	40	3.5	14.1	4.4	0.01	644.7	23.2
58-28	40	3.5	14.1	21.1	10	884.2	23.2
58-28	40	3.5	14.1	21.1	5	759.0	24.0
58-28	40	3.5	14.1	21.1	1	514.2	26.3
58-28	40	3.5	14.1	21.1	0.5	432.1	26.8
58-28	40	3.5	14.1	21.1	0.1	283.0	27.5
58-28	40	3.5	14.1	21.1	0.01	162.6	26.8
58-28	40	3.5	14.1	21.1	10	898.4	23.3
58-28	40	3.5	14.1	21.1	5	764.1	24.4
58-28	40	3.5	14.1	21.1	1	523.2	26.6
58-28	40	3.5	14.1	21.1	0.5	442.9	26.9
58-28	40	3.5	14.1	21.1	0.1	293.4	27.4
58-28	40	3.5	14.1	21.1	0.01	172.3	26.7
58-28	40	3.5	14.1	21.1	10	895.2	23.6
58-28	40	3.5	14.1	21.1	5	757.0	24.7
58-28	40	3.5	14.1	21.1	1	513.0	27.2
58-28	40	3.5	14.1	21.1	0.5	430.9	27.3
58-28	40	3.5	14.1	21.1	0.1	280.8	27.9

Base Binder	Thiopave (%)	Design Air Voids (%)	Curing Time (days)	Test Temp (Deg_C)	Frequency (Hz)	E* (ksi)	Phase Angle (Deg)
58-28	40	3.5	14.1	21.1	0.01	164.5	26.9
58-28	40	3.5	14.1	46.1	10	198.4	33.1
58-28	40	3.5	14.1	46.1	5	153.3	32.6
58-28	40	3.5	14.1	46.1	1	85.4	32.1
58-28	40	3.5	14.1	46.1	0.5	70.3	30.6
58-28	40	3.5	14.1	46.1	0.1	45.4	29.7
58-28	40	3.5	14.1	46.1	0.01	29.1	28.5
58-28	40	3.5	14.1	46.1	10	182.6	36.0
58-28	40	3.5	14.1	46.1	5	152.6	33.5
58-28	40	3.5	14.1	46.1	1	87.5	32.4
58-28	40	3.5	14.1	46.1	0.5	73.4	30.8
58-28	40	3.5	14.1	46.1	0.1	48.4	29.8
58-28	40	3.5	14.1	46.1	0.01	31.7	27.9
58-28	40	3.5	14.1	46.1	10	189.3	34.0
58-28	40	3.5	14.1	46.1	5	161.9	32.1
58-28	40	3.5	14.1	46.1	1	94.3	30.7
58-28	40	3.5	14.1	46.1	0.5	78.8	29.1
58-28	40	3.5	14.1	46.1	0.1	52.7	27.6
58-28	40	3.5	14.1	46.1	0.01	35.1	25.8
58-28	40	2	1	21.1	10	702.9	27.0
58-28	40	2	1	21.1	5	590.0	27.6
58-28	40	2	1	21.1	1	386.5	29.6
58-28	40	2	1	21.1	0.5	319.2	29.6
58-28	40	2	1	21.1	0.1	205.7	29.1
58-28	40	2	1	21.1	0.01	119.4	27.3
58-28	40	2	1	21.1	10	686.3	26.7
58-28	40	2	1	21.1	5	578.7	27.4
58-28	40	2	1	21.1	1	372.5	29.5
58-28	40	2	1	21.1	0.5	304.4	29.5
58-28	40	2	1	21.1	0.1	192.2	29.2
58-28	40	2	1	21.1	0.01	109.2	27.3
58-28	40	2	1	21.1	10	628.3	27.4
58-28	40	2	1	21.1	5	521.7	28.0
58-28	40	2	1	21.1	1	332.7	29.9
58-28	40	2	1	21.1	0.5	272.1	29.9
58-28	40	2	1	21.1	0.1	172.7	29.4
58-28	40	2	1	21.1	0.01	99.8	27.6
58-28	40	2	14	21.1	10	979.1	23.1
58-28	40	2	14	21.1	5	809.5	24.6

Base Binder	Thiopave (%)	Design Air Voids (%)	Curing Time (days)	Test Temp (Deg_C)	Frequency (Hz)	E* (ksi)	Phase Angle (Deg)
58-28	40	2	14	21.1	1	550.7	27.1
58-28	40	2	14	21.1	0.5	462.4	27.4
58-28	40	2	14	21.1	0.1	311.4	28.0
58-28	40	2	14	21.1	0.01	187.5	27.1
58-28	40	2	14	21.1	10	824.8	24.3
58-28	40	2	14	21.1	5	687.0	25.7
58-28	40	2	14	21.1	1	456.9	28.0
58-28	40	2	14	21.1	0.5	381.2	28.5
58-28	40	2	14	21.1	0.1	252.8	28.3
58-28	40	2	14	21.1	0.01	150.7	26.4
58-28	40	2	14	21.1	10	815.7	23.6
58-28	40	2	14	21.1	5	684.6	24.7
58-28	40	2	14	21.1	1	460.5	27.1
58-28	40	2	14	21.1	0.5	382.9	27.6
58-28	40	2	14	21.1	0.1	254.7	28.0
58-28	40	2	14	21.1	0.01	154.0	26.8
58-28	40	2	14.1	4.4	10	2081.4	12.9
58-28	40	2	14.1	4.4	5	1895.1	14.1
58-28	40	2	14.1	4.4	1	1470.1	16.7
58-28	40	2	14.1	4.4	0.5	1289.8	17.8
58-28	40	2	14.1	4.4	0.1	951.3	21.0
58-28	40	2	14.1	4.4	0.01	635.7	23.6
58-28	40	2	14.1	4.4	10	1939.4	12.7
58-28	40	2	14.1	4.4	5	1759.0	13.6
58-28	40	2	14.1	4.4	1	1364.2	16.4
58-28	40	2	14.1	4.4	0.5	1205.8	17.8
58-28	40	2	14.1	4.4	0.1	886.6	21.0
58-28	40	2	14.1	4.4	0.01	564.2	24.1
58-28	40	2	14.1	4.4	10	1946.8	12.8
58-28	40	2	14.1	4.4	5	1761.5	13.7
58-28	40	2	14.1	4.4	1	1362.9	16.5
58-28	40	2	14.1	4.4	0.5	1218.9	17.9
58-28	40	2	14.1	4.4	0.1	895.2	20.7
58-28	40	2	14.1	4.4	0.01	585.5	23.2
58-28	40	2	14.1	21.1	10	883.1	23.4
58-28	40	2	14.1	21.1	5	740.3	24.6
58-28	40	2	14.1	21.1	1	502.8	26.8
58-28	40	2	14.1	21.1	0.5	421.9	27.1
58-28	40	2	14.1	21.1	0.1	275.7	27.7

Base Binder	Thiopave (%)	Design Air Voids (%)	Curing Time (days)	Test Temp (Deg_C)	Frequency (Hz)	E* (ksi)	Phase Angle (Deg)
58-28	40	2	14.1	21.1	0.01	158.5	26.9
58-28	40	2	14.1	21.1	10	797.0	25.2
58-28	40	2	14.1	21.1	5	676.2	26.1
58-28	40	2	14.1	21.1	1	449.8	28.0
58-28	40	2	14.1	21.1	0.5	374.5	28.0
58-28	40	2	14.1	21.1	0.1	240.8	28.3
58-28	40	2	14.1	21.1	0.01	136.7	27.1
58-28	40	2	14.1	21.1	10	831.2	24.9
58-28	40	2	14.1	21.1	5	703.1	26.1
58-28	40	2	14.1	21.1	1	471.7	28.3
58-28	40	2	14.1	21.1	0.5	394.8	28.4
58-28	40	2	14.1	21.1	0.1	256.4	28.9
58-28	40	2	14.1	21.1	0.01	147.2	27.9
58-28	40	2	14.1	46.1	10	165.5	35.1
58-28	40	2	14.1	46.1	5	133.4	33.3
58-28	40	2	14.1	46.1	1	72.9	31.8
58-28	40	2	14.1	46.1	0.5	60.1	30.6
58-28	40	2	14.1	46.1	0.1	40.3	29.1
58-28	40	2	14.1	46.1	0.01	26.7	26.1
58-28	40	2	14.1	46.1	10	142.2	34.9
58-28	40	2	14.1	46.1	5	112.4	32.6
58-28	40	2	14.1	46.1	1	60.1	31.9
58-28	40	2	14.1	46.1	0.5	50.9	30.1
58-28	40	2	14.1	46.1	0.1	34.5	28.3
58-28	40	2	14.1	46.1	0.01	24.7	26.8
58-28	40	2	14.1	46.1	10	155.9	33.6
58-28	40	2	14.1	46.1	5	125.8	32.1
58-28	40	2	14.1	46.1	1	69.2	31.1
58-28	40	2	14.1	46.1	0.5	57.2	29.4
58-28	40	2	14.1	46.1	0.1	38.5	27.9
58-28	40	2	14.1	46.1	0.01	26.4	25.7

APPENDIX C Flow Number Test Results

TABLE C.1 Summary of Flow Number Test Results

Base Binder	Thiopave (%)	Design Air Voids (%)	No. of Cycles Tested	Flow Number		Microstrain at Flow Point	
				Power	Francken	Power	Francken
67-22	0	4	134	34	41	19933	22729
67-22	0	4	112	31	35	27629	29567
76-22	0	4	1244	155	311	9474	14347
76-22	0	4	1124	169	154	11260	10407
76-22	0	4	1687	375	281	13923	11996
67-22	30	2	902	259	336	17749	21354
67-22	30	2	859	238	298	20862	24351
67-22	30	3.5	926	281	385	17854	22252
67-22	30	3.5	783	212	318	19445	24949
67-22	40	2	496	143	188	19464	23706
67-22	40	2	664	161	262	16754	23184
67-22	40	2	984	166	176	18219	18604
67-22	40	2	797	157	159	19945	19945
67-22	40	3.5	1185	290	593	12168	19730
67-22	40	3.5	934	233	417	14381	21629
67-22	40	3.5	1728	241	287	13797	14726
67-22	40	3.5	1256	262	244	17401	16791
58-28	30	2	723	160	129	17234	14988
58-28	30	2	451	104	98	18602	17752
58-28	30	2	707	157	155	20926	20577
58-28	30	3.5	672	159	149	17215	16625
58-28	30	3.5	397	65		13055	
58-28	30	3.5	367	78	108	13912	17038
58-28	40	2	620	139		11011	
58-28	40	2	590	88		11373	
58-28	40	2	362	63	79	11416	13189
58-28	40	3.5	267	65	110	10724	16319
58-28	40	3.5	390	60	118	9475	14966
58-28	40	3.5	190	46	94	11464	19726

APPENDIX D Asphalt Pavement Analyzer Test Results

TABLE D.1 Summary of APA Test Results

Base Binder	Thiopave (%)	Design Air Voids (%)	Manual Rut Depth		Automated Rut Depth	
			Individual (mm)	Average (mm)	Individual (mm)	Average (mm)
67-22	0	4	8.79	9.9	N/A	N/A
67-22	0	4	8.67		N/A	
67-22	0	4	12.02		N/A	
67-22	0	4	10.06		N/A	
76-22	0	4	4.71	3.2	3.46	2.1
76-22	0	4	3.15		2.15	
76-22	0	4	1.55		1.80	
76-22	0	4	3.02		1.47	
76-22	0	4	2.84		1.65	
76-22	0	4	3.73		1.99	
67-22	30	2	6.21	7.1	4.39	5.2
67-22	30	2	6.87		5.09	
67-22	30	2	6.86		4.99	
67-22	30	2	7.46		5.55	
67-22	30	2	8.03		5.91	
67-22	30	2	7.25		5.30	
67-22	30	3.5	5.51	5.4	3.09	3.5
67-22	30	3.5	5.41		3.13	
67-22	30	3.5	5.83		3.76	
67-22	30	3.5	4.04		3.38	
67-22	30	3.5	5.91		4.01	
67-22	30	3.5	5.62		3.35	
67-22	40	2	6.04	5.5	4.43	4.3
67-22	40	2	6.25		4.34	
67-22	40	2	5.60		4.53	
67-22	40	2	5.09		3.98	
67-22	40	2	5.63		4.33	
67-22	40	2	4.42		4.01	
67-22	40	3.5	5.43	5.8	3.45	4.7
67-22	40	3.5	5.31		4.08	
67-22	40	3.5	4.75		4.22	
67-22	40	3.5	5.28		4.02	
67-22	40	3.5	6.91		6.24	
67-22	40	3.5	7.01		5.97	

Base Binder	Thiopave (%)	Design Air Voids (%)	Manual Rut Depth		Automated Rut Depth	
			Individual (mm)	Average (mm)	Individual (mm)	Average (mm)
58-28	30	2	5.12	5.7	4.25	4.3
58-28	30	2	3.51		3.60	
58-28	30	2	5.50		4.41	
58-28	30	2	6.31		4.42	
58-28	30	2	7.14		4.58	
58-28	30	2	6.48		4.62	
58-28	30	3.5	6.82	7.3	4.89	4.9
58-28	30	3.5	4.33		2.98	
58-28	30	3.5	5.78		4.62	
58-28	30	3.5	7.28		4.62	
58-28	30	3.5	9.38		6.32	
58-28	30	3.5	9.91		6.23	
58-28	40	2	4.47	4.7	3.26	3.2
58-28	40	2	4.64		3.28	
58-28	40	2	3.82		2.61	
58-28	40	2	4.28		2.25	
58-28	40	2	5.47		3.76	
58-28	40	2	5.78		3.89	
58-28	40	3.5	4.29	3.7	2.74	2.8
58-28	40	3.5	4.38		2.70	
58-28	40	3.5	2.91		2.58	
58-28	40	3.5	2.59		2.43	
58-28	40	3.5	4.22		2.95	
58-28	40	3.5	4.02		3.23	

APPENDIX E Hamburg Wheel-Tracking Test Results

TABLE E.1 Summary of Hamburg Raw Data Analysis

Base Binder	Thiopave (%)	Design Air Voids (%)	Slope of Steady-State Rutting Curve	Rutting Rate (mm/hr)	Total Rut Depth (Based on Rate) (mm)	Stripping Inflection Point (cycles)
67-22	0	4	0.0020	5.1610	20.5	10000
67-22	0	4	0.0031	7.9254	31.4	10000
67-22	0	4	0.0024	6.1312	24.3	6800
67-22	0	4	0.0022	5.5264	21.9	10000
76-22	0	4	0.0009	2.3688	9.4	10000
76-22	0	4	0.0012	3.0744	12.2	10000
76-22	0	4	0.0014	3.5028	13.9	10000
67-22	30	2	0.0013	3.1500	12.5	5550
67-22	30	2	0.0017	4.2336	16.8	3550
67-22	30	2	0.0008	1.9858	7.9	4875
67-22	30	3.5	0.0005	1.3608	5.4	3600
67-22	30	3.5	0.0003	0.7560	3.0	4500
67-22	30	3.5	0.0005	1.3104	5.2	4900
67-22	30	3.5	0.0014	3.4524	13.7	5250
67-22	40	2	0.0011	2.8728	11.4	3600
67-22	40	2	0.0010	2.5956	10.3	3900
67-22	40	2	0.0018	4.6368	18.4	5600
67-22	40	3.5	0.0007	1.7136	6.8	4300
67-22	40	3.5	0.0006	1.4944	5.9	5250
67-22	40	3.5	0.0008	2.0160	8.0	2850
67-22	40	3.5	0.0009	2.2932	9.1	2450
58-28	30	2	0.0013	3.2004	12.7	2250
58-28	30	2	0.0038	9.4752	37.6	2600
58-28	30	2	0.0038	9.4752	37.6	2500
58-28	30	3.5	0.0030	7.5398	29.9	3200
58-28	30	3.5	0.0024	6.1600	24.4	2200
58-28	30	3.5	0.0020	5.0715	20.1	1900
58-28	40	2	0.0011	2.6460	10.5	2500
58-28	40	2	0.0009	2.1420	8.5	3200
58-28	40	2	0.0011	2.7972	11.1	2000
58-28	40	3.5	0.0017	4.3344	17.2	1200
58-28	40	3.5	0.0013	3.1928	12.7	3100
58-28	40	3.5	0.0006	1.5876	6.3	2300

APPENDIX F Bending Beam Fatigue Test Results

TABLE F.1 Summary of Bending Beam Fatigue Test Results

Base Binder	Thiopave (%)	Design Air Voids (%)	Strain Level (ms)	Cycles to Failure (ASTM)	Cycles to Failure (AASHTO)	Initial Beam Stiffness (Mpa)
67-22	0	4	600	35,120	17,600	5905
67-22	0	4	600	28,500	24,540	5756
67-22	0	4	400	185,490	141,250	6344
67-22	0	4	400	364,470	254,090	6639
67-22	0	4	200	3,821,390	3,432,060	5861
67-22	0	4	200	6,606,930	6,674,890	6101
76-22	0	4	800	9,690	5,200	4462
76-22	0	4	800	12,420	6,360	4606
76-22	0	4	600	N/A	25,440	5843
76-22	0	4	600	40,940	22,440	5386
76-22	0	4	600	85,330	40,840	5333
76-22	0	4	400	1,634,300	568,850	5490
76-22	0	4	400	1,208,430	560,180	5503
76-22	0	4	200	N/A	218,159,415*	6016
76-22	0	4	200	N/A	60,600,263*	5933
67-22	30	2	600	31,780	12,300	6807
67-22	30	2	600	9,130	8,030	6923
67-22	30	2	400	86,870	84,240	7049
67-22	30	2	400	190,540	106,330	7043
67-22	30	2	200	3,841,000	4,105,190	7384
67-22	30	2	200	7,432,090	6,025,590	7255
67-22	30	3.5	600	11,680	5,200	6366
67-22	30	3.5	600	8,580	6,130	8175
67-22	30	3.5	400	29,890	24,990	7318
67-22	30	3.5	400	66,740	37,820	7736
67-22	30	3.5	200	1,944,860	1,810,410	8029
67-22	30	3.5	200	2,854,660	1,036,460	8587
67-22	40	2	600	3,480	3,170	6749
67-22	40	2	600	10,710	7,950	7162
67-22	40	2	400	189,810	62,930	7620
67-22	40	2	400	76,440	54,950	7726
67-22	40	2	200	2,524,770	2,165,480	8140
67-22	40	2	200	628,540	683,910	8664
67-22	40	3.5	600	3,610	2,970	7434
67-22	40	3.5	600	13,420	5,770	6817
67-22	40	3.5	400	48,720	31,540	7930
67-22	40	3.5	400	44,440	32,850	7742

Base Binder	Thiopave (%)	Design Air Voids (%)	Strain Level (ms)	Cycles to Failure (ASTM)	Cycles to Failure (AASHTO)	Initial Beam Stiffness (Mpa)
67-22	40	3.5	200	2,563,820	2,187,760	8624
67-22	40	3.5	200	1,915,230	2,026,120	7763
58-28	30	2	600	24,350	14,340	4066
58-28	30	2	600	28,840	16,720	3742
58-28	30	2	400	110,060	115,250	4261
58-28	30	2	400	213,790	149,050	4504
58-28	30	2	200	4,042,650	4,365,150	5202
58-28	30	2	200	2,630,260	2,670,950	4915
58-28	30	3.5	800	11,220	6,390	3636
58-28	30	3.5	800	6,340	2,490	3627
58-28	30	3.5	600	12,300	9,800	3877
58-28	30	3.5	600	14,190	9,260	3730
58-28	30	3.5	400	73,000	71,880	4873
58-28	30	3.5	400	230,850	151,350	3713
58-28	30	3.5	200	N/A	14,872,993*	5338
58-28	30	3.5	200	N/A	31,310,854*	5105
58-28	40	2	600	27,610	16,720	3465
58-28	40	2	600	8,520	6,650	3979
58-28	40	2	400	21,430	17,150	4833
58-28	40	2	400	77,030	43,870	4026
58-28	40	2	200	395,060	365,870	5394
58-28	40	2	200	1,452,850	1,460,300	5613
58-28	40	3.5	600	N/A	13,660	3842
58-28	40	3.5	600	50,890	18,710	4088
58-28	40	3.5	600	33,020	14,340	3768
58-28	40	3.5	400	50,110	38,410	5366
58-28	40	3.5	400	24,230	16,630	5051
58-28	40	3.5	200	1,505,830	1,452,850	5074
58-28	40	3.5	200	1,085,310	1,041,780	4550

* Extrapolation was used to estimate the number of cycles to failure.

APPENDIX G Thermal Stress-Restrained Specimen Test Results

TABLE G.1 Summary of Thermal Stress-Restrained Specimen Test Results

Base Binder	Thiopave (%)	Design Air Voids (%)	Sample Air Voids (%)	Sample Length (mm)	Sample Height (mm)	Sample Width (mm)	Fracture Stress (psi)	Fracture Temperature (^{o}C)
67-22	0	4	6.3	255.21	50.80	51.86	367	-19.6
67-22	0	4	7.3	252.38	49.91	51.65	367	-20.5
67-22	0	4	6.9	254.95	52.48	53.53	313	-21.4
76-22	0	4	5.7	254.43	49.85	51.21	387	-23.1
76-22	0	4	6.5	255.52	50.78	49.02	305	-24.0
76-22	0	4	6.8	255.87	51.59	50.18	322	-22.8
67-22	30	3.5	7.5	253.15	51.03	50.51	420	-18.0
67-22	30	3.5	7.2	254.41	51.25	50.39	366	-17.2
67-22	30	3.5	7.3	251.81	50.85	52.20	454	-22.6
67-22	40	3.5	7.4	253.72	51.81	53.19	435	-21.6
67-22	40	3.5	7.5	252.07	52.27	52.95	374	-17.5
67-22	40	3.5	7	253.13	51.92	52.80	480	-21.1
67-22	30	2	7.3	248.00	52.61	50.31	368	-22.6
67-22	30	2	6.2	250.98	50.95	50.96	386	-22.4
67-22	30	2	6.1	254.80	51.42	51.12	389	-20.7
67-22	40	2	5.7	249.05	51.42	50.12	373	-21.4
67-22	40	2	6	248.94	49.93	49.97	435	-20.7
67-22	40	2	6.1	254.68	51.89	50.96	477	-24.1
58-28	30	3.5	7.1	251.23	50.31	49.67	278	-31.0
58-28	30	3.5	7.3	252.43	50.79	49.67	381	-26.0
58-28	30	3.5	7.1	253.01	50.77	50.69	417	-28.0
58-28	40	3.5	7.7	253.21	50.89	50.44	436	-29.0
58-28	40	3.5	6.9	254.49	50.85	50.36	324	-26.0
58-28	40	3.5	7.9	253.06	50.54	50.21	389	-28.0
58-28	30	2	6.3	251.77	50.05	49.18	274	-26.0
58-28	30	2	6.3	252.15	49.82	49.54	366	-32.0
58-28	30	2	6.2	252.60	50.83	50.66	395	-29.0
58-28	40	2	6.4	251.67	50.47	50.33	304	-29.0
58-28	40	2	7.6	252.76	50.59	50.37	307	-26.0
58-28	40	2	6.7	253.12	50.76	50.02	381	-26.0

APPENDIX H Semi-Circular Bending Test Results

TABLE H.1 Fracture Toughness

Base Binder	Thiopave (%)	Design Air Voids (%)	Test Temp (°C)	K_{IC}, MPa/m^0.5					
				Rep1	Rep2	Rep3	Average	Std. Dev.	CV%
67-22	0	4	-18	0.654	0.801	0.710	0.722	0.074	10
67-22	0	4	-30	0.806	0.811	0.623	0.747	0.107	14
67-22	30	2	-18	0.921	0.756	0.600	0.759	0.160	21
67-22	30	2	-30	0.878	0.807	0.703	0.796	0.088	11
67-22	30	3.5	-18	0.668	0.737	0.766	0.724	0.050	7
67-22	30	3.5	-30	0.821	0.855	0.870	0.849	0.025	3
67-22	40	2	-18	0.621	0.606	0.790	0.673	0.102	15
67-22	40	2	-30	0.747	0.725	0.727	0.733	0.012	2
67-22	40	3.5	-18	0.788	0.622	0.605	0.672	0.101	15
67-22	40	3.5	-30	0.730	0.751	0.652	0.711	0.052	7
58-28	30	2	-18	0.802	0.678	0.705	0.728	0.065	9
58-28	30	2	-30	0.848	0.855	0.784	0.829	0.039	5
58-28	30	3.5	-18	0.711	0.735	0.697	0.714	0.019	3
58-28	30	3.5	-30	0.920	0.832	0.745	0.832	0.088	11
58-28	40	2	-18	0.604	0.672	0.611	0.629	0.037	6
58-28	40	2	-30	0.735	0.754	0.832	0.774	0.051	7
58-28	40	3.5	-18	0.712	0.639	0.739	0.697	0.052	7
58-28	40	3.5	-30	0.776	0.816	0.788	0.794	0.021	3

TABLE H.2 Fracture Energy (Method 1)

Base Binder	Thiopave (%)	Design Air Voids (%)	Test Temp (oC)	G_f (kN/m) -- Method 1					
				Rep1	Rep2	Rep3	Average	Std. Dev.	CV%
67-22	0	4	-18	0.219	0.290	0.367	0.292	0.074	25
67-22	0	4	-30	0.195	0.228	0.214	0.213	0.017	8
67-22	30	2	-18	0.457	0.188	0.335	0.327	0.135	41
67-22	30	2	-30	0.286	0.145	0.183	0.205	0.073	36
67-22	30	3.5	-18	0.296	0.249	0.254	0.266	0.026	10
67-22	30	3.5	-30	0.228	0.200	0.217	0.215	0.014	7
67-22	40	2	-18	0.207	0.241	0.269	0.239	0.031	13
67-22	40	2	-30	0.230	0.189	0.175	0.198	0.028	14
67-22	40	3.5	-18	0.300	0.232	0.301	0.278	0.039	14
67-22	40	3.5	-30	0.218	0.270	0.186	0.224	0.042	19
58-28	30	2	-18	0.383	0.380	0.394	0.385	0.008	2
58-28	30	2	-30	0.246	0.349	0.282	0.292	0.052	18
58-28	30	3.5	-18	0.294	0.503	0.464	0.420	0.111	26
58-28	30	3.5	-30	0.386	0.322	0.266	0.325	0.060	19
58-28	40	2	-18	0.278	0.331	0.302	0.303	0.026	9
58-28	40	2	-30	0.240	0.265	0.314	0.273	0.038	14
58-28	40	3.5	-18	0.311	0.279	0.384	0.325	0.054	17
58-28	40	3.5	-30	0.210	0.178	0.255	0.214	0.038	18

TABLE H.3 Fracture Energy (Method 2)

Base Binder	Thiopave (%)	Design Air Voids (%)	Test Temp (oC)	G_f (kN/m) -- Method 2					
				Rep1	Rep2	Rep3	Average	Std. Dev.	CV%
67-22	0	4	-18	0.227	0.242	0.300	0.256	0.039	15
67-22	0	4	-30	0.164	0.180	0.143	0.162	0.019	12
67-22	30	2	-18	0.368	0.192	1.016	0.526	0.434	83
67-22	30	2	-30	0.237	0.212	0.130	0.193	0.056	29
67-22	30	3.5	-18	0.225	0.236	0.302	0.254	0.042	16
67-22	30	3.5	-30	0.348	0.364	0.206	0.306	0.087	28
67-22	40	2	-18	0.193	0.192	0.213	0.199	0.012	6
67-22	40	2	-30	0.270	0.265	0.123	0.219	0.083	38
67-22	40	3.5	-18	0.228	0.337	0.265	0.277	0.055	20
67-22	40	3.5	-30	0.211	0.247	0.147	0.202	0.051	25
58-28	30	2	-18	0.333	0.372	0.419	0.375	0.043	11
58-28	30	2	-30	0.204	0.316	0.304	0.275	0.062	22
58-28	30	3.5	-18	0.361	0.462	0.387	0.403	0.052	13
58-28	30	3.5	-30	0.323	0.269	0.227	0.273	0.048	18
58-28	40	2	-18	0.316	0.339	0.301	0.319	0.019	6
58-28	40	2	-30	0.204	0.207	0.283	0.231	0.045	19
58-28	40	3.5	-18	0.395	0.242	0.294	0.310	0.078	25
58-28	40	3.5	-30	0.256	0.142	0.237	0.212	0.061	29

APPENDIX I Bending Beam Rheometer Test Results

TABLE I.1 Creep Stiffness (S-value) and Creep Rate (m-value) Measured using BBR

Base Binder	Thiopave (%)	Design Air Voids (%)	Test Temp. (°C)	S-value @ 60s (Mpa)	m-value @ 60s	COV S-value (%)	COV m-value (%)
67-22	0	4	16	155	0.510	13	2
67-22	30	2	16	677	0.378	37	5
67-22	30	3.5	16	898	0.338	4	7
67-22	40	2	16	442	0.398	30	9
67-22	40	3.5	16	1,051	0.317	6	8
67-22	0	4	-12	5,470	0.172	13	7
67-22	30	2	-12	8,173	0.139	16	9
67-22	30	3.5	-12	9,540	0.116	12	6
67-22	40	2	-12	5,953	0.135	17	5
67-22	40	3.5	-12	10,350	0.103	5	32
58-29	30	2	16	277	0.440	14	3
58-30	30	3.5	16	497	0.389	25	10
58-31	40	2	16	533	0.393	2	10
58-32	40	3.5	16	696	0.355	22	5
58-34	30	2	-12	4,230	0.139	6	12
58-35	30	3.5	-12	4,385	0.122	11	12
58-36	40	2	-12	5,105	0.097	10	25
58-37	40	3.5	-12	7,763	0.154	22	27

APPENDIX J Overlay Test Results

TABLE J.1 Number of Cycles to Failure Measured Using Overlay Test

Base Binder	Thiopave (%)	Design Air Voids (%)	Opening Width (in.)	Replicate No.	Number of Cycles to Failure
67-22	0	4	0.01	1	57
67-22	0	4	0.01	2	47
67-22	0	4	0.01	3	71
67-22	0	4	0.025	1	5
67-22	0	4	0.025	2	3
67-22	0	4	0.025	3	6
67-22	30	2	0.01	1	24
67-22	30	2	0.01	2	16
67-22	30	2	0.01	3	54
67-22	30	2	0.025	1	5
67-22	30	2	0.025	2	4
67-22	30	2	0.025	3	N.A.
67-22	30	3.5	0.01	1	80
67-22	30	3.5	0.01	2	117
67-22	30	3.5	0.01	3	68
67-22	30	3.5	0.025	1	3
67-22	30	3.5	0.025	2	8
67-22	30	3.5	0.025	3	2
67-22	40	2	0.01	1	19
67-22	40	2	0.01	2	28
67-22	40	2	0.01	3	7
67-22	40	2	0.025	1	17
67-22	40	2	0.025	2	15
67-22	40	2	0.025	3	63
67-22	40	3.5	0.01	1	32
67-22	40	3.5	0.01	2	52
67-22	40	3.5	0.01	3	11
67-22	40	3.5	0.025	1	49
67-22	40	3.5	0.025	2	30
67-22	40	3.5	0.025	3	32
58-28	30	2	0.01	1	1,178
58-28	30	2	0.01	2	1,853
58-28	30	2	0.01	3	N/A
58-28	30	2	0.025	1	15
58-28	30	2	0.025	2	23
58-28	30	2	0.025	3	17
58-28	30	2	0.025	4	34
58-28	30	3.5	0.01	1	555

Base Binder	Thiopave (%)	Design Air Voids (%)	Opening Width (in.)	Replicate No.	Number of Cycles to Failure
58-28	30	3.5	0.01	2	131
58-28	30	3.5	0.01	3	206
58-28	30	3.5	0.025	1	18
58-28	30	3.5	0.025	2	7
58-28	30	3.5	0.025	3	6
58-28	40	2	0.01	1	45
58-28	40	2	0.01	2	204
58-28	40	2	0.01	3	75
58-28	40	2	0.025	1	24
58-28	40	2	0.025	2	8
58-28	40	2	0.025	3	49
58-28	40	3.5	0.01	1	75
58-28	40	3.5	0.01	2	63
58-28	40	3.5	0.01	3	207
58-28	40	3.5	0.025	1	34
58-28	40	3.5	0.025	2	5
58-28	40	3.5	0.025	3	14